Subtle alterations in DNA methylation patterns in normal cells in response to dietary stilbenoids

Megan Beetch[1,a], Katarzyna Lubecka[2,a], Heather Kristofzski[3], Matthew Suderman[4,5], and Barbara Stefanska[1]*

[1] Food, Nutrition and Health, Faculty of Land and Food Systems, the University of British Columbia, Vancouver, BC, Canada
[2] Department of Biomedical Chemistry, Medical University of Lodz, Lodz, Poland
[3] Department of Nutrition Science, Purdue University, West Lafayette, IN, USA
[4] School of Social and Community Medicine, University of Bristol, Bristol, UK
[5] MRC Integrative Epidemiology Unit, University of Bristol, Bristol, UK

[a] These authors contributed equally to this work.

Keywords: diet, DNA methylation, exposure to stilbenoids, healthy cells

The Authors declare no conflict of interest.

*To whom correspondence should be addressed:
Dr. Barbara Stefanska
Assistant Professor
Faculty of Land and Food Systems
University of British Columbia
2205 East Mall, FNH 150
Vancouver, BC V6T 1Z4
Phone: +1 604-822-2524, Fax: +1 604-822–5143
barbara.stefanska@ubc.ca
http://www.landfood.ubc.ca/person/barbara-stefanska/

ABSTRACT

Scope: Searching for correlations between dietary polyphenols and risk of chronic diseases has been a challenge due to the lack of quantitative evaluation methods of long-term exposure. We previously observed substantial DNA methylation changes in human cancer cells upon treatment with polyphenols of the stilbenoid class. When induced in normal cells, such molecular changes might persist and reflect chronic exposure.

Methods and Results: Using Illumina-450K microarray, we delineated a genome-wide DNA methylation landscape in MCF10A human immortalized mammary epithelial cells exposed to resveratrol at non-cytotoxic 15μM dose for 9 days. We identified subtle alterations suggesting remodeling of DNA methylation patterns rather than switch on/off changes. Using pyrosequencing, we quantitatively measured DNA methylation at 8 CpG sites located within *KCNJ4*, *RNF169*, *BCHE*, *DAOA*, *HOXA9*, *RUNX3*, *KRTAP2-1*, and *TAGAP*, upon exposure to resveratrol or pterostilbene and detected similar differences induced by both stilbenoids. Two of the probes, *Runx3* and *Kcnj4*, were successfully verified in whole blood DNA from healthy rats on diets supplemented with stilbenoids.

Conclusions: Our study provides strong support for testing the utility of polyphenol-mediated changes in DNA methylation as quantitative measures of long-term dietary exposures in nutritional epidemiology and clinical trials.

GRAPHICAL ABSTRACT

Subtle alterations in DNA methylation were detected in normal cells exposed to polyphenols of the stilbenoid class, such as resveratrol or pterostilbene, and in whole blood of rats whose diets were supplemented with the compounds. Once confirmed in population-based studies, such molecular markers can be used as an excellent tool to reliably measure long-term polyphenol exposure and establish associations between polyphenol intake and risk of chronic diseases.

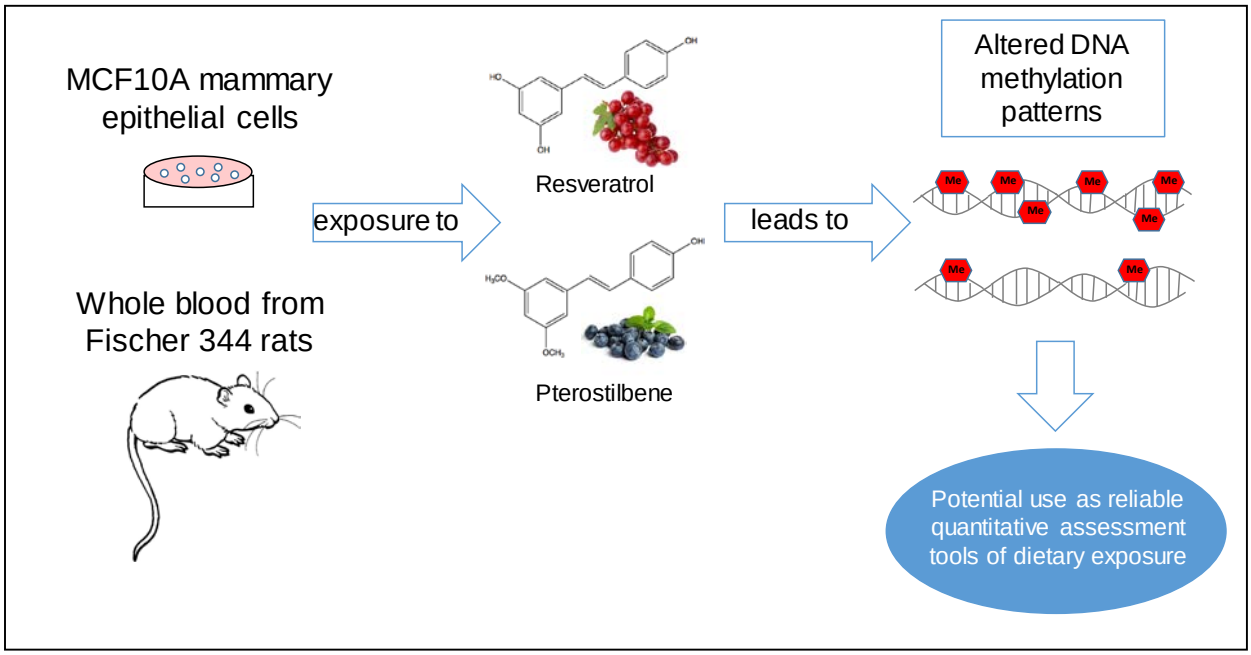

INTRODUCTION

Epidemiologic studies have been searching for associations between dietary factors and disease risk for many decades. Such studies compare rates of disease occurrence and dietary consumption in a population to estimate whether there is any association [1]. Thus, the accurate measurements of the intake are key for interpretation of the results. Variations in daily consumption patterns make it challenging to establish individuals' long-term exposures when using usual methods of dietary intake assessment. Self-reporting tools such as food frequency questionnaires, 24-hour recalls, and food diaries, that are commonly employed to estimate dietary consumption, introduce multiple errors, for example via conversion of food intake to nutrient exposure and via ignoring genetic polymorphisms affecting bioavailability. This may account for non-reliable results and lack of correlations between active ingredients and disease [2, 3]. One of the groups of dietary bioactive compounds with promising *in vitro* and *in vivo* effects well-studied in chronic diseases and health maintenance includes polyphenols [4-6]. Despite strong pre-clinical evidence, epidemiologic studies deliver inconsistent results for associations between polyphenol intake and disease risk in humans [5, 7-9].

Quantitative biochemical measurements that would reflect exposure to a certain group of compounds or foods including polyphenols have been under investigation [10]. Urine samples, blood draws, tissue biopsies, and stool specimens can be tested for metabolites, specific protein or gene expression level, or possibly status of epigenetic components, with varying capacities to distinguish acute versus chronic polyphenol intake [11]. Tracking of urinary polyphenols offers advantages relative to blood levels. Due to the short plasma half-life of polyphenol metabolites, blood levels may not consistently represent dietary intake or *in vivo* exposure. Urinary levels, on

the other hand, would be more representative of daily intake as opposed to chronic exposure [12, 13].

Myriad reviews assessing exposure detection indicate a vital need for new or improved methods to accurately measure chronic polyphenol intake in order to draw concrete conclusions about the impact of these dietary compounds in health and disease [11, 14]. Herein, we investigate whether polyphenols mediate molecular changes that could persist and be used as quantitative tools for chronic exposure assessment. We focus on resveratrol (RSV) and pterostilbene (PTS), two major polyphenols of the stilbenoid class, that are abundantly found in grapes and blueberries, respectively [15]. These polyphenols have raised considerable interest because of their possible role in beneficial disease outcomes such as prevention of degenerative diseases and anti-cancer action observed in intervention and preclinical studies [13, 16, 17]. Moreover, mechanistic studies indicate molecular changes, including epigenetics and specifically DNA methylation, that occur in response to the compounds [18-23]. We have recently shown that RSV and PTS modulate gene expression through altering DNA methylation patterns in gene regulatory regions in cancer cells [18]. DNA methylation is one of the components of the epigenome and is characterized by the addition of a methyl group to the 5th position of the cytosine ring within CpG dinucleotides in DNA [24]. This modification leads to changes in gene transcription that do not involve changes to the underlying DNA sequence [24]. Although DNA methylation is the gate-keeper of gene expression providing stable long-term regulation, it is also readily reversible and responsive to environmental factors, demonstrating potential as a useful tool to assess exposure to food bioactives [25]. Furthermore, changes in DNA methylation can easily and accurately be measured

using a straightforward laboratory technique called pyrosequencing which provides a percentage of methylation at a single CpG site resolution.

In the present study, we performed a genome-wide analysis of DNA methylation profiles in MCF10A mammary epithelial cells exposed to RSV and detected numerous subtle changes. Location of these RSV-mediated alterations in gene regulatory regions and enrichment with pathways associated with cardiovascular health, metabolism, cancer, and aging, might indicate a role in stabilizing control mechanisms to maintain a healthy phenotype. Statistically significant alterations of the highest magnitude were identified within regulatory regions of 8 genes, namely *KCNJ4*, *RNF169*, *BCHE*, *DAOA*, *HOXA9*, *RUNX3*, *KRTAP2-1*, and *TAGAP*. We further successfully quantitatively validated these changes by pyrosequencing in MCF10A cells exposed to RSV or PTS. Interestingly, the presence of changes within *Runx3* and *Kcnj4* was subsequently confirmed in peripheral blood, an easily accessible source of DNA, of healthy rats exposed to the compounds. Our study provides strong support for testing the utility of polyphenol-mediated changes in DNA methylation as quantitative measures of long-term dietary exposures in nutritional epidemiology and clinical trials.

MATERIALS AND METHODS

Cell culture and incubation with resveratrol (RSV) and pterostilbene (PTS)

Human mammary epithelial MCF10A cell line was purchased from ATCC (CRL-10317, USA). Please see Supporting Information for details on cell culture media and culture conditions. Resveratrol (RSV, Sigma-Aldrich, St. Louis, MO, USA) and pterostilbene (PTS, Cayman Chem., Ann Arbor, MI, USA) were resuspended in ethanol and 10 mM stock solutions were stored at -

20°C. Dilutions of the compounds were freshly prepared prior to adding to the cell medium. Cells were grown in a humidified atmosphere of 5% carbon dioxide at 37°C. 24 h prior to incubation with RSV or PTS, cells were plated at a density of 1-2 x 10^5 per a 10-cm tissue culture dish. Cells were exposed to different RSV or PTS concentrations ranging from 0 to 20 μM of RSV or to 15 μM of PTS for 4 days. Cells were then split 1:50, allowed to attach overnight and exposed to the compounds for additional 4 days (9-day exposure).

Illumina Infinium Human Methylation 450K BeadChip microarray

DNA from MCF10A control cells (incubated with ethanol) and cells cultured with RSV for 9 days was isolated using standard phenol:chloroform extraction protocol. Genomic DNA was processed for genome-wide DNA methylation analysis using Infinium HumanMethylation 450K BeadChip as described previously [18, 26]. Please see Supporting Information for details. The methylation score for each CpG was represented as a beta value according to the fluorescent intensity ratio with any values between 0 (unmethylated) and 1 (completely methylated). Raw microarray data and processed data are available from Gene Expression Omnibus (accession number GSE113299).

Animals and diets

Rats were treated strictly following the animal use protocol #1112000342 approved by the Institutional Animal Care and Use Committee at the involved institutions. A total of 18 male Fischer 344 rats, 4 weeks old, were obtained from Charles River (Indianapolis, IN, USA), housed 2/cage in a temperature-controlled (24°C) room with a 12-h light/dark cycle, and given ad libitum access to water and a chow diet [i.e., choline-sufficient amino acid-defined (CSAA) pelleted diet, Dyets Inc., Bethlehem, PA, USA]. After a week of acclimation period, five-week-old rats were

randomly divided into 3 groups each containing 6 animals (to reach statistical power) and fed the CSAA diet or a CSAA diet supplemented with resveratrol (CSAA+RSV, 1.2 g/kg of diet, 120 mg/kg of body weight per day) or pterostilbene (CSAA+PTS, 1.34 g/kg of diet, 134 mg/kg of body weight per day), pelleted at Dyets Inc. The compounds (BIOTANG Inc., Lexington, MA, USA) were used at equal molar concentrations. Following 20-day feeding period, retro-orbital Plexus sampling was used to collect blood from anesthetized rats. This method involves penetrating the retro-orbital plexus with a capillary tube to promote blood flow from the capillaries behind the eye. Whole blood amounts that did not exceed 10% of circulating blood volume based on body weight were collected from each rat into spray coated K2EDTA tubes (BD & Co,. Franklin Lakes, NJ, USA) and stored in -80°C until DNA and RNA extractions were performed.

In order to see a significant difference of 50% between groups at $P < 0.05$ when the variation of the endpoint is 25% of the sample mean, experiments need to have a power of 0.8. This requires a sample size of n=6 individual rats per group and was calculated using the biological and analytical variability from previous data [27, 28].

DNA extraction and pyrosequencing

DNA from human mammary epithelial MCF10A cells and rat peripheral blood was isolated using standard phenol:chloroform extraction protocol. DNA bisulfite conversion was performed as previously described [29, 30]. Specific regulatory gene sequences were amplified with HotStar Taq DNA polymerase (Qiagen) using biotinylated primers listed in Supplementary Table S1A (human) and S1B (rat). Pyrosequencing of the biotinylated DNA strands was performed in the PyroMarkTMQ24 instrument followed by data analysis using PyroMarkTMQ24 software (Biotage, Qiagen) [31].

RNA extraction and QPCR

Total RNA isolated using TRIzol (Roche Diagnostics) was processed for cDNA synthesis using 20U of AMV reverse transcriptase (Roche Diagnostics), as recommended by the manufacturer. Light Cycler 480 instrument (Roche) was used for QPCR reaction with the following cycles: denaturation at 95 °C for 10 min, amplification for 60 cycles at 95 °C for 10s, annealing temperature for 10s, 72 °C for 10s, and final extension at 72 °C for 10 min. Reaction mixture consisted of 2 µl of cDNA, 400 nM forward and reverse primers listed in Supplementary Table S1C and 10 µl of Light Cycler 480 SybrGreen I Master (Roche Diagnostics) in a final volume of 20 µl. Quantification of expression levels was performed using a standard curve and analyzed by the Roche LightCycler 480 software.

Statistical analysis

Raw methylation data from Human Methylation 450K microarrays were pre-processed using GenomeStudio and IMA (Illumina Methylation Analyzer for 450K, R/Bioconductor) including quality control, background correction, normalization, probe scaling, and adjustment for batch effect. Differential methylation analysis between sample groups was conducted using linear models (R Bioconductor package limma). Specifically, limma uses an empirical Bayes moderated t-test, computed for each probe, which is similar to a t-test, except that standard errors have been moderated using information from the full set of probes [32]. A methylation difference greater than 0.05 with a moderated t-test $P<0.05$ was considered statistically significant. Differentially methylated CpG sites were mapped into differentially methylated regions (DMRs) using DMRforPairs algorithm in R/Bioconductor [33, 34] (please see Supporting Information for details).

Statistical analysis of pyrosequencing and viability assays was performed using the unpaired *t*-test with two-tailed distribution. Each value represents the mean ± S.D. of three independent experiments. Mann-Whitney *U* test was used for statistical analysis of pyrosequencing in *in vivo* rat model with n=6 per group. The results were considered statistically significant when $P < 0.05$.

RESULTS

The landscape of DNA methylation in MCF10A human mammary epithelial cells upon resveratrol (RSV) exposure

The purpose of our study was to define polyphenol-mediated epigenetic response in MCF10A human immortalized mammary epithelial cells, used as an *in vitro* model of normal epithelial cells, and identify molecular changes occurring in response to polyphenols in normal cells. In our previous studies, we observed substantial changes in DNA methylation patterns in breast cancer cells treated with RSV or PTS [18-20]. Based on those pieces of evidence, we hypothesized that mere exposure to dietary polyphenols may leave a stable ”footprint” in normal human epithelial cells by remodeling the DNA methylation profile.

As follows, MCF10A mammary epithelial cells were incubated with 15μM RSV for 9 days to reflect prolonged exposure to stilbenoids. The dose of RSV was established based on its impact on cell growth (Supplementary Figure S1A). The 15μM dose of RSV was not toxic (< 10% of dead cells) and caused a negligible effect on the number of viable cells (<25% decrease in the number of viable cells) compared to control cells treated with ethanol (a vehicle control), as indicated by trypan blue exclusion test and further validated by MTT assay (Supplementary Figure S1A). A similar workflow was applied for PTS where 7μM concentration was selected for further

experiments (Supplementary Figure S1B). Simultaneously, these concentrations of RSV and PTS inhibited cancer cell growth by 50% with low cytotoxic effects as demonstrated in our previous study [18]. RSV-exposed and control MCF10A cells were subjected to Illumina 450K Methylation microarray to assess genome-wide DNA methylation effects of RSV exposure. The Illumina 450K microarray provides CpG-specific DNA methylation data for almost 500,000 CpG sequences that corresponds to 99% of all known protein coding genes (Please see Supporting Information for details).

We found 1,324 CpG sites differentially methylated upon 9-day exposure of MCF10A cells to 15μM RSV, as compared to control cells ($0.05 \leq$differential methylation≤ -0.05, $p<0.05$, limma t test). Chromosomal views of these differences were plotted using the Integrative Genomics Viewer (IGV) visualization tool (Figure 1A). Each vertical bar represents a single differentially methylated CpG site, with red indicating hypermethylation and blue indicating hypomethylation in RSV-exposed versus control cells. Among these changes, 889 CpG sites (67% of total number of changes) corresponding to 602 genes were hypermethylated whereas 435 CpG sites were hypomethylated and located within 305 genes (please see Supplementary Table S2 for differentially methylated CpG sites). The changes in DNA methylation were subtle ranging from 0.05 to 0.20 in differential methylation values. Only 15 hypermethylated CpG sites and 17 hypomethylated CpG sites were identified using a threshold for differential methylation ≥ 0.1 (Figure 1B). A heatmap in Figure 1C for 500 CpG sites with the highest change in DNA methylation between RSV and control further confirms mild alterations. It would suggest remodeling of the methylation patterns of normal cells upon RSV exposure rather than robust on/off switches that mediate a strong biological impact. RSV as a naturally-derived, bioactive

compound at physiologically relevant, non-toxic concentrations could possibly act through indirect mechanisms to induce subtle bidirectional changes in DNA methylation state of normal cells. Nearly half of differentially methylated sites are located in CpG islands (CpGIs), CpGI shores and shelves (Figure 1C). The distribution of hypermethylated and hypomethylated sites relative to TSS is similar with 30% of CpGs located in promoter regions (Figure 1C). Almost 30% of differentially methylated CpG loci are assigned to enhancer regions with equal distribution between hypermethylated and hypomethylated sites (Figure 1C).

Although our prediction was that RSV exposure leaves subtle marks in normal cells by slightly altering DNA methylation but does not have strong biological impact on corresponding genes, the location of changes in regions important for transcriptional regulation (e.g., promoters, enhancers, CpG islands) could indicate long-term regulation of the phenotype. Indeed, we found that differentially methylated genes are associated with cardiovascular and metabolic health (e.g., sodium-calcium exchanger SLC8A1, a family of calcium channel subunits CACNA, mitochondrial acetyl-CoA synthetase ACSS1/ACSS3, aminotransferase ABAT), immune functions (e.g., HLA class of major histocompatibility complex, interferon IFNA14), nervous system functions (e.g., synaptosome associated protein SNAP29, netrin NTN1 and netrin receptors UNC5 promoting neuronal cell survival), and cancer-relevant signaling such as cadherin and WNT pathways (e.g., numerous cadherins and protocadherins, protein kinase PRKCG, AXIN2, HDAC2, SFRP4) (Figure 1D). Alterations in DNA methylation mediated by RSV may therefore serve as a mechanism maintaining active or silenced transcription states crucial for a healthy phenotype.

These results led us to a question whether RSV treatment changes the epigenetic clock age of the normal cells. Maintaining a healthy phenotype could be associated with reversing age-related changes in the DNA methylation patterns. The epigenetic clock age is a type of a molecular age estimation method based on DNA methylation levels. We used Horvath's clock [35, 36] that includes 353 CpG sites, called epigenetic clock CpGs, whose methylation state is correlated with age. Among the 353 clock CpGs, there are 193 positively and 160 negatively correlated CpGs that become hypermethylated and hypomethylated with age, respectively. Using Horvath's R algorithms [35], we calculated DNA methylation age in control and RSV-treated MCF10A cells based on our Illumina 450K data. No significant alterations ($p=0.96199$) in the average DNA methylation age have been found between control (average DNA methylation age = 116.93±0.87) and RSV-exposed (average DNA methylation age = 117.01±2.39) MCF10A cells. Looking through all 353 CpGs, we found 20 sites of the epigenetic clock differentially methylated by RSV exposure. The highest change exceeding 0.05 was detected at cg18984151 located within C3orf75 (TMEM103) which is a subunit of RNA polymerase II (RNApolII) elongator complex acting as a histone acetyltransferase component of RNApolII. The locus is positively correlated with age and become hypermethylated with age. RSV treatment led to hypomethylation of this locus, possibly counteracting age-related alterations.

Differentially methylated CpG sites in response to resveratrol (RSV) in MCF10A human mammary epithelial cells are mapped into differentially methylated regions (DMRs)

In further bioinformatics analyses, we screened the genome-wide Illumina 450K data for differentially methylated regions (DMRs). DMRs are defined as regions that contain at least 4 CpG sites (Illumina probes) with a maximum distance of 200 bp between individual sites. Using R

bioconductor DMRforPairs package as described by Rijlaarsdam *et al.* [33], we found 30,417 DMRs among all samples (3 controls, 3 RSV-treated). Since DNA methylation changes in response to RSV are subtle, unsurprisingly we have not reached statistical significance for any of the DMRs. Importantly, there were 124 regions with median methylation levels (M-values) between the samples differed by at least 0.4 that is approximately equal to differential methylation 0.05 (delta beta value). To determine any DMRs between biological replicates, control samples and RSV-treated samples were separately computed in DMRforPairs. Any DMRs found between biological replicates were excluded from the 124 regions resulting in a final list of 80 unique regions differentially methylated in response to RSV in MCF10A cells (Supplementary Table S3).

These 80 regions are referred to as "relevant DMRs". As observed for differentially methylated CpG sites, 65% of relevant DMRs are located in regions with high regulatory role in gene transcription such as CpG islands and transcription start sites (TSS) (Figure 1E). It is reflected in the chromatin state analysis, where 52% of relevant DMRs are associated with promoters and only 12% with enhancers commonly located in gene body (Figure 1F). As described by Ernst *et al.* [34], we used data generated using 15-state ChromHMM model based on several chromatin marks (e.g., H3K4me3, H3K4me2, H3K4me1, H3K9ac, H3K27ac, H3K36me3, H4K20me1, H3K27me3 and H3K9me3) and selected Broad ChromHMM HMEC mammary epithelial cell track in UCSC Genome Browser (hg19) to determine chromatin states of relevant DMRs in breast cells. DMRs could correspond to the following chromatin states: active, weak or poised promoters, strong or weak enhancers, putative insulators, active or weak transcription, Polycomb-repressed regions or heterochromatin. Active promoters, strong enhancers and active transcription regions are linked to high expression levels, with the latter state determined based on the enrichment of histone marks along transcripts. Nearly 62% of relevant DMRs hypomethylated in response to RSV were

associated with active chromatin states whereas 79% of hypermethylated DMRs were characterized by chromatin states linked to low expression levels including weak and poised promoters, weak enhancers, weak transcription, repressed regions or heterochromatin (Figure 1F).

As for differentially methylated CpG sites upon exposure to RSV, functional pathway analysis for relevant DMRs confirms that RSV-mediated alterations may play a role in maintaining a healthy phenotype. Relevant DMRs are enriched for fatty acid metabolism, (e.g., acyl-CoA dehydrogenase ACADM catalyzing the initial step of fatty acid beta-oxidation, thioesterase PPT2 removing thioester-linked fatty acyl groups, dehydrogenase HSD17B12 catalyzing reactions of the long-chain fatty acids elongation cycle), branch-chain amino acid metabolism (e.g., dehydrogenase ACADM, malonyl-CoA synthetase ACSF3, carboxylase subunit PCCA), immune response to infections (e.g., HLA class of major histocompatibility complex, mRNA splicing regulators SRSF3 and ALYREF), oncogenic pathways (MAP2K3, KRAS, RASA1), and carbon metabolism linked to aging (e.g., ACADM, PCCA, pyruvate kinase PKLR) (Figure 1G).

Differential methylation occurring in response to resveratrol (RSV) or pterostilbene (PTS) in MCF10A mammary epithelial cells may serve as a quantitative measure of the dietary exposure

To investigate whether polyphenol-mediated changes in the DNA methylation patterns of normal cells could be quantitatively detectable, we selected 8 CpG sites for assessment of the methylation levels using pyrosequencing. Pyrosequencing is a quantitative method which measures the percentage of methylation at a single CpG site resolution and requires only PCR of bisulfite converted genomic DNA. In our selection, we took into account the magnitude of the difference in DNA methylation (differential methylation) between RSV-exposed and control cells, statistical

significance and location of change in gene regulatory regions. Hypermethylated CpG sites were located in the promoter or gene body of *KCNJ4* (potassium voltage-gated channel subfamily J member 4), *RNF169* (ring finger protein 169), *BCHE* (butyrylcholinesterase), and *DAOA* (D-amino acid oxidase activator) (Figure 2), whereas hypomethylated loci were located in the promoter of *HOXA9* (homeobox A9), *KRTAP2-1* (keratin associated protein 2-1), *TAGAP* (T-cell activation RhoGTPase activating protein), and CpG island in the body of *RUNX3* (runt-related transcription factor 3) (Figure 3). Functions of the selected genes reflected pathways observed in the integrative analysis of genes containing differentially methylated sites, such as nervous system functions (*KCNJ4*, *BCHE*, and *DAOA*), immune functions (*TAGAP*, and *HOXA9*), cancer and cancer-related signal transduction (*RNF169*, *HOXA9*, and *RUNX3*). Interestingly, the latter group contains a strong oncogene *RNF169* which negatively regulates DNA damage repair, and known tumor suppressor genes *HOXA9* and *RUNX3* which act as transcription factors regulating expression of a gene network linked to inflammatory response and signal transduction. While *RNF169* is hypermethylated (and potentially silenced) in response to RSV, *HOXA9* and *RUNX3* are hypomethylated (potentially activated).

For pyrosequencing, PCR primers were designed so that the tested fragment encompasses the CpG site differentially methylated on the microarray (CpG of interest, marked in square in charts in Figures 2 and 3) and if possible additional neighboring CpG sites (please see gene maps in Figure 2A and 3A). This allows us to obtain a pattern of methylation within a broader DNA region. We call the fragments tested by pyrosequencing “probes” and each probe corresponds to a single gene. Specifically, single CpG sites within *KCNJ4*, *RNF169*, *BCHE* and *DAOA*, all of which identified by Illumina 450K microarray as hypermethylated upon RSV exposure, showed increase in

methylation (Figure 2B). As observed in the array data, pyrosequencing revealed subtle RSV-mediated increases in DNA methylation within CpG sites located in these probes, ranging from 7 to 16% (Figure 2B). More profound changes in pyrosequenced regions were observed within probes hypomethylated in response to RSV, including *HOXA9, RUNX3, KRTAP2-1*, and *TAGAP* (Figure 3B). A robust 9-25% decrease in DNA methylation was detected throughout the entire region of *HOXA9* promoter spanning 13 CpG loci. On the other hand, significant hypomethylation was found mainly at CpG site covered on Illumina within *RUNX3* and *TAGAP*. A probe within *KRTAP2-1* showed the highest >30% decrease in DNA methylation at CpG#1 and CpG#2 (Figure 3B). Pyrosequencing successfully detected all differences in DNA methylation within 8 probes selected based on the microarray data. Thus, these subtle yet significant changes can be assessed by pyrosequencing, a straightforward technique that provides CpG-specific information in a timely manner and can be efficiently used to assess changes in methylation state in relation to exposure to environmental factors including diet [31].

A question arose whether epigenetic alterations are mediated only by RSV or if they are common to other compounds from stilbenoid class of polyphenols. We were especially interested in PTS. RSV is rapidly metabolized to glucuronide and sulfate conjugates that may limit its *in vivo* biological activity, compared to its analog, PTS. Upon oral administration of stilbenoids in *in vivo* models, PTS showed markedly greater total plasma levels of both the parent compound and its metabolites, having almost 80% bioavailability compared to 20% bioavailability of RSV [37, 38].

We therefore exposed MCF10A cells to PTS using the same schedule of treatments as for RSV followed by DNA methylation analysis within 8 selected probes using pyrosequencing. PTS was

used at 7 μM dose for 9 days. As described in the previous section, PTS at this concentration exerts cancer-specific effects with no toxicity towards normal cells and only a minor effect on the number of viable normal cells (<20% decrease in the number of viable cells) (Supplementary Figure S1B). Probes within *KCNJ4*, *RNF169*, *BCHE* and *DAOA* that were identified and validated in RSV-exposed cells as hypermethylated also showed significantly increased CpG-specific DNA methylation level by 8-34% in response to PTS (Figure 2C). Similarly, pyrosequencing of the tested regions within RSV-hypomethylated genes, *HOXA9*, *RUNX3*, *KRTAP2-1*, and *TAGAP*, demonstrated relevant 5-25% decrease in DNA methylation upon PTS exposure (Figure 3C). Collectively, we successfully confirmed using pyrosequencing that all 8 probes are targeted for DNA methylation changes in response to both RSV in PTS in mammary epithelial cells. The subtle changes in DNA methylation after PTS exposure presented similar trends of change as seen after RSV. Changes were slightly stronger for *KCNJ4* and *RNF169* at CpG of interest showing 18% higher increase in DNA methylation levels in response to PTS compared with RSV (Figure 2B and 2C).

The remodeled DNA methylation pattern at *Runx3* and *Kcnj4* promoters detectable in rat peripheral blood in response to exposure to stilbenoids

If the established quantitative molecular changes induced upon long-term exposure to stilbenoids could be detectable using non-invasive methods such as blood test, they would be of potential value in the development of biomarkers of exposure. We therefore tested whether our *in vitro* findings can be replicated in an *in vivo* animal model. In this model, rats were fed a chow CSAA diet or CSAA diet supplemented with RSV (CSAA+RSV, 1.2 g/kg of diet) or PTS (CSAA+PTS, 1.34 g/kg of diet) for 20 days. Compounds were used at equal molar concentrations and the selected

doses have been shown to be effective in attenuating cancer development based on previous studies in animal models [39-42]. At the 20 day-time point, whole blood was collected from 6 rats per group and subjected to DNA isolation, amplification of selected gene fragments, and pyrosequencing.

Four genes out of 8 validated probes in which methylation levels changed in MCF10A cells in response to RSV or PTS, were investigated in rats. The remaining genes were not well annotated in the rat genome and we were not able to obtain DNA sequence for these genes. Because fragments tested in the human genome did not match any sequence in the rat genome, we designed and optimized primers within promoters of *Kcnj4*, *Runx3*, *Bche*, and *Tagap*, in regions where CpG density was the highest (Figure 4A, Supplementary Figure S2). Based on pyrosequencing data, DNA methylation changes within 2 probes were upheld in whole blood of healthy rats upon 20-day RSV or PTS supplementation. Significant hypomethylation within *Runx3* was detected at CpGs #5 and #7 upon exposure to both RSV and PTS (Figure 4B and 4C). Hypermethylation within *Kcnj4* was observed at CpG #2 for RSV and both CpG #1 and #2 for PTS (Figure 4B and 4C). No significant changes in promoter methylation were identified by pyrosequencing in *Bche* or *Tagap* (Supplementary Figure S2).

Our present study establishes for the first time differences in DNA methylation at specific CpG sites after prolonged stilbenoid exposure that are detectable in normal cells and the whole blood of healthy rats. Upon validation in human cohorts, these novel DNA methylation probes may be used as candidates for developing quantitative exposure biomarkers with high application in epidemiologic studies where associations between the intake and disease risk are tested.

Subtle changes in DNA methylation may contribute to corresponding changes in gene expression: additional readout of exposure

In order to test whether the subtle changes in DNA methylation at the candidate genes affect transcriptional readout, we measured gene expression upon RSV treatment. RSV-mediated hypermethylation was reflected in downregulation of 3 out of 4 candidate genes, including *KCNJ4*, *RNF169*, and *DAOA* (trend of reduced expression for the latter) (Figure 5A). This would suggest that maintaining expression of those genes at low levels is beneficial for a healthy phenotype. Indeed, publicly available Oncomine expression data demonstrate up-regulation of *KCNJ4*, *RNF169*, and *DAOA* in breast cancer and other types of cancer compared to normal tissues, confirming potential cancer-promoting role of those genes (Figure 5B). On the other hand, 3 out of 4 genes hypomethylated upon RSV exposure, such as *RUNX3*, *KRTAP2-1*, and *TAGAP*, show increase in expression which suggests their potential health-promoting role (Figure 5C). This is further supported by down-regulation of those genes in breast tumors and other types of cancer compared to normal tissues as indicated by Oncomine expression data in clinical samples (Figure 5D). These results could imply that expression may be used as an additional measure of exposure to stilbenoids. However, not all the candidate genes are affected at the transcription level. Expression of *HOXA9*, a hypomethylated RSV target, stays unchanged (Figure 5C). It is possible that the slight remodeling of DNA methylation may not be enough for certain genes to affect transcription presumably due to co-existing chromatin structure. However, the altered methylation may help stabilize control mechanisms marking the genes to remain silenced (i.e., for cancer-promoting genes) or active (i.e., for guardian of a healthy phenotype). An interesting observation was noted for *BCHE* whose hypermethylation upon RSV treatment corresponded to increase in

expression rather than down-regulation as one would expect (Figure 5A). Additionally, Oncomine expression database clearly shows downregulation of *BCHE* in cancer compared to normal tissue and suggest a health-promoting role for *BCHE* (Figure 5B). An explanation may lie in the regulatory role of the CpG site where RSV-mediated hypermethylation occurs. The CpG site is located within the gene body as indicated in the gene map in Figure 2A. Increased methylation within body of the genes is associated with transcriptional activation and may constitute a signal for gene overexpression [43].

DISCUSSION

Improved quantitative evaluation methods of long-term exposure to dietary bioactive compounds are highly needed. Current measures of dietary exposures introduce inconsistencies in studies evaluating correlations between intake of various bioactive compounds and chronic disease. Polyphenols is a group of compounds with promising results in *in vitro* and *in vivo* studies [4-6], however without clear evidence from epidemiologic investigations [5, 7-9].

If we can provide adequate quantitative biomarkers, we may be able to accurately assess the importance of polyphenol intake in health maintenance and prevention of chronic diseases [11, 14]. An excellent example of how measurement methods influence interpretation of results is a study evaluating polyphenol intake among over 800 older adults living in the Chianti region of Tuscany in Italy [3, 44]. No significant correlations between polyphenol consumption and longevity were found when the intake measured based on dietary questionnaires was taken into account. Interestingly, using total urinary polyphenol concentration as a proxy measure of the intake showed that participants with the highest urinary polyphenol concentration had a lower

mortality rate than individuals with the lowest concentration. The results led to an important conclusion that high dietary intake of polyphenols may be associated with longevity and emphasized the importance of the accurate assessment of the intake.

While urinary metabolites reflect daily consumption, blood levels will be representative of just an hourly intake. Measures of chronic exposure to polyphenols are largely missing. In the present study, we investigated two polyphenols of the stilbenoid class, RSV and PTS, and their potential in inducing molecular changes in normal cells that would be informative of the intake. RSV is highly absorbed by humans but is lowly bioavailable due to its rapid conversion to metabolites [37, 38]. On the other hand, PTS, a naturally occurring dimethylated analog of RSV, is a highly bioavailable [37, 38]. We and others previously observed epigenetic changes, specifically alterations in DNA methylation, at candidate gene loci in human cancer cells treated with RSV or PTS [19-21]. Our recent study further demonstrates remodeling of the DNA methylation patterns in breast cancer cells exposed to polyphenols [18]. These pieces of evidence together with dynamic nature and responsiveness of DNA methylation to environmental factors make it highly probable that normal cells may also respond to long-term exposure to polyphenols by inducing alterations in DNA methylation patterns. Contrary to cancer cells, changes in normal cells would be subtle and without strong biological effects. There is evidence that in normal cells dynamics of DNA methylation allows for long-lasting changes upon a wide range of exogenous and endogenous exposures including toxicants, nutrients, behavioral and social stimuli, leaving so called "methylation memory" [45]. Indeed, we found in the present investigation that exposure of MCF10A mammary epithelial cells to RSV results in alterations at 1,324 CpG sites, of which only 32 sites have a magnitude of the difference in methylation greater than 0.1 (Figure 1). These

changes are induced at non-cytotoxic doses of RSV which supports their value as a “footprint” of exposure rather than a biologically relevant intervention, not necessarily desirable in normal cells. On the other hand, although without the acute biological response, the observed effects on the epigenome might be associated long-term with maintenance of a healthy phenotype. This intriguing hypothesis requires further investigation in future studies.

Although mechanisms underlying stilbenoid-mediated remodeling of DNA methylation patterns remain to be elucidated, the mode of action marking genes by subtle hypermethylation and hypomethylation in the normal cell model seems promising for providing relevant new insights into associations between the epigenome, polyphenol exposure, and health status. We selected 8 probes corresponding to 8 genes, including *KCNJ4*, *RNF169*, *BCHE*, *DAOA*, *HOXA9*, *RUNX3*, *KRTAP2-1*, and *TAGAP*, for validation by pyrosequencing as a straightforward laboratory technique to detect changes in DNA methylation with high reproducibility. All probes showed a high concordance between microarray and pyrosequencing (Figure 2 and 3). We also confirmed that exposure to RSV analog, PTS, causes similar changes in DNA methylation at selected probes (Figure 2C and 3C). Hence, these subtle but detectable changes in the DNA methylation pattern of normal epithelial cells exposed to stilbenoids could have potential to be utilized as a valuable substitute or complementary tool in quantification of polyphenol exposure.

Such an assessment approach would be of value only if minimally-invasive specimens serve as a source of DNA. There is evidence of using blood to detect changes in DNA methylation for cancer risk prediction or cancer early detection [46, 47]. For instance, hypomethylation of BLCA-4 repeats detectable in blood cell DNA was associated with higher risk of bladder cancer [48].

Methylation within *CNKSR1*, *IFI44L*, *PENK*, and *WNK2* as well as lack of methylation within *TPO* and *MYT1L* in white blood cell DNA was demonstrated as a potential biomarker for risk prediction of HCC [49-51]. Similar association was found in breast cancer where methylation in *ATM* intragenic loci was linked to high cancer risk [52]. We therefore tested whether the changes in DNA methylation occurring in response to stilbenoids in MCF10A cells are also present in blood of healthy animals on diets supplemented with RSV or PTS. Out of 8 probes established based on our *in vitro* data, 4 probes were found in the rat genome. Of those 4 probes, CpG loci in promoters of *Runx3* and *Kcnj4* were verified and confirmed to have an altered DNA methylation status upon exposure to stilbenoids in rat blood DNA (Figure 4).

Since our studies demonstrate subtle changes in DNA methylation, a question arises whether such small changes can impact transcriptional activity of genes. We found that most but not all of the selected genes were differentially expressed upon stilbenoid-mediated subtle changes in DNA methylation (Figure 5). This clearly indicates that these gentle alterations in DNA methylation can act as a guardian of active or silenced chromatin state, and would explain lack of a strong biological response of normal cells to stilbenoids. This suggestion is further supported by the genome-wide characterization of RSV-mediated changes. We found that differentially methylated CpG sites and corresponding DMRs are located mostly in promoters, CpG islands, and enhancers; regions of transcriptional regulation (Figure 1). Interestingly, genes encompassing differentially methylated sites or regions were enriched with pathways associated with cardiovascular health, metabolism, cancer, and aging, indicating a role in stabilizing control mechanisms to maintain a healthy phenotype.

Our study is the first to establish DNA methylation changes in normal cells and blood DNA of healthy animals which occur upon prolonged exposure to stilbenoid compounds, RSV and PTS. Such quantitative molecular changes possess high potential to be developed into biomarkers of exposure to dietary polyphenols after validation in humans and verification in large cohorts. Recent guidelines for biomarkers in nutritional epidemiology emphasize that combining dietary reporting tools with molecular biomarkers of exposure like those proposed in our study can produce complementary information and increase accuracy of studied associations between diet and health status [10].

AUTHOR CONTRIBUTIONS

M.B., K.L., and B.S. conceived and design the study and performed the experiments. The data were analyzed by all the Authors. M.S. was specifically involved in bioinformatics analysis of the genome-wide data. M.B., K.L., and B.S. wrote the manuscript, and M.S. reviewed it.

ACKNOWLEDGEMENTS

This research was supported by the University of British Columbia VP Academic (10R76632), Purdue University Center for Cancer Research (Biological Evaluation Shared Resource, National Institutes of Health P30CA023168), and USDA National Institute of Food and Agriculture (1005656) Awards, granted to B.S.

The Authors declare no conflict of interest.

REFERENCES

[1] Tarasuk, V. S., Brooker, A. S., Interpreting epidemiologic studies of diet-disease relationships. *The Journal of nutrition* 1997, *127,* 1847-1852.

[2] Tucker, K. L., Assessment of usual dietary intake in population studies of gene-diet interaction. *Nutrition, metabolism, and cardiovascular diseases : NMCD* 2007, *17*, 74-81.
[3] Shim, C. S., Moon, J. H., Cho, Y. D., Lee, M. S., Jeon, H. B., Jin, S. Y., Lee, H. K., Neuroendocrine carcinoma of the ampulla of vater. *Gastrointestinal endoscopy* 2000, *51*, 593.
[4] Sinha, D., Sarkar, N., Biswas, J., Bishayee, A., Resveratrol for breast cancer prevention and therapy: Preclinical evidence and molecular mechanisms. *Seminars in cancer biology* 2016, *40-41*, 209-232.
[5] Grosso, G., Buscemi, S., Galvano, F., Mistretta, A., Marventano, S., La Vela, V., Drago, F., Gangi, S., Basile, F., Biondi, A., Mediterranean diet and cancer: epidemiological evidence and mechanism of selected aspects. *BMC surgery* 2013, *13 Suppl 2*, S14.
[6] Aires, V., Delmas, D., Common pathways in health benefit properties of RSV in cardiovascular diseases, cancers and degenerative pathologies. *Current pharmaceutical biotechnology* 2015, *16*, 219-244.
[7] Chao, C., Li, Q., Zhang, F., White, E., Alcohol consumption and risk of lung cancer in the VITamins And Lifestyle Study. *Nutrition and cancer* 2011, *63*, 880-888.
[8] Chao, C., Haque, R., Caan, B. J., Poon, K. Y., Tseng, H. F., Quinn, V. P., Red wine consumption not associated with reduced risk of colorectal cancer. *Nutrition and cancer* 2010, *62*, 849-855.
[9] Sutcliffe, S., Giovannucci, E., Leitzmann, M. F., Rimm, E. B., Stampfer, M. J., Willett, W. C., Platz, E. A., A prospective cohort study of red wine consumption and risk of prostate cancer. *International journal of cancer. Journal international du cancer* 2007, *120*, 1529-1535.
[10] Corella, D., Ordovas, J. M., Biomarkers: background, classification and guidelines for applications in nutritional epidemiology. *Nutricion hospitalaria* 2015, *31 Suppl 3*, 177-188.
[11] Zamora-Ros, R., Touillaud, M., Rothwell, J. A., Romieu, I., Scalbert, A., Measuring exposure to the polyphenol metabolome in observational epidemiologic studies: current tools and applications and their limits. *The American journal of clinical nutrition* 2014, *100*, 11-26.
[12] Perez-Jimenez, J., Hubert, J., Hooper, L., Cassidy, A., Manach, C., Williamson, G., Scalbert, A., Urinary metabolites as biomarkers of polyphenol intake in humans: a systematic review. *The American journal of clinical nutrition* 2010, *92*, 801-809.
[13] Arts, I. C., Hollman, P. C., Polyphenols and disease risk in epidemiologic studies. *The American journal of clinical nutrition* 2005, *81*, 317S-325S.
[14] Spencer, J. P., Abd El Mohsen, M. M., Minihane, A. M., Mathers, J. C., Biomarkers of the intake of dietary polyphenols: strengths, limitations and application in nutrition research. *The British journal of nutrition* 2008, *99*, 12-22.
[15] Burns, J., Yokota, T., Ashihara, H., Lean, M. E., Crozier, A., Plant foods and herbal sources of resveratrol. *Journal of agricultural and food chemistry* 2002, *50*, 3337-3340.
[16] Manach, C., Williamson, G., Morand, C., Scalbert, A., Remesy, C., Bioavailability and bioefficacy of polyphenols in humans. I. Review of 97 bioavailability studies. *The American journal of clinical nutrition* 2005, *81*, 230S-242S.
[17] Williamson, G., Manach, C., Bioavailability and bioefficacy of polyphenols in humans. II. Review of 93 intervention studies. *The American journal of clinical nutrition* 2005, *81*, 243S-255S.
[18] Lubecka, K., Kurzava, L., Flower, K., Buvala, H., Zhang, H., Teegarden, D., Camarillo, I., Suderman, M., Kuang, S., Andrisani, O., Flanagan, J. M., Stefanska, B., Stilbenoids remodel the DNA methylation patterns in breast cancer cells and inhibit oncogenic NOTCH signaling

through epigenetic regulation of MAML2 transcriptional activity. *Carcinogenesis* 2016, *37*, 656-668.
[19] Stefanska, B., Rudnicka, K., Bednarek, A., Fabianowska-Majewska, K., Hypomethylation and induction of retinoic acid receptor beta 2 by concurrent action of adenosine analogues and natural compounds in breast cancer cells. *European journal of pharmacology* 2010, *638*, 47-53.
[20] Stefanska, B., Salame, P., Bednarek, A., Fabianowska-Majewska, K., Comparative effects of retinoic acid, vitamin D and resveratrol alone and in combination with adenosine analogues on methylation and expression of phosphatase and tensin homologue tumour suppressor gene in breast cancer cells. *The British journal of nutrition* 2012, *107*, 781-790.
[21] Papoutsis, A. J., Borg, J. L., Selmin, O. I., Romagnolo, D. F., BRCA-1 promoter hypermethylation and silencing induced by the aromatic hydrocarbon receptor-ligand TCDD are prevented by resveratrol in MCF-7 cells. *The Journal of nutritional biochemistry* 2012, *23*, 1324-1332.
[22] Lou, X. D., Wang, H. D., Xia, S. J., Skog, S., Sun, J., Effects of resveratrol on the expression and DNA methylation of cytokine genes in diabetic rat aortas. *Archivum immunologiae et therapiae experimentalis* 2014, *62*, 329-340.
[23] Gracia, A., Elcoroaristizabal, X., Fernandez-Quintela, A., Miranda, J., Bediaga, N. G., M, M. d. P., Rimando, A. M., Portillo, M. P., Fatty acid synthase methylation levels in adipose tissue: effects of an obesogenic diet and phenol compounds. *Genes & nutrition* 2014, *9*, 411.
[24] Jones, P. A., Issa, J. P., Baylin, S., Targeting the cancer epigenome for therapy. *Nature reviews. Genetics* 2016, *17*, 630-641.
[25] Lim, U., Song, M. A., Dietary and lifestyle factors of DNA methylation. *Methods in molecular biology* 2012, *863*, 359-376.
[26] Cheishvili, D., Stefanska, B., Yi, C., Li, C. C., Yu, P., Arakelian, A., Tanvir, I., Khan, H. A., Rabbani, S., Szyf, M., A common promoter hypomethylation signature in invasive breast, liver and prostate cancer cell lines reveals novel targets involved in cancer invasiveness. *Oncotarget* 2015, *6*, 33253-33268.
[27] Stefanska, B., Cheishvili, D., Suderman, M., Arakelian, A., Huang, J., Hallett, M., Han, Z. G., Al-Mahtab, M., Akbar, S. M., Khan, W. A., Raqib, R., Tanvir, I., Khan, H. A., Rabbani, S. A., Szyf, M., Genome-wide study of hypomethylated and induced genes in patients with liver cancer unravels novel anticancer targets. *Clinical cancer research : an official journal of the American Association for Cancer Research* 2014, *20*, 3118-3132.
[28] Siddiqui, R. A., Harvey, K. A., Walker, C., Altenburg, J., Xu, Z., Terry, C., Camarillo, I., Jones-Hall, Y., Mariash, C., Characterization of synergistic anti-cancer effects of docosahexaenoic acid and curcumin on DMBA-induced mammary tumorigenesis in mice. *BMC cancer* 2013, *13*, 418.
[29] Stefanska, B., Huang, J., Bhattacharyya, B., Suderman, M., Hallett, M., Han, Z. G., Szyf, M., Definition of the landscape of promoter DNA hypomethylation in liver cancer. *Cancer research* 2011, *71*, 5891-5903.
[30] Colella, S., Shen, L., Baggerly, K. A., Issa, J. P., Krahe, R., Sensitive and quantitative universal Pyrosequencing methylation analysis of CpG sites. *BioTechniques* 2003, *35*, 146-150.
[31] Tost, J., Gut, I. G., DNA methylation analysis by pyrosequencing. *Nature protocols* 2007, *2*, 2265-2275.
[32] Wilhelm-Benartzi, C. S., Koestler, D. C., Karagas, M. R., Flanagan, J. M., Christensen, B. C., Kelsey, K. T., Marsit, C. J., Houseman, E. A., Brown, R., Review of processing and analysis methods for DNA methylation array data. *British journal of cancer* 2013, *109*, 1394-1402.

[33] Rijlaarsdam, M. A., van der Zwan, Y. G., Dorssers, L. C., Looijenga, L. H., DMRforPairs: identifying differentially methylated regions between unique samples using array based methylation profiles. *BMC bioinformatics* 2014, *15*, 141.
[34] Ernst, J., Kheradpour, P., Mikkelsen, T. S., Shoresh, N., Ward, L. D., Epstein, C. B., Zhang, X., Wang, L., Issner, R., Coyne, M., Ku, M., Durham, T., Kellis, M., Bernstein, B. E., Mapping and analysis of chromatin state dynamics in nine human cell types. *Nature* 2011, *473*, 43-49.
[35] Horvath, S., DNA methylation age of human tissues and cell types. *Genome biology* 2013, *14*, R115.
[36] Horvath, S., Erratum to: DNA methylation age of human tissues and cell types. *Genome biology* 2015, *16*, 96.
[37] Kapetanovic, I. M., Muzzio, M., Huang, Z., Thompson, T. N., McCormick, D. L., Pharmacokinetics, oral bioavailability, and metabolic profile of resveratrol and its dimethylether analog, pterostilbene, in rats. *Cancer chemotherapy and pharmacology* 2011, *68*, 593-601.
[38] Walle, T., Hsieh, F., DeLegge, M. H., Oatis, J. E., Jr., Walle, U. K., High absorption but very low bioavailability of oral resveratrol in humans. *Drug metabolism and disposition: the biological fate of chemicals* 2004, *32*, 1377-1382.
[39] Kiskova, T., Ekmekcioglu, C., Garajova, M., Orendas, P., Bojkova, B., Bobrov, N., Jager, W., Kassayova, M., Thalhammer, T., A combination of resveratrol and melatonin exerts chemopreventive effects in N-methyl-N-nitrosourea-induced rat mammary carcinogenesis. *European journal of cancer prevention : the official journal of the European Cancer Prevention Organisation* 2012, *21*, 163-170.
[40] Sengottuvelan, M., Viswanathan, P., Nalini, N., Chemopreventive effect of trans-resveratrol--a phytoalexin against colonic aberrant crypt foci and cell proliferation in 1,2-dimethylhydrazine induced colon carcinogenesis. *Carcinogenesis* 2006, *27*, 1038-1046.
[41] Paul, S., DeCastro, A. J., Lee, H. J., Smolarek, A. K., So, J. Y., Simi, B., Wang, C. X., Zhou, R., Rimando, A. M., Suh, N., Dietary intake of pterostilbene, a constituent of blueberries, inhibits the beta-catenin/p65 downstream signaling pathway and colon carcinogenesis in rats. *Carcinogenesis* 2010, *31*, 1272-1278.
[42] Jeyabalan, J., Aqil, F., Munagala, R., Annamalai, L., Vadhanam, M. V., Gupta, R. C., Chemopreventive and therapeutic activity of dietary blueberry against estrogen-mediated breast cancer. *Journal of agricultural and food chemistry* 2014, *62*, 3963-3971.
[43] Yang, X., Han, H., De Carvalho, D. D., Lay, F. D., Jones, P. A., Liang, G., Gene body methylation can alter gene expression and is a therapeutic target in cancer. *Cancer cell* 2014, *26*, 577-590.
[44] Warden, B. A., Smith, L. S., Beecher, G. R., Balentine, D. A., Clevidence, B. A., Catechins are bioavailable in men and women drinking black tea throughout the day. *The Journal of nutrition* 2001, *131*, 1731-1737.
[45] Vineis, P., Chatziioannou, A., Cunliffe, V. T., Flanagan, J. M., Hanson, M., Kirsch-Volders, M., Kyrtopoulos, S., Epigenetic memory in response to environmental stressors. *FASEB journal : official publication of the Federation of American Societies for Experimental Biology* 2017, *31*, 2241-2251.
[46] Friso, S., Udali, S., Guarini, P., Pellegrini, C., Pattini, P., Moruzzi, S., Girelli, D., Pizzolo, F., Martinelli, N., Corrocher, R., Olivieri, O., Choi, S. W., Global DNA hypomethylation in peripheral blood mononuclear cells as a biomarker of cancer risk. *Cancer epidemiology, biomarkers & prevention : a publication of the American Association for Cancer Research, cosponsored by the American Society of Preventive Oncology* 2013, *22*, 348-355.

[47] Huang, W. Y., Su, L. J., Hayes, R. B., Moore, L. E., Katki, H. A., Berndt, S. I., Weissfeld, J. L., Yegnasubramanian, S., Purdue, M. P., Prospective study of genomic hypomethylation of leukocyte DNA and colorectal cancer risk. *Cancer epidemiology, biomarkers & prevention : a publication of the American Association for Cancer Research, cosponsored by the American Society of Preventive Oncology* 2012, *21*, 2014-2021.
[48] Ji, H. X., Zhao, Q., Pan, J. H., Shen, W. H., Chen, Z. W., Zhou, Z. S., Association of BLCA-4 hypomethylation in blood leukocyte DNA and the risk of bladder cancer in a Chinese population. *Pathology oncology research : POR* 2013, *19*, 205-210.
[49] Kao, W. Y., Yang, S. H., Liu, W. J., Yeh, M. Y., Lin, C. L., Liu, C. J., Huang, C. J., Lin, S. M., Lee, S. D., Chen, P. J., Yu, M. W., Genome-wide identification of blood DNA methylation patterns associated with early-onset hepatocellular carcinoma development in hepatitis B carriers. *Molecular carcinogenesis* 2017, *56*, 425-435.
[50] Wu, H. C., Shen, J., Yang, H. I., Tsai, W. Y., Chen, C. J., Santella, R. M., Blood DNA methylation markers in prospectively identified hepatocellular carcinoma cases and controls from Taiwan. *World journal of hepatology* 2016, *8*, 301-306.
[51] Liu, Z., Yan, H., Zhang, J., Blood DNA methylation markers in potentially identified Chinese patients with hepatocellular carcinoma. *Pakistan journal of pharmaceutical sciences* 2016, *29*, 1451-1456.
[52] Brennan, K., Garcia-Closas, M., Orr, N., Fletcher, O., Jones, M., Ashworth, A., Swerdlow, A., Thorne, H., Investigators, K. C., Riboli, E., Vineis, P., Dorronsoro, M., Clavel-Chapelon, F., Panico, S., Onland-Moret, N. C., Trichopoulos, D., Kaaks, R., Khaw, K. T., Brown, R., Flanagan, J. M., Intragenic ATM methylation in peripheral blood DNA as a biomarker of breast cancer risk. *Cancer research* 2012, *72*, 2304-2313.

FIGURE LEGENDS

Figure 1. Subtle changes of the landscape of DNA methylation in MCF10A human mammary epithelial cells upon exposure to resveratrol (RSV). The genome-wide DNA methylation patterns were delineated using Illumina 450K microarray platform in MCF10A cells incubated with RSV at 15 μM for 9 days vs. MCF10A cells treated with ethanol as a vehicle control. (A) Chromosomal view of differentially methylated CpG sites ($P<0.05$, limma t-test). Each CpG site with significant difference of at least 0.05 between RSV-treated and control untreated cells was plotted into a bar track of a chromosomal view using Integrative Genomics Viewer (IGV) visualization tool. Each bar corresponds to a single, differentially methylated CpG site, with red indicating hypermethylation and blue indicating hypomethylation in RSV vs. control (RSV minus Ctrl). (B) Pie charts of statistically significant differentially methylated CpG sites with the

difference of at least 0.05 or 0.1 between RSV-exposed and control MCF10A cells ($P<0.05$, limma t-test). Diff. refers to differential methylation (delta beta, RSV minus control). (C) A heatmap showing methylation levels (beta values) for the top 500 differentially methylated CpG loci ($P<0.05$, limma t-test). The heatmap presents subtle pattern separating data sets obtained from controls (untreated MCF10A cells) and RSV-exposed cells. Columns "a-c" show classification of the CpG sites according to their location relative to transcription start site (TSS) (a), CpG islands (b) and enhancer region (c). (D) Pathways associated with genes containing CpG loci that are differentially methylated upon exposure of MCF10A cells to RSV. Integrative pathway analysis was performed using DAVID knowledgebase. (E) Differentially methylated regions (DMRs) were determined using DMRforPairs algorithm in R/Bioconductor. Regions with median methylation levels (M-values) between the samples differed at least by 0.4 that is approximately equal to differential methylation 0.05 (delta beta value) were considered relevant. Their location relative to transcription start site (TSS), CpG islands and body of the genes is depicted in the pie chart. (F) Chromatin states associated with relevant DMRs were determined using broad ChromHMM HMEC track in UCSC Genome Browser (hg19). DMRs could correspond to the following chromatin states: active, weak or poised promoters, strong or weak enhancers, putative insulators, active or weak transcription, Polycomb-repressed regions or heterochromatin. Active promoters, strong enhancers and active transcription regions are linked to high expression levels, with the latter state determined based on the enrichment of histone marks along transcripts. Weak or poised promoters, weak enhancers, weak transcription, Polycomb-repressed regions or heterochromatin, in turn, are linked to low expression. (G) Genes of overlapping transcripts were determined for the exact DMR region and within a margin of 10000 bp of the region. Pathways associated with genes for all relevant DMRs were determined using DAVID knowledgebase.

Figure 2. Stilbenoid-mediated hypermethylation of CpG loci within *KCNJ4, RNF169, BCHE,* and *DAOA* in human mammary epithelial cells. Four hypermethylated CpG sites corresponding to 4 genes (probes) in response to resveratrol (RSV) in MCF10A human mammary epithelial cells were identified based on Illumina 450K microarray. The difference in DNA methylation and statistical significance were taken into account in the selection. Each region encompasses a differentially methylated CpG site covered on Illumina 450K microarray (marked in square). The exact position of validated CpG sites relative to transcription start site (TSS) is shown in gene maps (A). The tested region is shaded, and pyrosequenced CpGs are circled and numbered. The putative transcription factor binding sites are indicated as predicted by TransFac. The difference in DNA methylation status at the selected CpG sites was quatitatively validated by pyrosequencing in MCF10A cells exposed for 9 days to 15 μM RSV (B) and 7 μM pterostilbene (PTS) (C), a dimethylated analog of RSV. Average methylation status of CpG site covered on Illumina and neighboring CpG sites in the tested fragment of *KCNJ4*, *RNF169*, *BCHE*, and *DAOA* is displayed. All results represent mean ± S.D. of three independent experiments; ***$P < 0.001$, **$P < 0.01$, *$P < 0.05$.

Figure 3. Stilbenoid-mediated hypomethylation of CpG loci within *HOXA9, RUNX3, KRTAP2-1,* and *TAGAP* in human mammary epithelial cells. Four hypomethylated CpG sites corresponding to 4 genes (probes) in response to resveratrol (RSV) in MCF10A human mammary epithelial cells were identified based on Illumina 450K microarray. The difference in DNA methylation and statistical significance were taken into account in the selection. Each region

encompasses a hypomethylated CpG site covered on Illumina 450K microarray (marked in square). The exact position of validated CpG sites relative to transcription start site (TSS) is shown in gene maps (A). The tested region is shaded, and pyrosequenced CpGs are circled and numbered. The putative transcription factor binding sites are indicated as predicted by TransFac. The difference in DNA methylation status at the selected CpG sites was quatitatively validated by pyrosequencing in MCF10A cells exposed for 9 days to 15 μM RSV (B) and 7 μM pterostilbene (PTS) (C), a dimethylated analog of RSV. Average methylation status of CpG site covered on Illumina and neighboring CpG sites in the tested fragment of *HOXA9, RUNX3*, *KRTAP2-1*, and *TAGAP* is displayed. All results represent mean ± S.D. of three independent experiments; ***$P < 0.001$, **$P < 0.01$, *$P < 0.05$.

Figure 4. Resveratrol (RSV) and pterostilbene (PTS) change methylation states of CpG sites located in regulatory regions of *Runx3* and *Kcnj4* in rat peripheral blood. Fischer 344 rats were exposed for 20 days to chow diet [choline sufficient amino acid defined (CSAA) diet] supplemented with resveratrol (CSAA+RSV) or pterostilbene (CSAA+PTS). Collected peripheral blood was subjected to DNA isolation followed by DNA methylation analysis by pyrosequencing at loci identified in *in vitro* MCF10A experiment. DNA methylation changes were detected within *Runx3* and *Kcnj4* regulatory regions. The exact position of tested CpG sites is shown in gene maps (A). Average methylation status of CpG sites in the tested fragments of *Runx3* and *Kcnj4* in rats on CSAA diet and CSAA diet supplemented with RSV or PTS is displayed in panels B and C. All results represent mean ± SEM of n=6 per group; ***$P < 0.001$, **$P < 0.01$, *$P < 0.05$.

Figure 5. Resveratrol (RSV)-mediated changes in expression of genes which responded to exposure to stilbenoids with subtle alterations in DNA methylation: additional readout of exposure. (A,C) Effect of 9-day exposure of MCF10A mammary epithelium cells to 15 μM RSV on expression of *KCNJ4*, *RNF169*, *BCHE*, and *DAOA* as well as *HOXA9*, *RUNX3*, *KRTAP2-1*, and *TAGAP* that were respectively hypermethylated or hypomethylated by stilbenoids. Gene expression was determined by QPCR. All results represent mean ± S.D. of three independent experiments; ***$P < 0.001$, **$P < 0.01$, *$P < 0.05$. (B,D) Cancer gene expression microarray data for *KCNJ4*, *RNF169*, *BCHE*, and *DAOA* as well as *HOXA9*, *RUNX3*, *KRTAP2-1*, and *TAGAP* that were respectively hypermethylated or hypomethylated by stilbenoids. The normal versus tumor gene expression data were obtained from Oncomine and are presented as $\log_2$-transformed median centered per array, and SD-normalized to 1 per array. All the presented changes are statistically significant ($P < 0.05$).

Figure 1

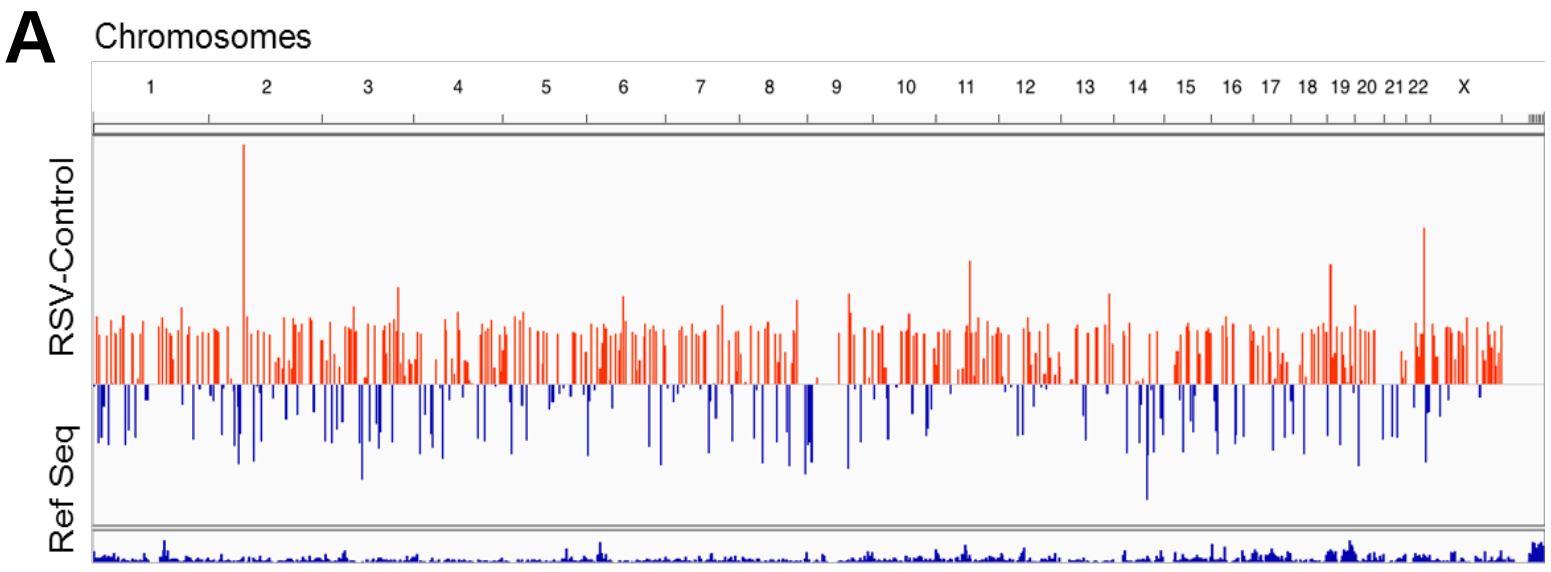
A
Chromosomes
1 2 3 4 5 6 7 8 9 10 11 12 13 14 15 16 17 18 19 20 21 22 X
RSV-Control
Ref Seq

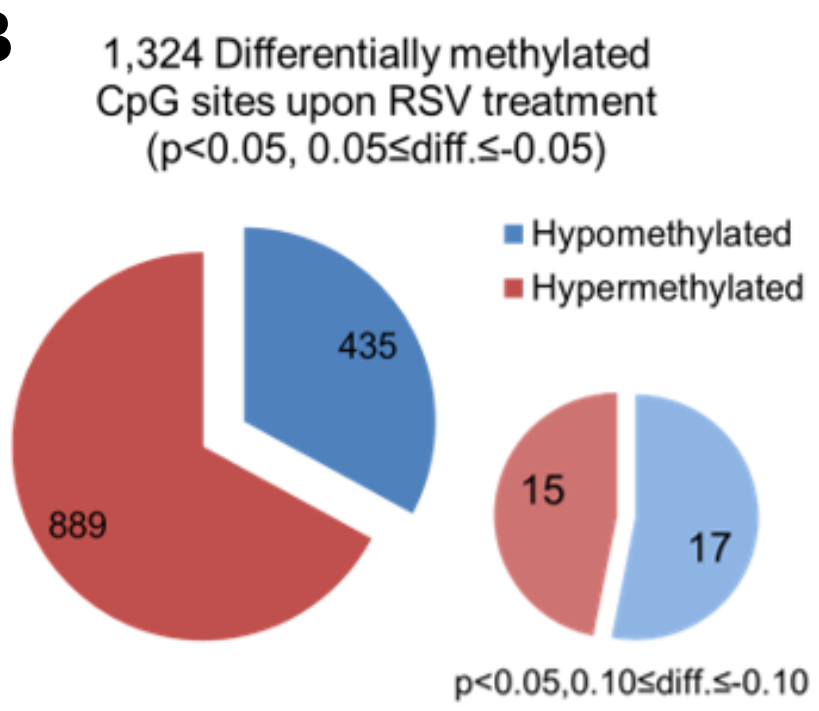
B
1,324 Differentially methylated CpG sites upon RSV treatment (p<0.05, 0.05≤diff.≤-0.05)
Hypomethylated
Hypermethylated
435
889
15
17
p<0.05,0.10≤diff.≤-0.10

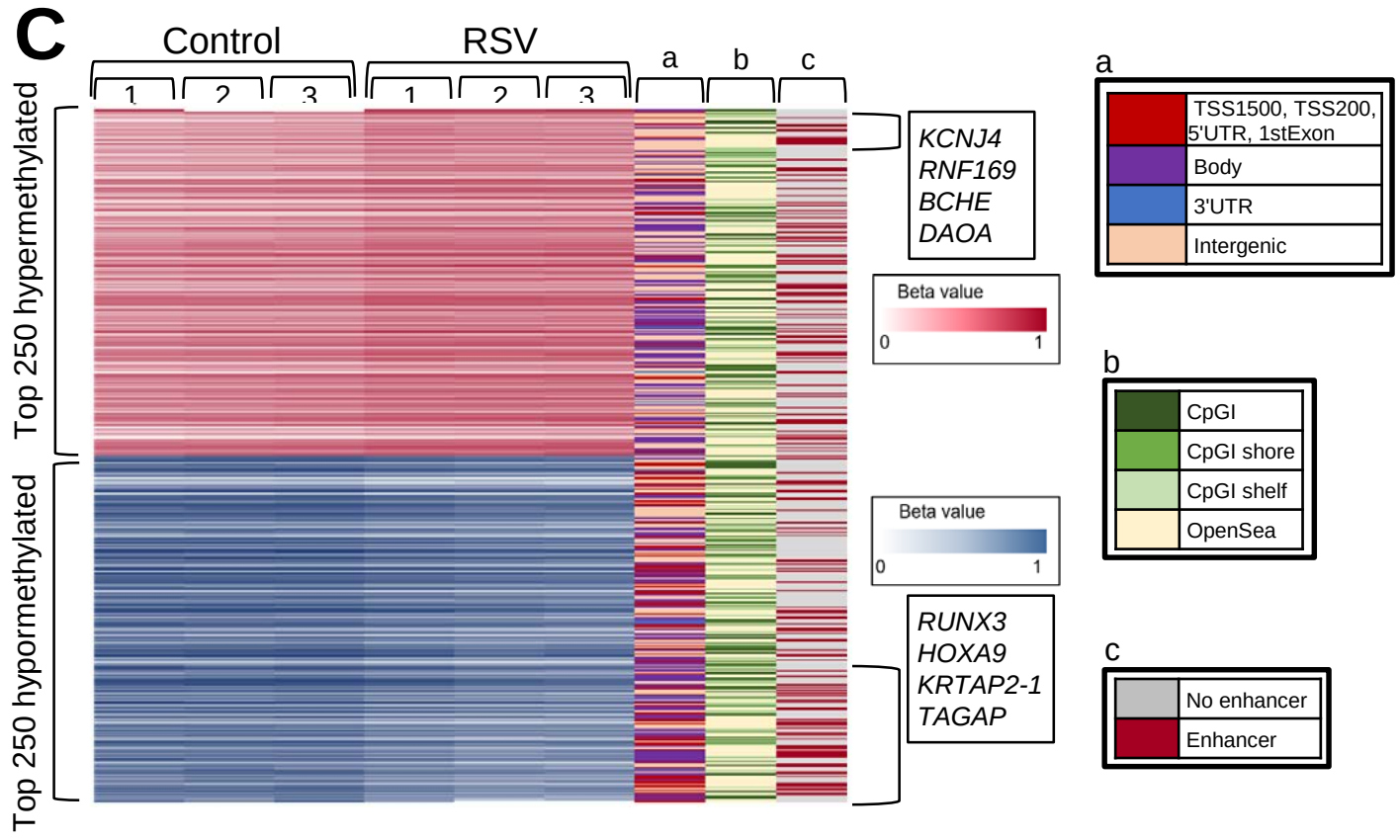
C
Control
RSV
a b c
1 2 3 1 2 3
Top 250 hypermethylated
Top 250 hypormethylated
KCNJ4
RNF169
BCHE
DAOA
RUNX3
HOXA9
KRTAP2-1
TAGAP
Beta value
0 1
a
TSS1500, TSS200, 5'UTR, 1stExon
Body
3'UTR
Intergenic
b
CpGI
CpGI shore
CpGI shelf
OpenSea
c
No enhancer
Enhancer

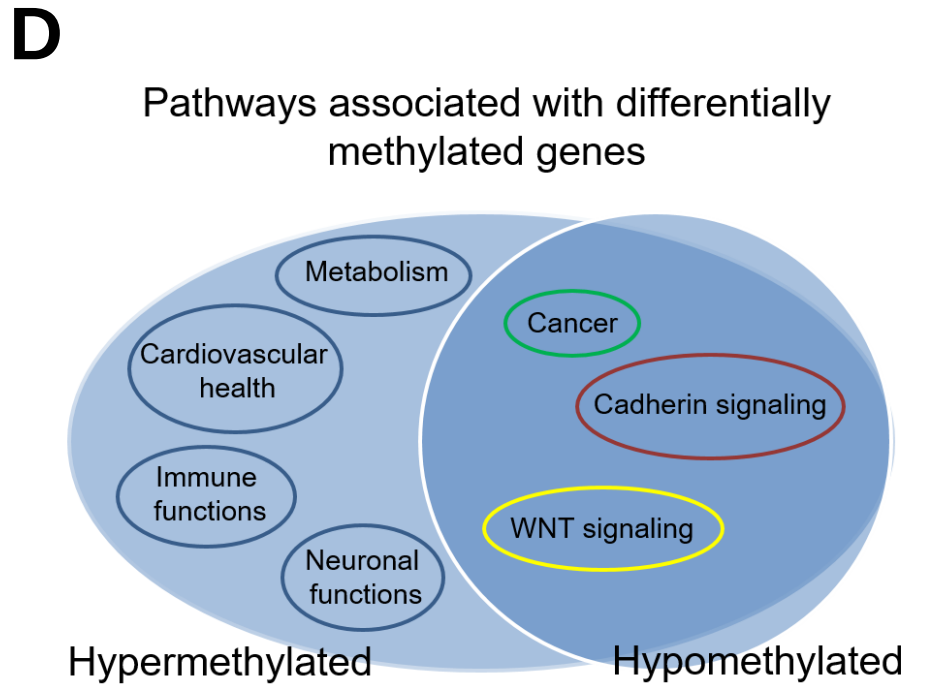
D
Pathways associated with differentially methylated genes
Metabolism
Cancer
Cardiovascular health
Cadherin signaling
Immune functions
WNT signaling
Neuronal functions
Hypermethylated genes
Hypomethylated genes

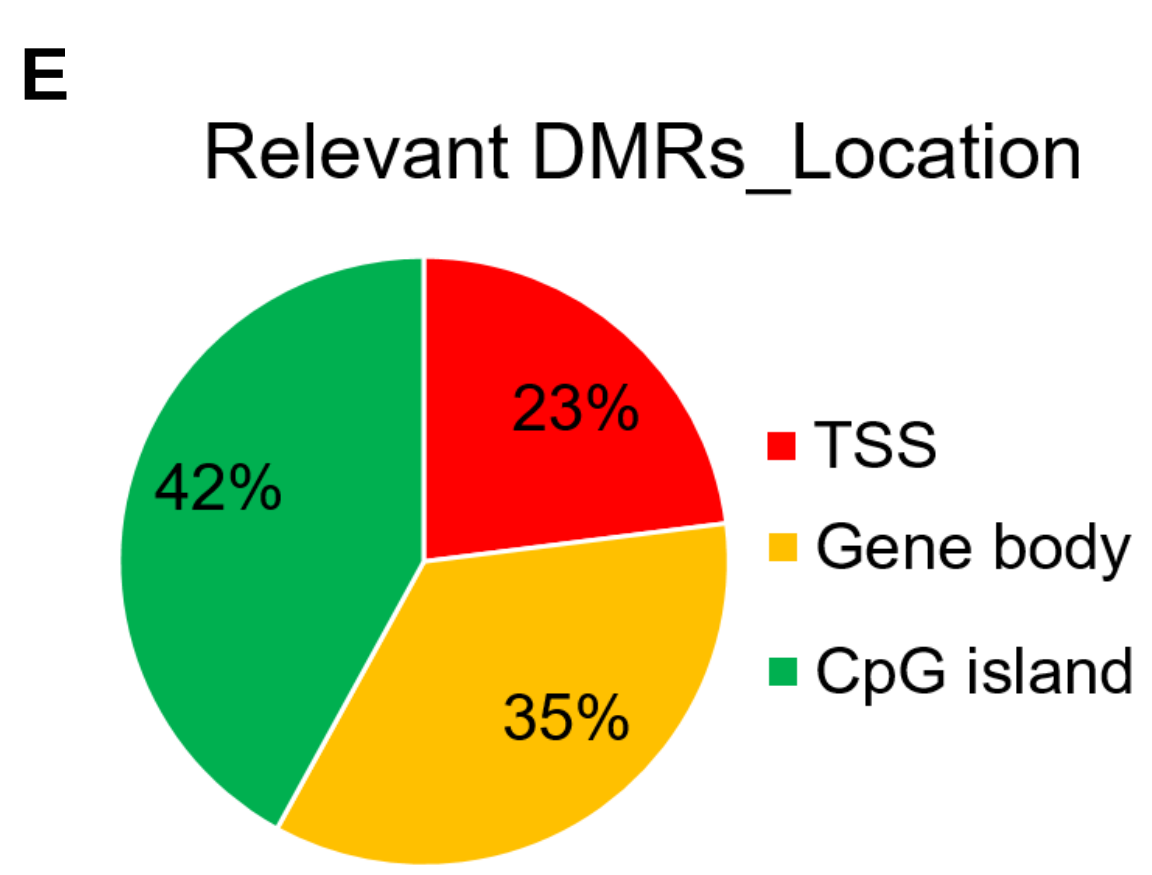
E
Relevant DMRs_Location
23%
35%
42%
TSS
Gene body
CpG island

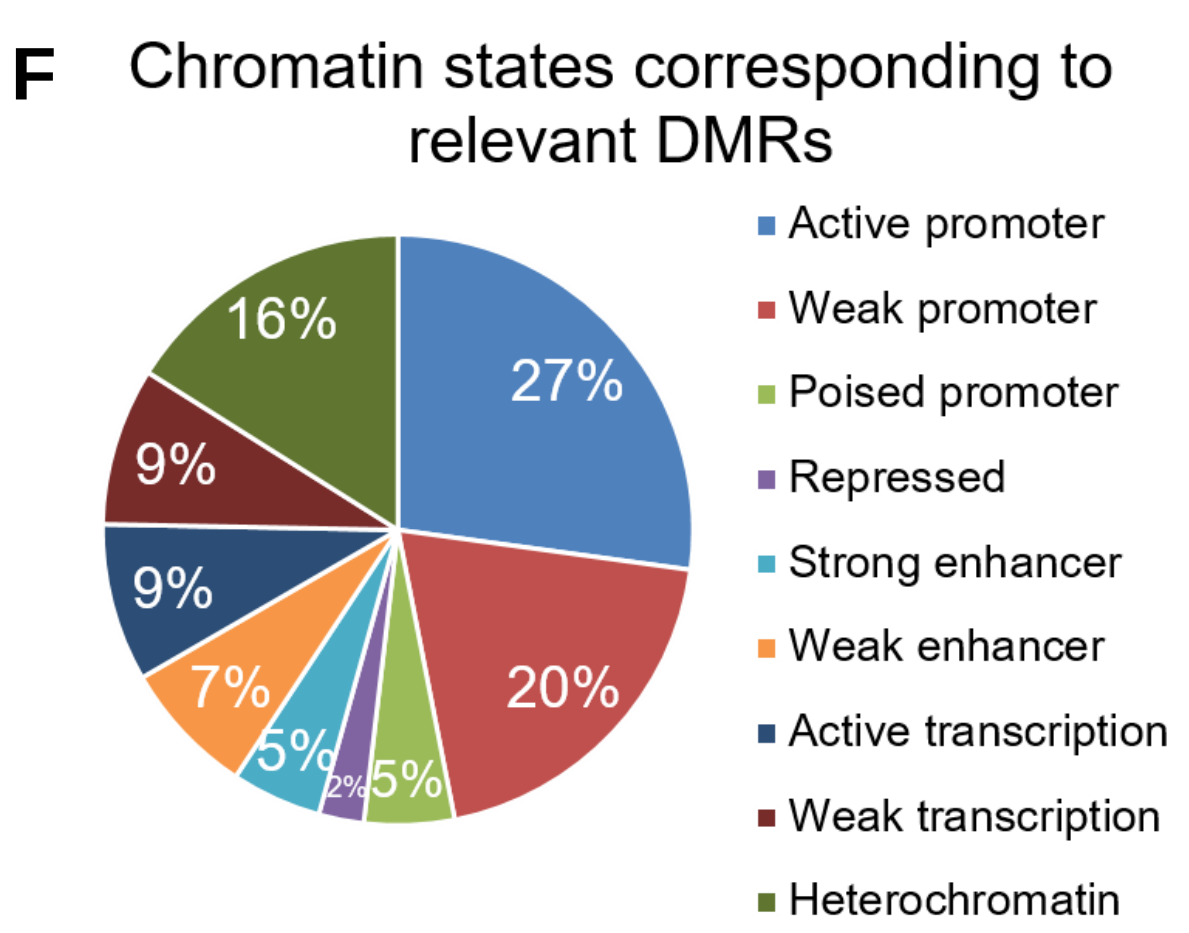
F
Chromatin states corresponding to relevant DMRs
27%
20%
5%
2%
5%
7%
9%
9%
16%
Active promoter
Weak promoter
Poised promoter
Repressed
Strong enhancer
Weak enhancer
Active transcription
Weak transcription
Heterochromatin

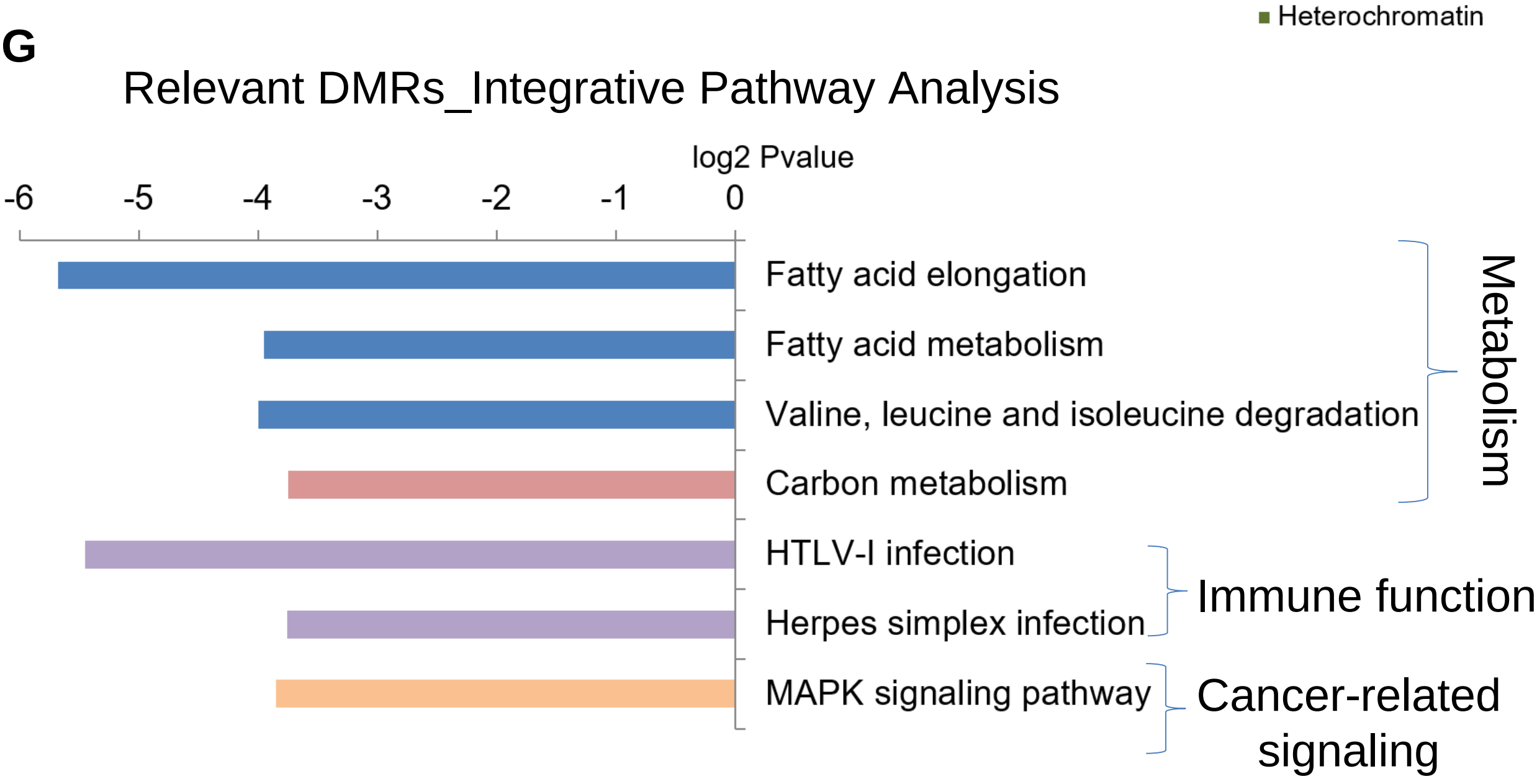
G
Relevant DMRs_Integrative Pathway Analysis
log2 Pvalue
-6 -5 -4 -3 -2 -1 0
Fatty acid elongation
Fatty acid metabolism
Valine, leucine and isoleucine degradation
Carbon metabolism
HTLV-I infection
Herpes simplex infection
MAPK signaling pathway
Metabolism
Immune function
Cancer-related signaling

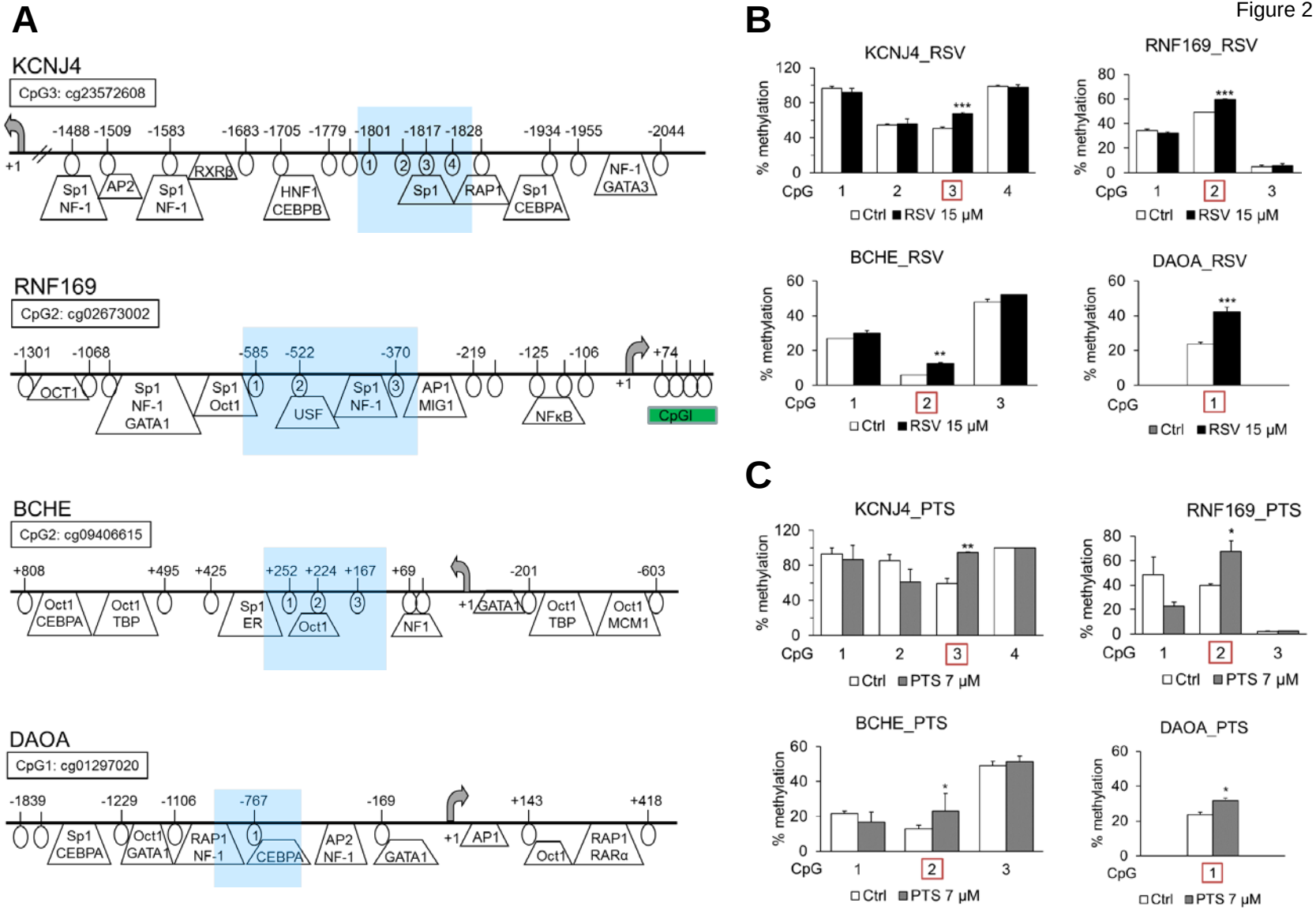
A
KCNJ4
CpG3: cg23572608
-1488 -1509 -1583 -1683 -1705 -1779 -1801 -1817 -1828 -1934 -1955 -2044
+1
Sp1 NF-1
AP2
Sp1 NF-1
RXRβ
HNF1 CEBPB
Sp1
RAP1
Sp1 CEBPA
NF-1 GATA3
RNF169
CpG2: cg02673002
-1301 -1068 -585 -522 -370 -219 -125 -106 +74
OCT1
Sp1 NF-1 GATA1
Sp1 Oct1
USF
Sp1 NF-1
AP1 MIG1
NFκB
CpGI
BCHE
CpG2: cg09406615
+808 +495 +425 +252 +224 +167 +69 -201 -603
Oct1 CEBPA
Oct1 TBP
Sp1 ER
Oct1
NF1
GATA1
Oct1 TBP
Oct1 MCM1
DAOA
CpG1: cg01297020
-1839 -1229 -1106 -767 -169 +143 +418
Sp1 CEBPA
Oct1 GATA1
RAP1 NF-1
CEBPA
AP2 NF-1
GATA1
AP1
Oct1
RAP1 RARα
B
KCNJ4_RSV
RNF169_RSV
BCHE_RSV
DAOA_RSV
% methylation
CpG
Ctrl
RSV 15 μM
C
KCNJ4_PTS
RNF169_PTS
BCHE_PTS
DAOA_PTS
Ctrl
PTS 7 μM

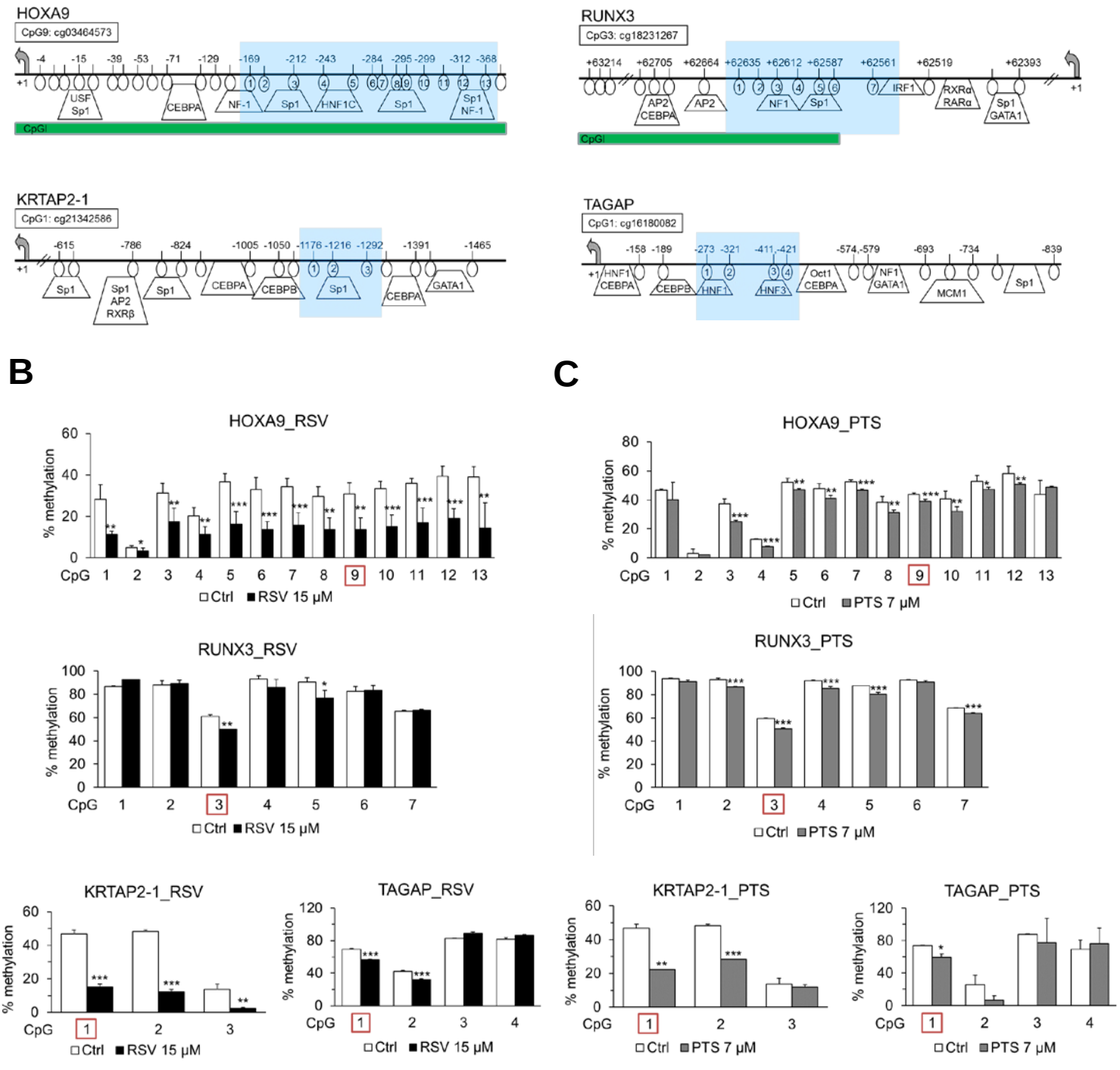
A
HOXA9
CpG9: cg03464573
-4 -15 -39 -53 -71 -129 -169 -212 -243 -284 -295 -299 -312 -368
+1
USF
Sp1
CEBPA
NF-1
Sp1
HNF1C
Sp1
Sp1
NF-1
CpGi
RUNX3
CpG3: cg18231267
+63214 +62705 +62664 +62635 +62612 +62587 +62561 +62519 +62393
AP2
CEBPA
AP2
NF1
Sp1
IRF1
RXRα
RARα
Sp1
GATA1
+1
CpGi
KRTAP2-1
CpG1: cg21342586
-615 -786 -824 -1005 -1050 -1176 -1216 -1292 -1391 -1465
+1
Sp1
Sp1
AP2
RXRβ
Sp1
CEBPA
CEBPB
Sp1
CEBPA
GATA1
TAGAP
CpG1: cg16180082
-158 -189 -273 -321 -411 -421 -574 -579 -693 -734 -839
+1
HNF1
CEBPA
CEBPB
HNF1
HNF3
Oct1
CEBPA
NF1
GATA1
MCM1
Sp1
B
HOXA9_RSV
% methylation
CpG 1 2 3 4 5 6 7 8 9 10 11 12 13
Ctrl
RSV 15 μM
RUNX3_RSV
% methylation
CpG 1 2 3 4 5 6 7
Ctrl
RSV 15 μM
KRTAP2-1_RSV
% methylation
CpG 1 2 3
Ctrl
RSV 15 μM
TAGAP_RSV
% methylation
CpG 1 2 3 4
Ctrl
RSV 15 μM
C
HOXA9_PTS
% methylation
CpG 1 2 3 4 5 6 7 8 9 10 11 12 13
Ctrl
PTS 7 μM
RUNX3_PTS
% methylation
CpG 1 2 3 4 5 6 7
Ctrl
PTS 7 μM
KRTAP2-1_PTS
% methylation
CpG 1 2 3
Ctrl
PTS 7 μM
TAGAP_PTS
% methylation
CpG 1 2 3 4
Ctrl
PTS 7 μM

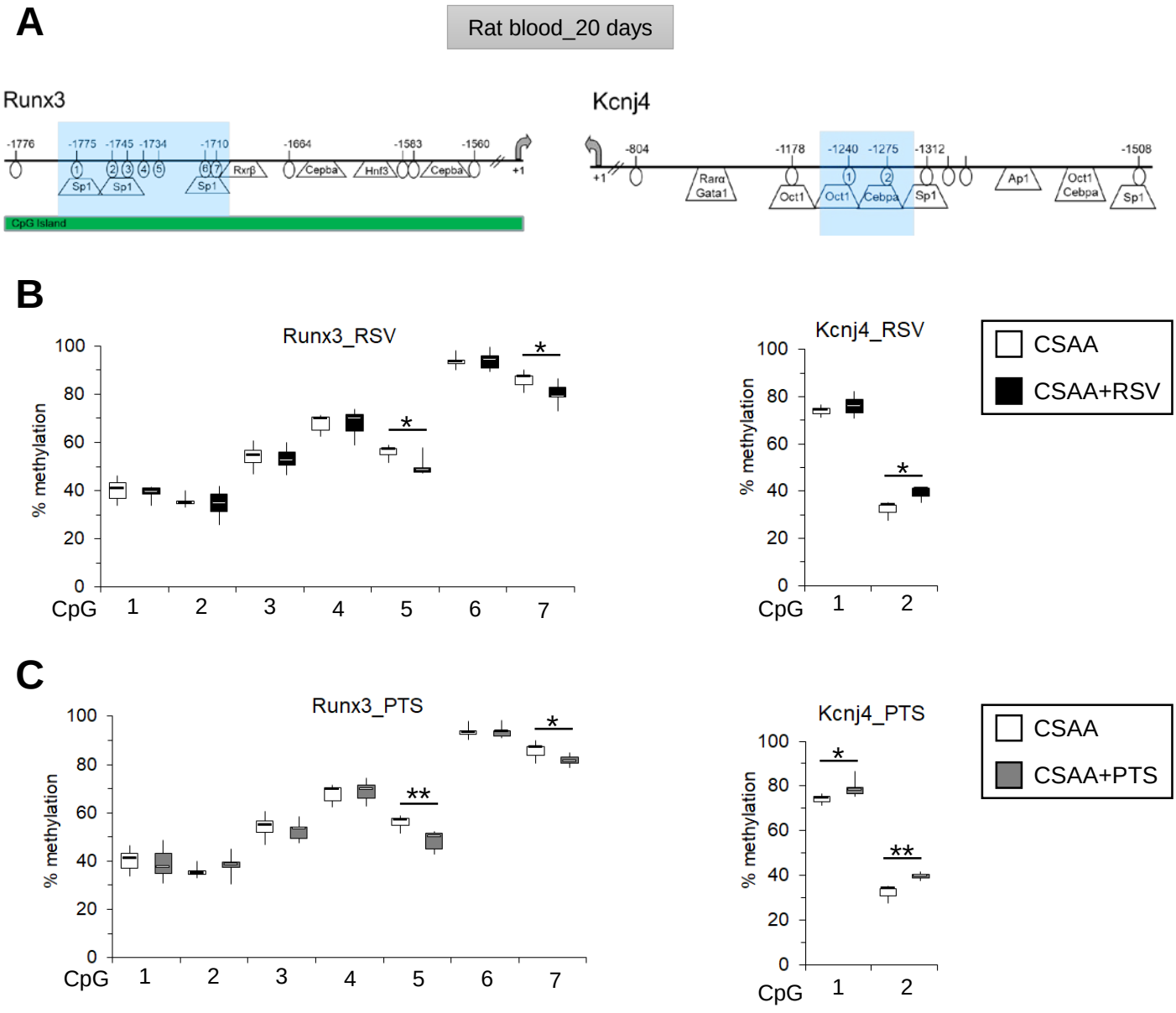
A
Rat blood_20 days
Runx3
-1776
-1775
-1745
-1734
-1710
-1664
-1583
-1560
+1
Sp1
Sp1
Sp1
Rxrβ
Cepba
Hnf3
Cepba
CpG Island
Kcnj4
-804
-1178
-1240
-1275
-1312
-1508
+1
Rarα
Gata1
Oct1
Oct1
Cebpa
Sp1
Ap1
Oct1
Cebpa
Sp1
B
Runx3_RSV
% methylation
CpG
Kcnj4_RSV
% methylation
CpG
CSAA
CSAA+RSV
C
Runx3_PTS
% methylation
CpG
Kcnj4_PTS
% methylation
CpG
CSAA
CSAA+PTS

A

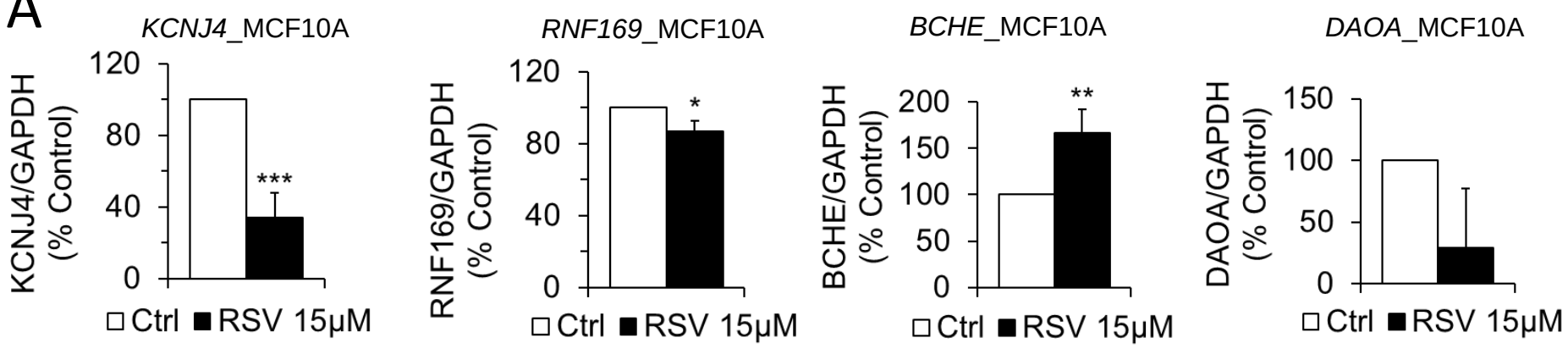
KCNJ4_MCF10A
KCNJ4/GAPDH (% Control)
120
80
40
0
***
Ctrl
RSV 15μM
RNF169_MCF10A
RNF169/GAPDH (% Control)
120
80
40
0
*
Ctrl
RSV 15μM
BCHE_MCF10A
BCHE/GAPDH (% Control)
200
150
100
50
0
**
Ctrl
RSV 15μM
DAOA_MCF10A
DAOA/GAPDH (% Control)
150
100
50
0
Ctrl
RSV 15μM

B

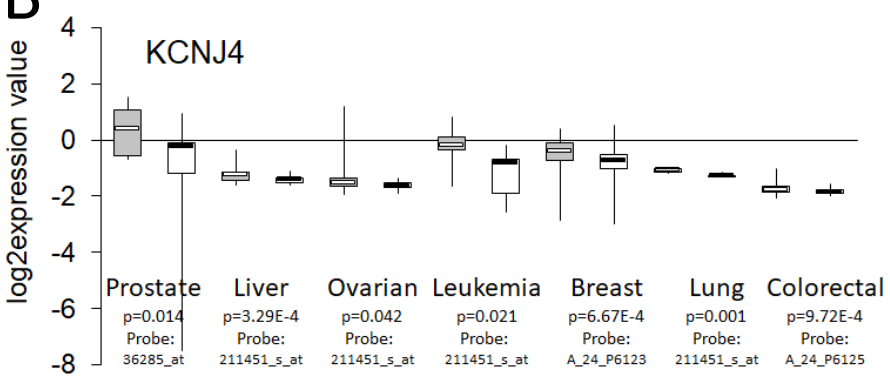
KCNJ4
log2expression value
4
2
0
-2
-4
-6
-8
Prostate p=0.014 Probe: 36285_at
Liver p=3.29E-4 Probe: 211451_s_at
Ovarian p=0.042 Probe: 211451_s_at
Leukemia p=0.021 Probe: 211451_s_at
Breast p=6.67E-4 Probe: A_24_P6123
Lung p=0.001 Probe: 211451_s_at
Colorectal p=9.72E-4 Probe: A_24_P6125

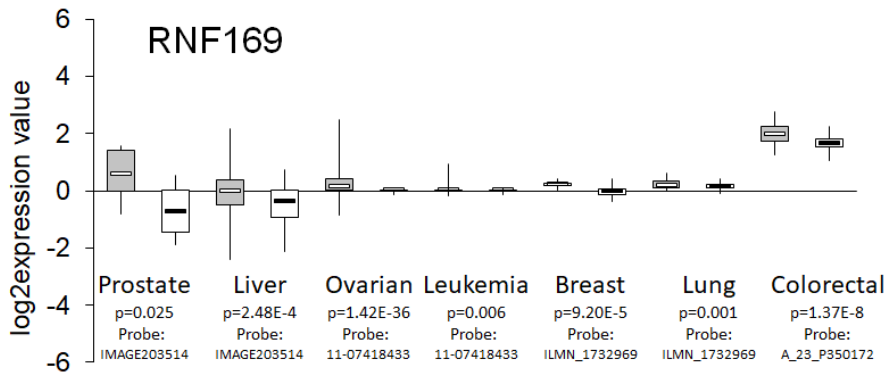
RNF169
log2expression value
6
4
2
0
-2
-4
-6
Prostate p=0.025 Probe: IMAGE203514
Liver p=2.48E-4 Probe: IMAGE203514
Ovarian p=1.42E-36 Probe: 11-07418433
Leukemia p=0.006 Probe: 11-07418433
Breast p=9.20E-5 Probe: ILMN_1732969
Lung p=0.001 Probe: ILMN_1732969
Colorectal p=1.37E-8 Probe: A_23_P350172

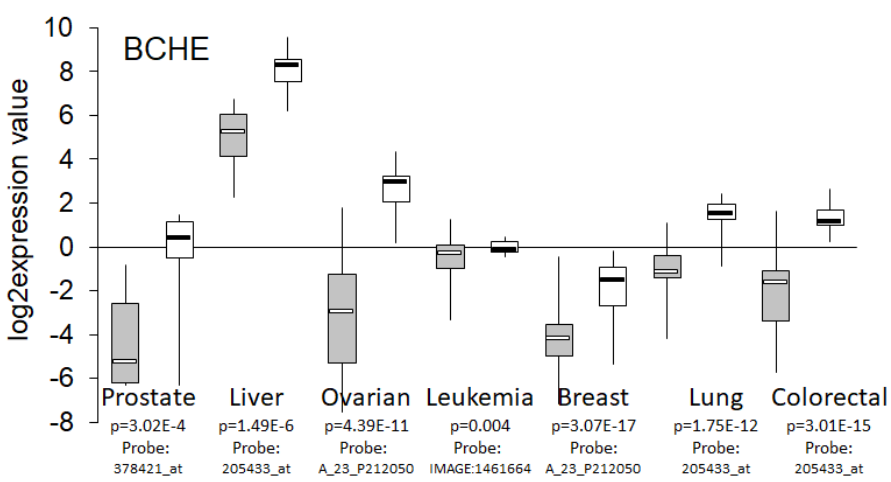
BCHE
log2expression value
10
8
6
4
2
0
-2
-4
-6
-8
Prostate p=3.02E-4 Probe: 378421_at
Liver p=1.49E-6 Probe: 205433_at
Ovarian p=4.39E-11 Probe: A_23_P212050
Leukemia p=0.004 Probe: IMAGE:1461664
Breast p=3.07E-17 Probe: A_23_P212050
Lung p=1.75E-12 Probe: 205433_at
Colorectal p=3.01E-15 Probe: 205433_at

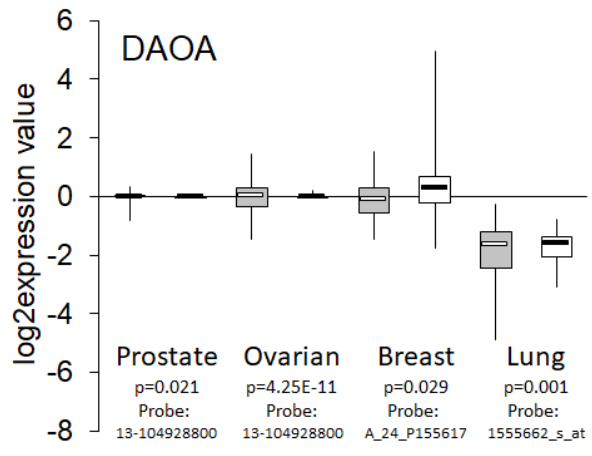
DAOA
log2expression value
6
4
2
0
-2
-4
-6
-8
Prostate p=0.021 Probe: 13-104928800
Ovarian p=4.25E-11 Probe: 13-104928800
Breast p=0.029 Probe: A_24_P155617
Lung p=0.001 Probe: 1555662_s_at

C

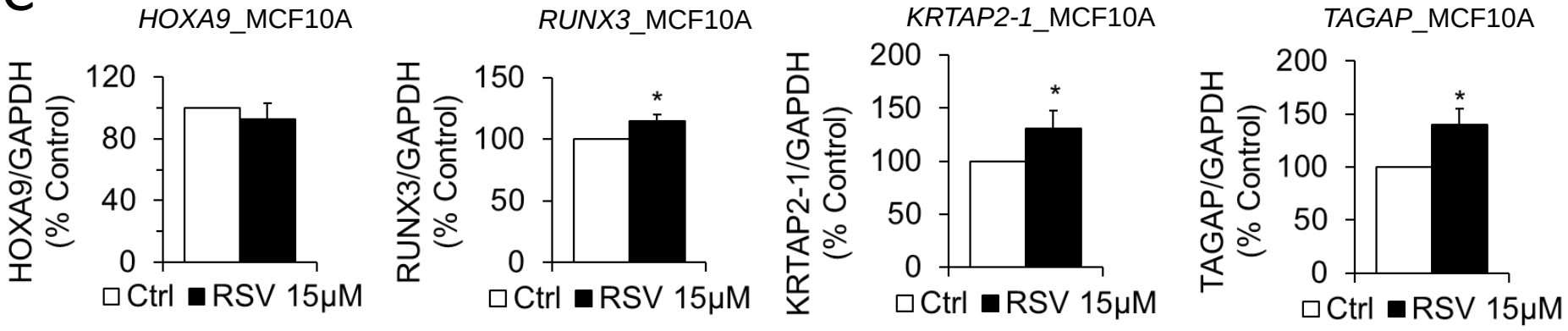
HOXA9_MCF10A
HOXA9/GAPDH (% Control)
120
80
40
0
Ctrl
RSV 15μM
RUNX3_MCF10A
RUNX3/GAPDH (% Control)
150
100
50
0
*
Ctrl
RSV 15μM
KRTAP2-1_MCF10A
KRTAP2-1/GAPDH (% Control)
200
150
100
50
0
*
Ctrl
RSV 15μM
TAGAP_MCF10A
TAGAP/GAPDH (% Control)
200
150
100
50
0
*
Ctrl
RSV 15μM

D

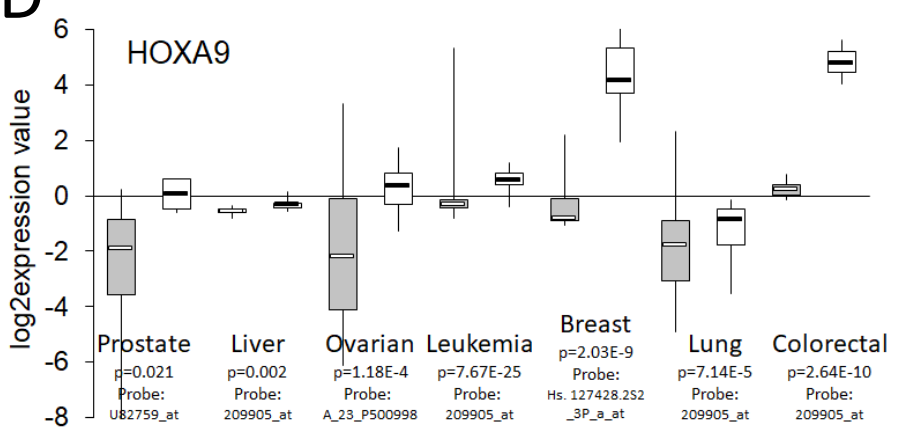
HOXA9
log2expression value
6
4
2
0
-2
-4
-6
-8
Prostate p=0.021 Probe: U82759_at
Liver p=0.002 Probe: 209905_at
Ovarian p=1.18E-4 Probe: A_23_P500998
Leukemia p=7.67E-25 Probe: 209905_at
Breast p=2.03E-9 Probe: Hs. 127428.2S2 _3P_a_at
Lung p=7.14E-5 Probe: 209905_at
Colorectal p=2.64E-10 Probe: 209905_at

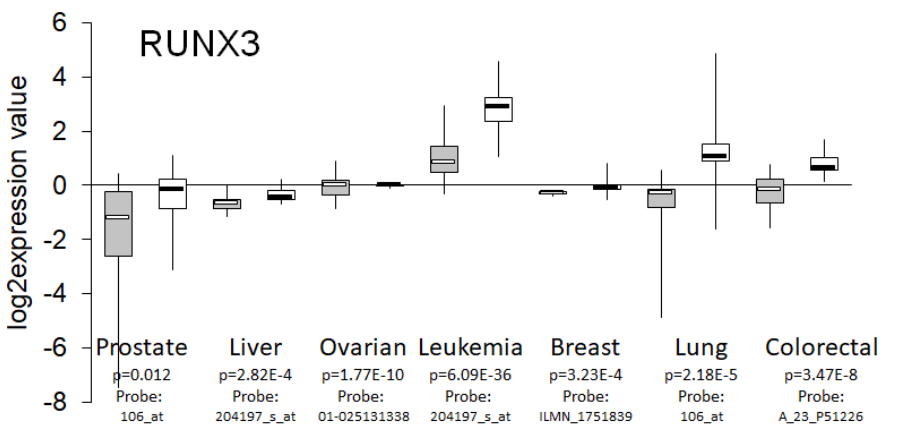
RUNX3
log2expression value
6
4
2
0
-2
-4
-6
-8
Prostate p=0.012 Probe: 106_at
Liver p=2.82E-4 Probe: 204197_s_at
Ovarian p=1.77E-10 Probe: 01-025131338
Leukemia p=6.09E-36 Probe: 204197_s_at
Breast p=3.23E-4 Probe: ILMN_1751839
Lung p=2.18E-5 Probe: 106_at
Colorectal p=3.47E-8 Probe: A_23_P51226

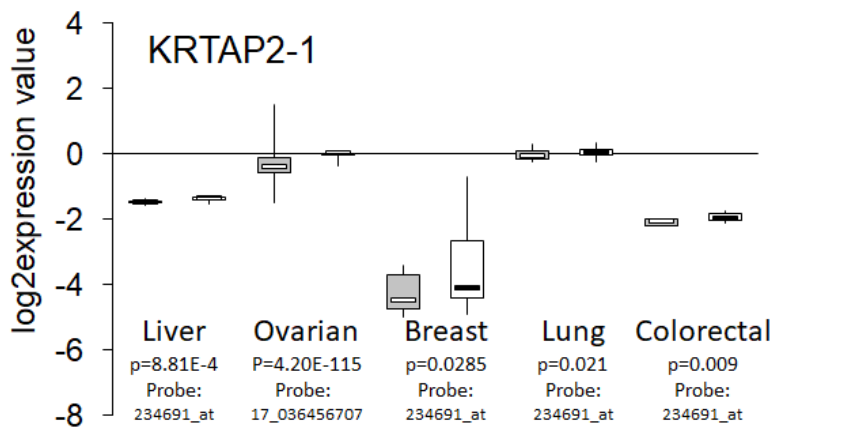
KRTAP2-1
log2expression value
4
2
0
-2
-4
-6
-8
Liver p=8.81E-4 Probe: 234691_at
Ovarian P=4.20E-115 Probe: 17_036456707
Breast p=0.0285 Probe: 234691_at
Lung p=0.021 Probe: 234691_at
Colorectal p=0.009 Probe: 234691_at

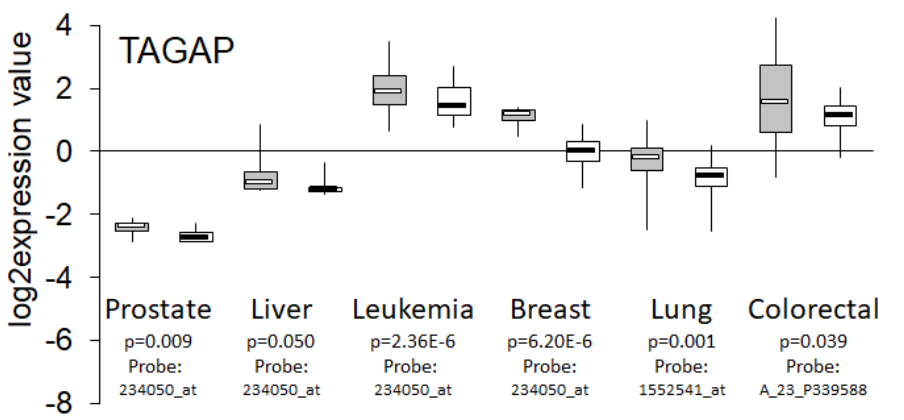
TAGAP
log2expression value
4
2
0
-2
-4
-6
-8
Prostate p=0.009 Probe: 234050_at
Liver p=0.050 Probe: 234050_at
Leukemia p=2.36E-6 Probe: 234050_at
Breast p=6.20E-6 Probe: 234050_at
Lung p=0.001 Probe: 1552541_at
Colorectal p=0.039 Probe: A_23_P339588

SUPPLEMENTARY MATERIALS AND METHODS

Cell culture and exposure to resveratrol (RSV) and pterostilbene (PTS)

Human mammary epithelial MCF10A cell line was purchased from ATCC (CRL-10317, USA) and maintained in DMEM/F12 (1:1) medium (Gibco) supplemented with 20 ng/ml epidermal growth factor (Sigma-Aldrich, St. Louis, MO, USA), 100 ng/ml cholera toxin (Calbiochem, EMD Millipore, Billerica, MA, USA), 0.01 mg/ml insulin (Sigma-Aldrich, St. Louis, MO, USA), 500 ng/ml hydrocortisone (Sigma-Aldrich, St. Louis, MO, USA), 5% horse serum (Gibco), 1U/ml penicillin and 1µg/ml streptomycin (Gibco). MCF10A cell line was routinely verified by morphology, invasion and growth rate. Resveratrol (RSV, Sigma-Aldrich, St. Louis, MO, USA) and pterostilbene (PTS, Cayman Chem., Ann Arbor, MI, USA) were resuspended in ethanol and 10mM solutions were stored at -20°C. Dilutions of the compounds were freshly prepared prior to adding to the cell medium. Cells were grown in a humidified atmosphere of 5% carbon dioxide at 37°C. 24 h prior to incubation with RSV or PTS, cells were plated at a density of 1-2 x 10^5 per a 10-cm tissue culture dish. Cells were exposed to different RSV or PTS concentrations ranging from 0 to 20 µM of RSV and 0 to 15 µM of PTS for 4 days. Cells were then split 1:50, allowed to attach overnight and exposed to the compounds for additional 4 days (9-day exposure).

Illumina Infinium Human Methylation 450K BeadChip microarray

DNA from control untreated cells (cultured with ethanol as a vehicle control) and cells cultured with RSV or PTS was isolated using standard phenol:chloroform extraction protocol. Genomic

DNA was quantified using Picogreen protocol (Quant-iT™ PicoGreen® dsDNA Products, Invitrogen, P-7589) and read on SpectraMAXGeminiXS Spectrophotometer. Bisulphite conversion of 500 ng of each DNA sample was performed using the EZ-96 DNA Methylation-Gold Kit according to the manufacturer's protocol (Zymo Research). Then, 4 μL of bisulphite-converted DNA was used for hybridization on the Infinium HumanMethylation 450K BeadChip, following the Illumina Infinium HD Methylation protocol (Illumina). Hybridization and scanning were performed in the University of Chicago Genomics Facility. Raw data processing was performed using the Methylation module (version 1.9.0) of the GenomeStudio software (Illumina; version 2011.1) using HumanMethylation450_15017482_v.1.2.bpm manifest, which normalizes within-sample data using different internal controls that are present on the HumanMethylation 450K BeadChip and internal background probes. The methylation score for each CpG was represented as a beta value according to the fluorescent intensity ratio with any values between 0 (unmethylated) and 1 (completely methylated). Raw microarray data and processed data will be available from Gene Expression Omnibus (accession number pending).

The Illumina 450K microarray platform covers more than 485,000 methylation sites (CpG sequences) per sample at single-nucleotide resolution. This coverage corresponds to 99% of RefSeq genes (all known protein coding genes), with an average of 17 CpG sites per gene region. These CpG sites are distributed across regulatory gene regions including CpG islands, promoters, 5'UTR, first exon, gene body, 3'UTR, and CpG island shelves and open seas. The latter two refer respectively to regions between 2kb-4kb and more than 4kb from CpG islands. CpG islands are regions with high CpG density whose methylation is important in gene regulation.

Viability assays

Cell viability was determined by trypan blue (Sigma-Aldrich, St.Louis, MO, USA) exclusion test. Cells were harvested after incubation with RSV or PTS on day 4 and day 9. Following 3-5 minute incubation with trypan blue, the viable and dead cells were counted under the microscope. The results were confirmed by a viability assay using MTT (Supplementary Figure S1).

Mapping differentially methylated CpG sites into differentially methylated regions (DMRs)

We utilized GenomeStudio (Illumina) to generate final reports that were used as input into the lumi pipeline for pre-processing and normalization of the data in R/Bioconductor. Differentially methylated regions (DMRs) were identified using DMRforPairs algorithm [1]. Default parameters were applied, except min_dM parameter was lowered to 0.4 (lower bound of range). dM value of 0.4 is approximately equal to delta beta-value of 0.05. DMRs were defined as regions containing minimum of 4 probes with maximum of 200bp between them. DMRs were ranked according to dM value (dM indicates the largest median difference (absolute) between any of the sample pairs). No significant DMRs were detected in the analysis of control- versus RSV-treated MCF10A samples, but DMRs considered relevant (dM>0.4) were further assessed.

124 relevant DMRs were detected among all samples (3 controls, 3 RSV-treated). Further, control samples were compared to each other and RSV samples were compared to each other to determine DMRs within biological replicates. No significant DMRs were observed. 9 relevant DMRs were detected among control samples and 35 relevant DMRs were detected among RSV samples. Relevant DMRs detected in biological replicates were removed from further analysis.

We then used broad ChromHMM HMEC track in UCSC Genome Browser (hg19) to determine chromatin states of relevant DMRs in breast cells [2]. DMRs could correspond to the following chromatin states: active, weak or poised promoters, strong or weak enhancers, putative insulators, active or weak transcription, Polycomb-repressed regions or heterochromatin. Active promoters, strong enhancers and active transcription regions are linked to high expression levels, with the latter state determined based on the enrichment of histone marks along transcripts. Weak or poised promoters, weak enhancers, weak transcription, Polycomb-repressed regions or heterochromatin, in turn, are linked to low expression.

REFERENCES

[1] Rijlaarsdam, M. A., van der Zwan, Y. G., Dorssers, L. C., Looijenga, L. H., DMRforPairs: identifying differentially methylated regions between unique samples using array based methylation profiles. *BMC bioinformatics* 2014, *15*, 141.

[2] Ernst, J., Kheradpour, P., Mikkelsen, T. S., Shoresh, N.*, et al.*, Mapping and analysis of chromatin state dynamics in nine human cell types. *Nature* 2011, *473*, 43-49.

SUPPLEMENTARY FIGURES and TABLES

Supplementary Figure S1. Exposure of MCF10A mammary epithelial cells to resveratrol (RSV) or pterostilbene (PTS) leads to negligible effects on cell viability within a defined range of concentrations. (A,B) Effects of 9 day-exposure of MCF10A mammary epithelial cells to resveratrol (RSV) (A) or pterostilbene (PTS) (B) at a range of concentrations 0-20 μM for RSV or 0-15 μM for PTS on cell viability as measured by a trypan blue exclusion test (top panels) and MTT assay (bottom panels). All results represent mean ± S.D. of three independent experiments; ***$P < 0.001$, **$P < 0.01$, *$P < 0.05$.

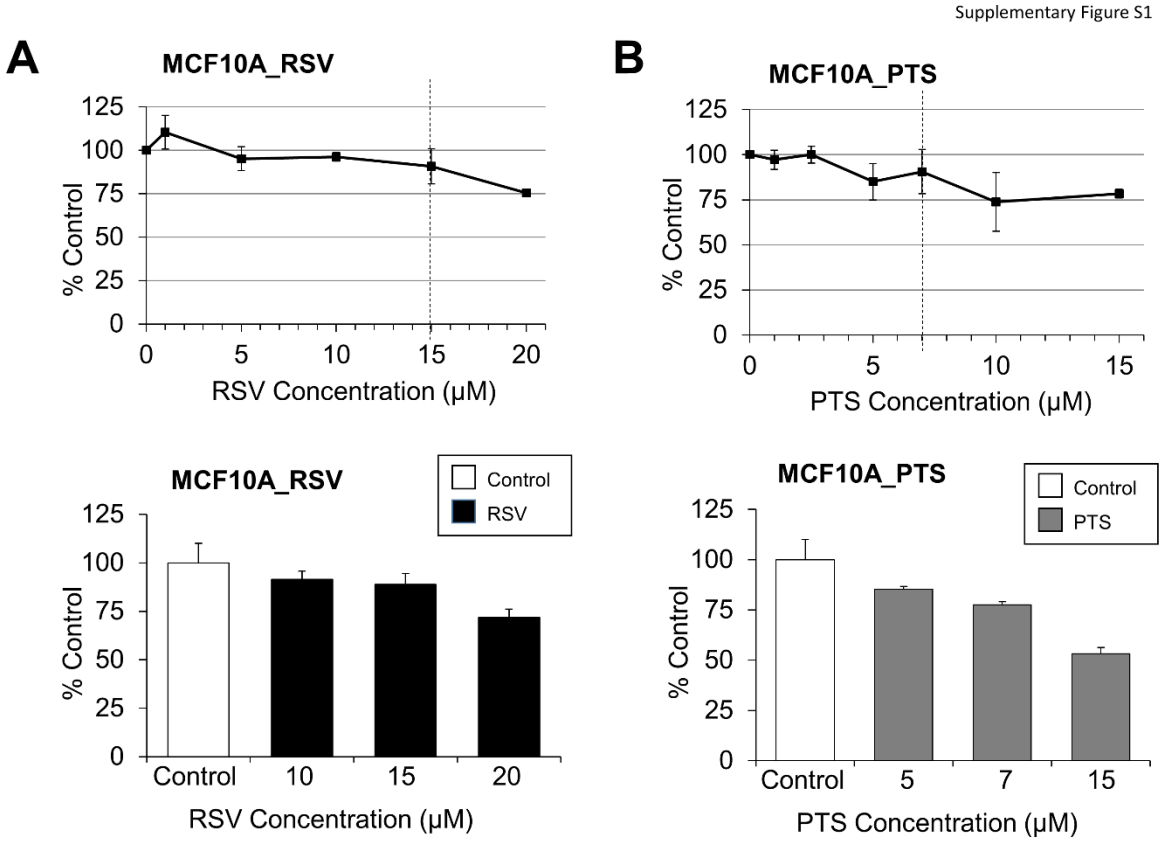

Supplementary Figure S2. Resveratrol (RSV) and pterostilbene (PTS) effects on methylation states of CpG sites located in regulatory regions of *Tagap* and *Bche* in rat peripheral blood. Fischer 344 rats were exposed for 20 days to chow diet [choline sufficient amino acid defined (CSAA) diet] supplemented with resveratrol (CSAA+RSV) or pterostilbene (CSAA+PTS). Collected peripheral blood was subjected to DNA isolation followed by DNA methylation analysis by pyrosequencing at loci identified in *in vitro* MCF10A experiment. Average methylation status of CpG sites in the tested fragments of *Tagap* and *Bche* in rats on CSAA diet and CSAA diet supplemented with RSV (A) or PTS (B) indicates no significant changes. All results represent mean ± SEM of n=6 per group.

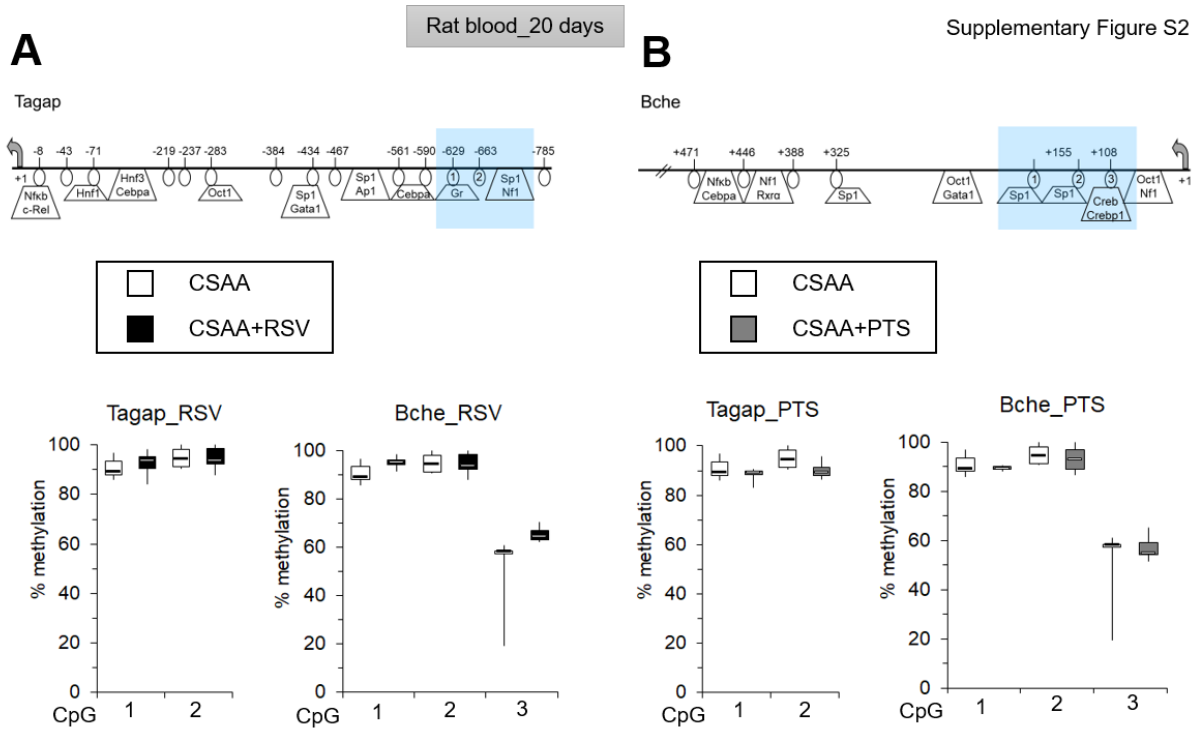

Supplementary Table S1. Primer sequences used in DNA methylation analysis by pyrosequencing in human mammary epithelial MCF10A cells (A) and rat peripheral blood (B), and in expression analysis by QPCR (C).

Supplementary Table S1A. Primer sequences used in DNA methylation analysis by pyrosequencing in MCF10A mammary epithelial cells.			
Gene	**Primer sequences for pyrosequencing**	**Annealing temperature [°C]**	**Amplicon length [bp]**
BCHE (Assay 3, three CpG sites)	FW 5'-GTTTTTTGAATAATAGGAAGATTTGATG-3' RVBio 5'-AAACTAAAACAACAACTACATCCTACAT-3' Seq 5'-TGAGTTTTATAGTAATTTGGATT-3'	56	292
DAOA (Assay 1, one CpG site)	FW 5'-TGGTTATGGTAGTTATGTTTTGTGAA-3' RVBio 5'-AAACAAAAAAAAAAACCAAATATCCACAT-3' Seq 5'-TTTGTGAAAAATTTTATTAATGA-3'	55	129
HOXA9 (Assay 2, thirteen CpG sites)	FW 5'-ATGGGGTTTGTTTTAATTGTG-3' RVBio 5'-CAACCTATATAACTTCTAAAACAATAACTC-3' Seq1 5'-GGGTTTGTTTTAATTGTGG-3' (CpGs 1-4) Seq2 5'-ATAATTAATTAAGTTATTAAGAAGG-3' (CpGs 5-11) Seq3 5'-AATTGAAGTTATAAAAAAGTAGTT-3' (CpGs 12-13)	54	305
KCNJ4 (Assay 2, four CpG sites)	FW 5'-GGTGTTTGGATTTGGGTGGTTTA-3' RVBio 5'-CAACCTAAACATTAAAACAAAACTCTATCT-3' Seq1 5'-GGTGGTTTATTGAGTAAGG-3' (CpG 1) Seq2 5'-AGGAATTAAATATTTAGGGAAAT-3' (CpG 2-4)	59	292
KRTAP2-1 (Assay 1, three CpG sites)	FW 5'-AGGAATTATATGGGGGAAATAGTTT-3' RVBio 5'-AAATTATACCTAATATCTCCCTCTTCT-3' Seq 5'-AGTTATTAGATAGGGTTTTGA-3'	53	247
RNF169 (Assay 2, three CpG sites)	FW 5'-TGGATTTAGGAGGTTTGGGTTGTA-3' RVBio 5'-ATAACTTTATAACTAAAACCAAACCCAC-3' Seq1 5'-AGAAAATGTGGATTAGTGTA-3' (CpGs 1-2) Seq2 5'-AGGTTGTTTTTTTTGGTAG-3' (CpG 3)	59	319
RUNX3 (Assay 1, seven CpG sites)	FW 5'-TAGGGGAAGGTAGTTGATATGGTT-3' RVBio 5'-AACTAAAACTAACCTCTTCCCTACT-3' Seq 5'-GGATAATGTATTTTGGGG-3'	54	170
TAGAP (Assay 1, four CpG sites)	FW 5'-TGGATGTGGGATATTGTTATAGAATTAGA-3' RVBio 5'-AAATTCACCATCTCTTTCCTACTT-3' Seq 5'-AGATAGTTTTTTTTTTGAGGAATA-3'	59	285

Supplementary Table S1B. Primer sequences used in DNA methylation analysis by pyrosequencing in rat peripheral blood samples.			
Gene	**Primer sequences for pyrosequencing**	**Annealing temperature [°C]**	**Amplicon length [bp]**
Runx3	FW 5'-GGGTAGATGTAAATTGGAATTATTTAAGAA-3' RVBio 5'-CCACCAAATAAAACCCACACCT-3' Seq 5'-AAATAGAATTTATATATTATAGAGG-3'	49	126
Tagap	FW 5'-GGAATTTTTAAATTTTTAAGTTGTAGTT-3' RVBio 5'-AAACCAATACTATTAAAAACAACTCTACT-3' Seq 5'-TTTAAATTTTTAAGTTGTAGTTTAT-3'	46	116
Bche	FW 5'-GGTTATTTAGAGGAGGTTGTGTATAGG-3' RVBio 5'-TCCTCCTATAAATTCTTCTACTCTACAT-3' Seq 5'-GGTTGTGTATAGGGGAT-3'	55.5	171
Kcnj4	FW 5'-AGGGAAAAGAGAGATAAGAGTGT-3' RVBio 5'-AACCCTAAATTCCATCCCCAACTCTA-3' Seq1 5'-TTTTTATAATTTGATTTTGAATATG -3'	49	219

Supplementary Table S1C. Primer sequences used in expression analysis (QPCR).			
Gene	**Primer sequences for QPCR**	**Annealing temperature [°C]**	**Amplicon length [bp]**
BCHE	FW 5'-CCAGAATGGATGGGAGTGATG-3' RV 5'-CCACCGTTTCACTATGGATCTAC-3'	59	123
DAOA	FW 5'-CTGATGGGTGCTGATTCTCTC-3' RV 5'-TGCTCAGAAGAATGCTCCTTT-3'	59	94
HOXA9	FW 5'-CATTAAACCTGAACCGCTGTC-3' RV 5'-CTCTATCAACTGGAGGAGAACC-3'	59	107
KCNJ4	FW 5'-GTGTACTTCGCCAACCTGAG-3' RV 5'-CGGAGAAGATCATGAGCATGTAG-3'	59	103
KRTAP2-1	FW 5'-GAGCACTGGGCTCATCTATT-3' RV 5'-GCCACGAAATCTTAAGAAGAAGG-3'	59	83
RNF169	FW 5'-TCAGAGCACCAATCAAATTAAGC-3' RV 5'-CAGCTTGTGGATTTGATCTTCAG-3'	59	122
RUNX3	FW 5'-GTTTCACCCTGACCATCACT-3' RV 5'-GTCCACGGTCACCTTGATG-3'	59	80
TAGAP	FW 5'-GAGAGCAGCCAACGAGAAA-3' RV 5'-CTTAAAGACCACAGCGAGGAG-3'	59	109
GAPDH	FW 5'-TGCACCACCAACTGCTTA-3' RV 5'-AGAGGCAGGGATGATGTTC-3'	59	177

Supplementary Table S2. A list of CpG sites that are differentially methylated upon 9-day exposure of MCF10A mammary epithelial cells to 15 µM RSV (0.05≤differential methylation≤-0.05, p<0.05, limma t test). Among these changes, 889 CpG sites (67% of total number of changes) corresponding to 602 genes were hypermethylated whereas 435 CpG sites were hypomethylated and located within 305 genes. The changes in DNA methylation were subtle ranging from 0.05 to 0.20 in differential methylation values.

Supplementary Table S3. A list of relevant differentially methylated regions (DMRs) between control MCF10A cells and cells treated with 15 µM RSV for 9 days. DMRs are defined as regions that contain at least 4 CpG sites (Illumina probes) with a maximum distance of 200 bp between individual sites. Regions in which median methylation levels (M-values) between the samples differed at least by 0.4 which referred as relevant DMRs. Chromosomal positions are indicated in bp, n indicates the number of probes in a region, ID indicates the region ID. Values in the columns per sample indicate median beta values. dM indicates the largest median difference (absolute) between any of the sample pairs and p indicates uncorrected p-value from Mann-Whitney U test (n=2) or Kruskal Wallis test (n>2), p.adj denotes the multiple testing corrected p-value (method:fdr). Gene symbols of overlapping transcripts are listed for the exact region and within a margin of 10000 bp of the region.

	Ctrl MCF10A 9	Ctrl MCF10A 9	Ctrl MCF10A 9	RSV 15uM MC	RSV 15uM MC	RSV 15uM MC	methylation di	average methy	t	P.Value	adj.P.Val	B	CHR	MAPINFO	CHROMOSOM	STRAND	PROBE SNPS	PROBE SNPS	UCSC REFGEN	UCSC REFGEN	UCSC REFGEN	UCSC CPG ISL	RELATION TO	DMR	ENHANCER
cg08441918	0.763467774	0.028714881	0.022939304	0.795198065	0.7736602	0.815996204	0.52324417	0.533329405	2.792616272	0.027160093	0.803196548	-4.18437055	19	6495210	19	F	rs61731566		TUBB4;MIR22(	NM 006087;N	Body;TSS1500	chr19:649519:	Island		
cg15135990	0.800011315	0.121382966	0.10856122	0.769575233	0.757968399	0.78485351	0.427480547	0.557058774	2.457896253	0.044032805	0.829725495	-4.68156117	2	74665089	2	R			RTKN;RTKN;RT	NM 033046;N	Body;5'UTR;Bc	chr2:7466331!	S Shore		
cg23572608	0.433244326	0.682140494	0.441927991	0.683194562	0.685310328	0.670073619	0.160421899	0.59931522	2.572485909	0.037279707	0.819266878	-4.51133063	22	38841396	22	R			KCNJ4;KCNJ4	NM 152868;N	5'UTR;TSS1500				
cg02673002	0.433244326	0.44047619	0.55340693	0.639170552	0.606414592	0.563049853	0.127169184	0.539293741	3.697044068	0.007862262	0.773451347	-2.87652999	11	74459317	11	R			RNF169	NM 0010986:	TSS1500	chr11:744598!	N Shore		
cg14829303	0.170132325	0.354444666	0.218222493	0.366812227	0.322940138	0.397821875	0.114924919	0.305062287	2.530647412	0.039611668	0.823066205	-4.57351241	12	11287271	12	R		rs2599396	TAS2R30;PRR4	NM 0010976	TSS1500;5'UTR;5'UTR				
cg26247795	0.272094372	0.261828591	0.320334262	0.399749111	0.370252101	0.428337428	0.114693805	0.342099311	5.908102465	0.000623696	0.773451347	-0.14459017	21	14407237	21	F	rs57764991	rs60432368				chr21:144094:	N Shelf		
cg00431317	0.538096315	0.491783567	0.556032939	0.6860648	0.565147739	0.675748792	0.113682837	0.585479025	3.420219845	0.011353788	0.777995215	-3.26779973	8	85267094	8	F			RALYL;RALYL;R	NM 173848;N	5'UTR;5'UTR;5'UTR;Body				TRUE
cg23954274	0.152122699	0.291908238	0.313136711	0.400625	0.35546875	0.331067146	0.109997749	0.307388091	2.63503996	0.034055751	0.813674675	-4.41834673	10	133195058	10	R		rs7085446							
cg17287725	0.009621258	0.010778558	0.154355348	0.135786119	0.203382354	0.15850707	0.107640126	0.112071785	2.698933079	0.031061534	0.809865645	-4.32340552	19	12267592	19	F		rs35242769	ZNF625	NM 145233	TSS200	chr19:122669!	Island	DMR	
cg22170936	0.321629145	0.393059911	0.437628412	0.458108022	0.500160738	0.497315837	0.101089043	0.434650344	3.589757529	0.009053557	0.776859249	-3.02702552	X	53111391	X	R			TSPYL2	NM 022117	TSS200	chrX:5311128:	Island		
cg12424965	0.488870569	0.527583799	0.564336075	0.644520548	0.615406809	0.623803446	0.10098012	0.577420208	5.445207625	0.001002827	0.773451347	-0.65799929	6	520807	6	F	rs10458176		EXOC2	NM 018303	Body	chr6:519079-5	Island		
cg09406615	0.276225279	0.308380197	0.225499955	0.356932153	0.373218869	0.378658426	0.099568006	0.319819147	5.058991241	0.001522343	0.773451347	-1.10940055	3	165555103	3	R			BCHE;BCHE	NM 000055;N	1stExon;5'UTR				TRUE
cg07698793	0.496936692	0.527419355	0.58642251	0.685399871	0.619673617	0.603698151	0.099331027	0.586591699	3.540974598	0.009658813	0.776859249	-3.09594428	3	177471540	3	F	rs71812455								TRUE
cg09326409	0.195602837	0.239544928	0.267221025	0.386935198	0.324521703	0.288510552	0.099199554	0.283722707	3.607982379	0.008838096	0.776859249	-3.00135551	16	31342453	16	R			ITGAM;ITGAM	NM 0011458(	Body;Body	chr16:313424!	Island		
cg04728978	0.576876967	0.642532131	0.670272519	0.779161478	0.686240417	0.713430435	0.096383571	0.678085658	3.195059574	0.015433689	0.785810238	-3.59264707	2	167660297	2	R									TRUE
cg23290674	0.377567141	0.313061958	0.314481707	0.499549143	0.417779545	0.375177305	0.095798396	0.382936133	2.944621059	0.02188874	0.793784429	-3.9595737	8	112906823	8	F									TRUE
cg24336839	0.309429701	0.36259542	0.375988142	0.445519348	0.428320912	0.460031763	0.095286253	0.396980881	5.381095631	0.001073306	0.773451347	-0.73145259	22	24384397	22	R			GSTT1	NM 000853	TSS200	chr22:243841:	Island		
cg14006741	0.3733277	0.45573187	0.486404834	0.572844851	0.548831714	0.474965229	0.093725797	0.485351033	2.719668881	0.030150034	0.808256584	-4.29260969	20	1294814	20	F	rs6041333		SDCBP2;SDCBI	NM 015685;N	TSS1500;Body	chr20:129368:	S Shore		
cg21265404	0.463870432	0.448681397	0.439301973	0.572877917	0.492016944	0.567276642	0.093439234	0.497337551	4.410277217	0.003215892	0.773451347	-1.91692998	9	90531866	9	R			FAM75C1	NM 0011451:	TSS1500				
cg01297020	0.388084576	0.434928941	0.437276794	0.487580337	0.531379515	0.519648161	0.092772567	0.466483054	5.609074857	0.000845041	0.773451347	-0.47288029	13	106117425	13	R			DAOA;DAOA;D	NM 172370;N	TSS1500;TSS1500;TSS1500				
cg12690369	0.145994894	0.157171837	0.284506191	0.282476068	0.28521407	0.296046544	0.092021253	0.241901601	2.681033913	0.03187153	0.81121464	-4.34999602	12	71314144	12	R			PTPRR	NM 002849	1stExon				TRUE
cg24244747	0.300634092	0.382335148	0.375971503	0.443652679	0.482218354	0.404419502	0.090449931	0.398205213	3.379736102	0.011991835	0.780421619	-3.32580054	6	80885001	6	F			BCKDHB;BCKD	NM 183050;N	Body;Body				TRUE
cg07290652	0.848569893	0.80255739	0.817180421	0.919944882	0.897899732	0.921024375	0.090187095	0.867862782	7.014060106	0.00022168	0.773451347	0.970167981	7	137700005	7	R									TRUE
cg06484303	0.166872901	0.197586727	0.217665078	0.28319607	0.272220223	0.291713748	0.088335112	0.238209125	6.764826886	0.000276709	0.773451347	0.731844678	5	27387958	5	F									TRUE
cg21833076	0.511484992	0.571541294	0.591735006	0.641630901	0.618859029	0.679261025	0.088329888	0.602418708	3.795740916	0.006915757	0.773451347	-2.73943291	11	104643591	11	F									TRUE
cg24693225	0.673402735	0.682258065	0.712559047	0.828524545	0.776394542	0.727350574	0.088016605	0.733414918	3.590104487	0.009049403	0.776859249	-3.02653643	1	63539613	1	R		rs11809015							TRUE
cg27595127	0.329904482	0.348079413	0.354779412	0.455953097	0.392319873	0.447705207	0.08773829	0.388123581	5.162648787	0.00135832	0.773451347	-0.98613457	6	33875991	6	R									
cg16831889	0.201934281	0.192764378	0.229093592	0.346301588	0.31262449	0.227585429	0.087573085	0.251717293	3.06400992	0.018511692	0.7871227	-3.78402026	15	50558051	15	F			HDC	NM 002112	TSS200				
cg26223899	0.339841485	0.365949119	0.402871622	0.439098011	0.465703971	0.465654125	0.087264627	0.413186389	5.362917169	0.001094284	0.773451347	-0.75238577	6	41407766	6	R		rs2496660				chr6:4141058!	N Shelf		
cg15382620	0.39826969	0.468027619	0.453016102	0.596664318	0.469478357	0.513174404	0.086667889	0.483105082	2.623143316	0.034645753	0.813914277	-4.43602976	5	76921025	5	R		rs62362477				chr5:7692388:	N Shelf		
cg16903025	0.444208809	0.331628179	0.441435342	0.516267238	0.499780798	0.460873664	0.08654979	0.449032338	2.768358969	0.028118197	0.804381388	-4.22034378	8	124549553	8	R			FBXO32	NM 058229	Body	chr8:1245525:	N Shelf	RDMR	
cg00366190	0.462919854	0.470455188	0.561913412	0.608459215	0.540731632	0.604991087	0.086297827	0.541578398	2.88880837	0.023686303	0.798424782	-4.04197086	19	33622942	19	R		rs1270591	WDR88	NM 173479	TSS200	chr19:336229:	Island		
cg07473976	0.228647772	0.28216138	0.35174998	0.385267932	0.340165024	0.396012981	0.086295602	0.330667512	2.829227499	0.025778545	0.802600013	-4.13012122	21	39292764	21	F						chr21:392879	S Shelf		
cg08484992	0.168462847	0.255466941	0.181967985	0.305253342	0.272121789	0.286555972	0.08601111	0.244971479	3.838671094	0.006543447	0.773451347	-2.68021454	16	88977278	16	R			CBFA2T3;CBFA	NM 175931;N	5'UTR;Body	chr16:889758!	S Shore		
cg26792288	0.399496729	0.409700242	0.437554378	0.509819893	0.494105038	0.50040858	0.085860721	0.458514143	8.085371993	9.13E-05	0.773451347	1.918464421	16	80578423	16	R			DYNLRB2	NM 130897	Body	chr16:805747	S Shelf		
cg15672543	0.440765269	0.41694778	0.460020465	0.529542775	0.511899791	0.532193732	0.085300928	0.481894969	7.231731303	0.000183566	0.773451347	1.172589395	1	149135501	1	F		rs35503008				chr1:1491375	N Shelf		
cg09143012	0.312322792	0.325498974	0.281451141	0.43336291	0.366857738	0.372206853	0.084384865	0.348616735	4.284791303	0.003742853	0.773451347	-2.08038709	2	161587758	2	F									TRUE
cg22233843	0.394639556	0.413752914	0.376072041	0.456015779	0.50570676	0.473009447	0.083422492	0.43653275	5.658089815	0.000803391	0.773451347	-0.41823364	6	32632565	6	R	rs9274371	rs9274372	HLA-DQB1	NM 002123	Body	chr6:3263215!	Island		
cg06799747	0.214677592	0.271672235	0.317011701	0.34057971	0.408536585	0.301357466	0.082370744	0.308972548	2.483033903	0.042450239	0.82822212	-4.64424257	11	49017551	11	R									
cg20801892	0.225885827	0.25041876	0.18798178	0.280035492	0.339438085	0.291323125	0.082170112	0.262513845	4.064326601	0.004914334	0.773451347	-2.37320777	20	2678368	20	R			EBF4	NM 0011105:	Body	chr20:267290	S Shelf		
cg17194154	0.63337931	0.630832037	0.684978386	0.740883352	0.725427594	0.727393264	0.081504826	0.690482324	5.500232299	0.000946442	0.773451347	-0.59541976	13	95359974	13	F						chr13:953596	S Shore	CDMR	
cg20929922	0.245015167	0.276301807	0.280129777	0.311114363	0.362764192	0.371938217	0.081456674	0.307877254	4.665139079	0.002379934	0.773451347	-1.59219157	5	43484725	5	R			C5orf28	NM 022483	TSS1500	chr5:4348351!	S Shore		
cg13362636	0.49027296	0.478221179	0.586628059	0.577169275	0.608663837	0.61304133	0.081250748	0.55899944	2.907702396	0.023060896	0.798025093	-4.01405657	2	82289309	2	R									TRUE
cg17830420	0.33294373	0.362435111	0.378739741	0.442243375	0.444818613	0.43000182	0.080981742	0.398530398	6.798753583	0.000268383	0.773451347	0.764707098	7	122388911	7	R			CADPS2;CADP!	NM 0010095:	Body;Body;Body				TRUE
cg00985817	0.543077837	0.526049973	0.54262398	0.599865112	0.622263624	0.631899456	0.080758801	0.577629997	8.237622032	8.11E-05	0.773451347	2.043980018	4	23584720	4	F	rs75023074								TRUE
cg20909686	0.269170101	0.297100119	0.339426211	0.375554197	0.395439509	0.375182145	0.080159807	0.341978714	4.681745685	0.002334474	0.773451347	-1.57136911	11	65554042	11	R			OVOL1	NM 004561	TSS1500	chr11:655537	Island		
cg08855630	0.214944431	0.313526868	0.236387321	0.366053748	0.30591378	0.333014262	0.080041057	0.294973402	2.984031111	0.020706851	0.792058824	-3.90151082	3	68978377	3	R			FAM19A4;FAN	NM 182522;N	5'UTR;5'UTR	chr3:6898078:	N Shelf		
cg05298252	0.395373477	0.412644968	0.453300825	0.528583264	0.502637687	0.468979853	0.079627178	0.460253346	4.14644435	0.004436534	0.773451347	-2.26330463	12	123311608	12	R			CCDC62;CCDC(	NM 032573;N	3'UTR;Body;3'UTR				TRUE
cg21643086	0.210641799	0.239292365	0.232790698	0.325347759	0.288207298	0.306313037	0.079047744	0.267098826	6.780552499	0.000272814	0.773451347	0.747093675	6	27243037	6	F									
cg01034654	0.142571714	0.16939739	0.175917535	0.201575191	0.278522757	0.24435776	0.078856356	0.202057058	4.083716735	0.004796627	0.773451347	-2.34716811	9	94484698	9	F						chr9:9448629:	N Shore	CDMR	
cg19632206	0.306684687	0.329899053	0.38679078	0.433376455	0.429751213	0.396087429	0.078613526	0.380431603	3.768563923	0.007163348	0.773451347	-2.77705205	1	190446756	1	F			FAM5C;FAM5(	NM 199051;N	1stExon;5'UTR				
cg26943588	0.716680779	0.7328	0.7885212	0.830840046	0.833752776	0.807866109	0.078152317	0.785076818	4.246064596	0.003924162	0.773451347	-2.1313051	5	74139966	5	F			FAM169A	NM 015566	5'UTR				TRUE
cg26793447	0.430874786	0.408272143	0.433296069	0.508181045	0.504696306	0.493797011	0.078077121	0.463186227	9.110328154	4.26E-05	0.773451347	2.723796872	13	113670930	13	R			MCF2L;MCF2L	NM 0011127:	Body;Body	chr13:113670!	Island		
cg16914890	0.602592388	0.60540429	0.629799302	0.737121052	0.662094763	0.672440254	0.077953363	0.651575342	3.957511428	0.005622203	0.773451347	-2.51762728	2	242839615	2	R		rs13025557							
cg23238483	0.334180971	0.447932388	0.378370941	0.453817405	0.469083755	0.471113199	0.077843353	0.425749777	2.9905783	0.020517154	0.791731075	-3.89187511	3	3886090	3	F			LRRN1	NM 020873	5'UTR				
cg22956547	0.179246566	0.209923664	0.251535164	0.260221836	0.325809465	0.287468279	0.077598062	0.252367496	3.508135477	0.010090859	0.776859249	-3.1425054	19	44493005	19	R		rs35767372	ZNF155;ZNF15	NM 003445;N	Body;Body				
cg10790672	0.608308336	0.64510729	0.626038206	0.707415668	0.709366118	0.69477155	0.077366501	0.665167861	7.612452959	0.00013338	0.773451347	1.514385315	5	78384465	5	R			BHMT2	NM 017614	3'UTR				
cg13168698	0.569105691	0.591168445	0.569918899	0.648383372	0.649579832	0.663771712	0.077180627	0.615321325	9.214145126	3.96E-05	0.773451347	2.800437398	15	77481069	15	F			SGK269	NM 024776	5'UTR				TRUE
cg01472503	0.52426539	0.49460072	0.523846654	0.564152691	0.612373552	0.595071336	0.076294938	0.552385057	5.43891312	0.001009512	0.773451347	-0.6651852	10	79997887	10	F	rs1904422								
cg13844248	0.612440191	0.716502845	0.711340206	0.777096979	0.764690722	0.727199571	0.076234677	0.718211752	2.662833899	0.03271781	0.812133784	-4.37703931	17	59846164	17	F			BRIP1	NM 032043	Body				
cg18850127	0.30543911	0.338514775	0.428596845	0.422051804	0.432579072	0.446361429	0.076147192	0.395590506	2.629913749	0.034308686	0.813749416	-4.42596615	7	39170497	7	F	rs36052669		POU6F2;POU6	NM 007252;N	Body;Body				
cg16877946	0.390430351	0.452199105	0.430031447	0.5072095	0.474389518	0.519100431	0.076012849	0.462226725	4.261174017	0.003852298	0.773451347	-2.11141273	11	84018870	11	R			DLG2;DLG2	NM 0011426!	Body;Body				
cg15099418	0.111777799	0.138431938	0.14594729	0.145157057	0.248019146	0.230647936	0.075889037	0.169996861	2.925352172	0.022492441	0.795556441	-3.98799941	3	117593637	3	R									TRUE
cg01612037	0.579710145	0.671811779	0.687777619	0.713186522	0.729632188	0.723710092	0.075743086	0.684304724	2.871629802	0.024270496	0.800468744	-4.06736796	12	130765389	12	F	rs7298008								
cg01944484	0.662870159	0.663550237	0.652949405	0.712751678	0.736257872	0.757206845	0.075615531	0.697597699	6.682157127	0.000298243	0.773451347	0.651203099	12	149764	12	F		rs2368808	FAM138D	NR 026823	TSS1500				
cg10293542	0.207852828	0.221235103	0.250164438	0.297832234	0.313112078	0.293985385	0.075225776	0.264030344	6.454916316	0.000367824	0.773451347	0.425332798	6	34229016	6	F						chr6:3423109:	N Shelf		
cg21923959	0.165977423	0.182471824	0.18189053	0.235609543	0.204357012	0.314563825	0.074730201	0.214145026	2.897612705	0.023392671	0.798025093	-4.02896068	11	111250566	11	R			POU2AF1	NM 006235	TSS1500				
cg15691325	0.150597196	0.176323161	0.184872876	0.201510989	0.28427831	0.24943719	0.074477752	0.20783662	3.632357337	0.008558577	0.77348616	-2.96708968	2	172387940	2	R			CYBRD1;CYBRE	NM 0011273!	Body;Body				TRUE
cg22490991	0.641325776	0.597826087	0.631047842	0.700634324	0.654956689	0.737394702	0.074262003	0.660530903	3.482844774	0.010437842	0.776859249	-3.178454	4	96465502	4	R			UNC5C	NM 003728	Body	chr4:9646945(	N Shelf		
cg04284993	0.207468237	0.239000806	0.246133683	0.266111952	0.314484481	0.333959116	0.073984274	0.267859713	3.994952751	0.005362114	0.773451347	-2.46681797	5	45038752	5	R									TRUE
cg01238044	0.447630923	0.498349835	0.505124724	0.593594306	0.556453942	0.522763965	0.073872244	0.520667949	3.448571908	0.010928792	0.776859249	-3.2272929	22	24384105	22	F	rs11550606		GSTT1	NM 000853	Body	chr22:243841:	N Shore		
cg14072126	0.197770701	0.221153846	0.222278481	0.261584864	0.333058759	0.26634034	0.073260312	0.250364499	3.804008018	0.006842302	0.773451347	-2.72800942	2	48132074	2	F			FBXO11;FBXO:	NM 018693;N	5'UTR;5'UTR;5	chr2:4813373!	N Shore		
cg16288617	0.682454246	0.719540313	0.708423967	0.788202637	0.752790093	0.788390588	0.072988264	0.739966974	5.48926428	0.000957392	0.773451347	-0.60785974	8	61190272	8	F	rs10099424		CA8	NM 004056	Body	chr8:6119331:	N Shelf		
cg01883540	0.511858812	0.532466208	0.536923915	0.612418547	0.594134515	0.593634521	0.072979549	0.563572753	8.038067954	9.47E-05	0.773451347	1.879023762	4	120646965	4	F									TRUE
cg18273817	0.109016393	0.125508508	0.113088066	0.177313293	0.18737911	0.201815142	0.072964859	0.152353419	8.762637871	5.47E-05	0.773451347	2.460754975	1	8936178	1	F			ENO1	NM 001428	5'UTR	chr1:8938098	N Shore	CDMR	
cg20415809	0.265272938	0.205561819	0.253116531	0.306599342	0.320347336	0.315723794	0.072906395	0.277770293	4.834787578	0.001957987	0.773451347	-1.38141205	2	182321855	2	F			ITGA4;ITGA4	NM 000885;N	5'UTR;1stExon	chr2:1823217(	Island		TRUE
cg13521077	0.163103575	0.199413037	0.183393391	0.226807057	0.240416764	0.29534076	0.072218193	0.218079097	3.895423691	0.006084437	0.773451347	-2.60232245	4	81260418	4	R			C4orf22	NM 152770	Body	chr4:8125704(	S Shelf		
cg26979339	0.26126903	0.283170641	0.298667431	0.336236105	0.348814774	0.373688209	0.071877329	0.316974365	5.612018138	0.000842473	0.773451347	-0.46958947	12	107168153	12	F			RIC8B	NM 018157	TSS1500	chr12:107167:	Island		
cg14003416	0.640105079	0.597020725	0.670321813	0.705761565	0.702406184	0.711960471	0.070893534	0.67126264	4.14739944	0.004431286	0.773451347	-2.26203218	2	12557155	2	R									TRUE
cg04293307	0.313571034	0.317319848	0.371289753	0.426046512	0.433655363	0.354557996	0.070693079	0.369406751	2.899490456	0.023330545	0.798025093	-4.02618649	17	63553581	17	F			AXIN2	NM 004655	Body	chr17:635559(	N Shelf		
cg10615711	0.586840832	0.567759779	0.573489279	0.648613377	0.636242505	0.654950869	0.070572287	0.611316107	8.977547171	4.68E-05	0.773451347	2.62451454	9	140675616	9	R	rs76736785		EHMT1;EHMT1	NM 024757;N	Body;Body	chr9:1406754!	Island		
cg07685034	0.071506083	0.11410602	0.116983032	0.179386482	0.195272582	0.139353375	0.070472435	0.136101262	3.995138271	0.005360859	0.773451347	-2.46656671	21	47269627	21	F			PCBP3;PCBP3	NM 020528;N	TSS1500;TSS1500				
cg16239218	0.515991389	0.51964476	0.542549251	0.590654176	0.594660459	0.603703375	0.070277537	0.561200568	8.145840949	8.71E-05	0.773451347	1.968574226	10	117715809	10	R									TRUE
cg16424311	0.369720102	0.445439148	0.427889447	0.480840009	0.492924528	0.480021311	0.070245717	0.449472424	3.815388788	0.006742571	0.773451347	-2.71229885	6	49700271	6	F	rs77745275		CRISP3	NM 006061	Body				
cg04089420	0.207589025	0.177959099	0.228468433	0.339723584	0.231433812	0.253562176	0.070234338	0.239789355	2.512130234	0.040691533	0.82436524	-4.6010255	10	1378575	10	R			ADARB2	NM 018702	Body	chr10:138250(	N Shelf		TRUE
cg09639890	0.585517584	0.635623229	0.579827991	0.674008811	0.660164356	0.677027027	0.07007713	0.6353615	4.689499442	0.002313578	0.773451347	-1.56166105	3	192135072	3	F			FGF12	NM 004113	Body				TRUE
cg16172329	0.563550575	0.643323442	0.641220087	0.676232334	0.716024161	0.665431747	0.069864713	0.650963724	2.948235859	0.021777411	0.793784429	-3.95424373	2	162907368	2	R			DPP4	NM 001935	Body				
cg20348196	0.365442404	0.439360807	0.424848485	0.490630092	0.445532436	0.502859594	0.069790142	0.44477897	3.128430701	0.016923933	0.785810238	-3.68975612	6	32408284	6	F			HLA-DRA	NM 019111	Body				
cg10821127	0.552026647	0.558498127	0.604917079	0.626771475	0.64250792	0.654901898	0.069579813	0.606603858	4.641080272	0.002447542	0.773451347	-1.62243124	11	91987297	11	R									TRUE
cg04655834	0.133333333	0.152282924	0.166809974	0.202631915	0.217037929	0.24067406	0.069305891	0.185461689	5.633049015	0.000824375	0.773451347	-0.44611017	15	25031239	15	R									TRUE
cg21107549	0.391032989	0.418569953	0.439811495	0.470980126	0.521423812	0.464867065	0.069285522	0.45111424	3.830845121	0.006609654	0.773451347	-2.69099079	6	28979307	6	R						chr6:2897924(	Island	DMR	
cg21884062	0.194183865	0.23718892	0.255733821	0.294790797	0.288580769	0.311474321	0.069246427	0.263658749	4.421987455	0.003171052	0.773451347	-1.90179611	13	36050844	13	R			MIR548F5;NBI	NR 031646;NI	Body;Body;TS!	chr13:360525!	N Shore	RDMR	
cg26627687	0.520317609	0.485883583	0.522561238	0.614214683	0.548785684	0.573463268	0.069233735	0.544204344	3.882331497	0.006187116	0.773451347	-2.62025129	17	58823592	17	R		rs77711639	BCAS3;BCAS3	NM 0010994:	Body;Body				TRUE
cg15695738	0.333860759	0.343147946	0.393825043	0.401842949	0.452595937	0.424057451	0.069220863	0.391555014	3.691087239	0.007923736	0.773451347	-2.88484633	19	35329860	19	R		rs56190201				chr19:353297:	Island		TRUE
cg10121058	0.543996287	0.557998483	0.614882092	0.666214383	0.627512597	0.630679522	0.069176547	0.606880561	3.517129578	0.009970486	0.776859249	-3.12973985	16	84553063	16	R									
cg11307865	0.395054096	0.428012911	0.416564999	0.507951692	0.478085283	0.461023505	0.069142825	0.447782081	5.033212209	0.00156648	0.773451347	-1.14029983	12	27587175	12	F									TRUE
cg25350252	0.533988884	0.556836903	0.493962047	0.609465958	0.577287987	0.605432243	0.069132785	0.562829004	4.127470028	0.004542225	0.773451347	-2.2886116	2	220381129	2	F		rs79585435	ACCN4;ACCN4	NM 182847;N	Body;Body	chr2:2203777	S Shelf		
cg12663553	0.434828776	0.537181378	0.504371934	0.577335914	0.533686441	0.57265657	0.069098946	0.526676836	2.682317702	0.031812706	0.81121464	-4.34808865	3	111852312	3	F	rs79019553	rs61645341	GCET2;GCET2	NM 152785;N	TSS200;TSS200				
cg09047034	0.58499244	0.629830109	0.61775008	0.667443013	0.664695503	0.707390735	0.068985541	0.645350313	4.454400811	0.003050496	0.773451347	-1.86001321	2	38762714	2	F						chr2:3876311	N Shore		TRUE
cg15706017	0.435789474	0.516532968	0.459193548	0.559267241	0.529926026	0.529274005	0.068983761	0.50499721	3.38453188	0.011914271	0.780421619	-3.31891989	6	32269111	6	F			C6orf10	NM 006781	Body				
cg15969149	0.554886598	0.548276867	0.580841235	0.63210438	0.639785347	0.619047619	0.068977549	0.595823674	6.757136835	0.000278636	0.773451347	0.724377173	10	77352287	10	F									
cg09137745	0.588369658	0.603922342	0.618139006	0.62657606	0.66612719	0.724482837	0.06891836	0.637936182	2.97503607	0.020970514	0.792290172	-3.91475398	X	154063101	X	R			LOC10013296:	NM 0011629:	TSS200				
cg14975881	0.139504045	0.174698795	0.126641322	0.22229064	0.216514827	0.208741031	0.068900779	0.181398443	5.549189897	0.000899239	0.773451347	-0.54009711	19	54389945	19	F			PRKCG	NM 002739	Body	chr19:543930:	N Shelf		
cg20116199	0.529931305	0.535443038	0.488718195	0.548660085	0.570569181	0.640855833	0.068664187	0.55236294	2.804975843	0.026685181	0.803015828	-4.16605021	12	64784686	12	R			C12orf56;C12c	NM 0010996:	TSS1500;TSS1!	chr12:647840:	S Shore		
cg15023513	0.625470061	0.649484536	0.670817247	0.704692664	0.714064116	0.732852843	0.068612593	0.682896911	5.344588754	0.001115899	0.773451347	-0.77353922	15	87667171	15	F									
cg07502050	0.636580992	0.686906353	0.731439241	0.754055901	0.743061647	0.763611143	0.068600702	0.71927588	3.12863667	0.016919096	0.785810238	-3.68945531	2	218169223	2	R		rs34960128	DIRC3	NR 026597	Body				TRUE
cg17862558	0.480201765	0.526010218	0.53200247	0.565868263	0.574297189	0.603740757	0.068563919	0.54702011	4.276661895	0.003780134	0.773451347	-2.09105722	4	106137048	4	F			TET2;TET2	NM 0011272(	5'UTR;5'UTR				TRUE
cg07897695	0.221162884	0.27978636	0.312921571	0.348240275	0.332968596	0.338281063	0.068539706	0.305560125	3.216793701	0.014978466	0.785810238	-3.56106084	15	25327919	15	R			SNORD116-16;	NR 003331;NI	Body;TSS1500;TSS1500				
cg21896142	0.251155624	0.222891017	0.240042434	0.329533251	0.30835356	0.281787663	0.068528466	0.272293925	5.174755069	0.001340482	0.773451347	-0.97184017	X	80457315	X	R			HMGN5;HMGI	NM 030763;N	1stExon;5'UTR;5'UTR;1stExon				
cg25214900	0.573629865	0.56297043	0.592124948	0.624533264	0.648672566	0.660913458	0.068464682	0.610474089	5.915965315	0.000618826	0.773451347	-0.13612047	12	79693302	12	F			SYT1;SYT1;SYT	NM 005639;N	Body;Body;Body				TRUE
cg22282280	0.22964229	0.254153714	0.23993607	0.313029447	0.289025461	0.326681989	0.068334941	0.275411495	6.107727018	0.0005123	0.773451347	0.067919762	17	33678143	17	R			SLFN11;SLFN1	NM 0011045!	3'UTR;3'UTR;3'UTR;3'UTR;3'UTR				
cg03900581	0.508103497	0.519745801	0.486586494	0.550681663	0.560300867	0.608433735	0.068326831	0.538975346	4.196053755	0.004172745	0.773451347	-2.19738796	1	96468567	1	R									TRUE
cg07263979	0.688374337	0.747577368	0.75849306	0.758058282	0.82364545	0.817612688	0.068290552	0.765626864	2.901372807	0.023268443	0.798025093	-4.02340571	2	241585888	2	R						chr2:2415866!	N Shore		
cg01632300	0.662607127	0.671985457	0.629552858	0.730364593	0.73692274	0.701626898	0.068256263	0.688843279	4.95589611	0.001707621	0.773451347	-1.23355786	6	152957223	6	F			SYNE1;SYNE1	NM 182961;N	5'UTR;5'UTR	chr6:1529578:	N Shore		
cg26909813	0.112669882	0.113869987	0.145304671	0.158205431	0.171339564	0.246246246	0.067982234	0.157939297	2.96103008	0.021388173	0.793159331	-3.93538565	17	45057218	17	R		rs9901534	RPRML	NM 203400	TSS1500	chr17:450553:	S Shore		
cg26623696	0.403370787	0.420090039	0.424271846	0.483503535	0.545600772	0.422555464	0.0679757	0.449898741	2.434372136	0.045568873	0.830879737	-4.7164649	11	90797970	11	R								RDMR	
cg20101012	0.343003413	0.376644081	0.387967605	0.446057741	0.43803492	0.42743808	0.067971881	0.403190973	5.583747913	0.000867504	0.773451347	-0.50124733	6	168570436	6	R	rs12175962								
cg05971102	0.608522727	0.656768559	0.646473145	0.743608473	0.689136836	0.682681909	0.067887596	0.671198608	3.546059075	0.009593279	0.776859249	-3.08874717	2	3753297	2	R						chr2:3750828	S Shore	RDMR	TRUE
cg25029689	0.446748351	0.509655341	0.495853659	0.537002603	0.538266599	0.580607477	0.067873109	0.518022338	3.599380046	0.008939095	0.776859249	-3.01346675	2	182458107	2	F			CERKL;CERKL;C	NM 0010303:	Body;Body;Body;Body;Body;Body;Body				TRUE
cg17644776	0.436386483	0.421069452	0.379702926	0.488062368	0.44518647	0.507323819	0.067804599	0.446288586	3.447084367	0.010950658	0.776859249	-3.22941582	2	200775616	2	F			C2orf69	NM 153689	TSS1500	chr2:2007757	N Shore		
cg01109012	0.252598203	0.260404789	0.271540118	0.257049345	0.374114522	0.356630824	0.067750527	0.295389634	2.376579098	0.049580915	0.833631366	-4.80211256	X	37707161	X	R			DYNLT3	NM 006520	TSS1500	chrX:3770629!	S Shore		
cg12954928	0.222428174	0.184992571	0.24638169	0.260899654	0.27608092	0.319946452	0.067708197	0.251788244	3.420115871	0.011355379	0.777995215	-3.26794845	4	126235794	4	F						chr4:1262358!	N Shore	DMR	
cg00843787	0.576644585	0.635112594	0.580507267	0.662233265	0.645833333	0.687211339	0.067671164	0.631257064	3.807518064	0.006811373	0.773451347	-2.72316208	15	24119320	15	R						chr15:241232:	N Shelf		
cg14023589	0.512995313	0.579247817	0.498222129	0.566208142	0.628556375	0.598627787	0.067642348	0.563976261	2.82654758	0.025877118	0.802600013	-4.13409026	12	72875216	12	R			TRHDE	NM 013381	Body				
cg12015991	0.320478723	0.37173806	0.391442155	0.413043478	0.46932698	0.404150737	0.067620752	0.395030022	2.949144672	0.021749516	0.793784429	-3.95290383	6	32490043	6	F			HLA-DRB5	NM 002125	Body	chr6:3248974:	Island		
cg23746638	0.182493369	0.205303948	0.260094787	0.292991362	0.266055046	0.29150638	0.067553561	0.249740815	3.479338009	0.010486963	0.776859249	-3.18344469	6	40991828	6	R						chr6:4099580:	N Shelf		
cg08646313	0.498526523	0.483146067	0.488746509	0.596951819	0.526959093	0.548930297	0.067474037	0.523876718	3.998725036	0.005336649	0.773451347	-2.46170997	8	98058371	8	R			PGCP	NM 016134	Body				TRUE
cg13932501	0.138200138	0.163287443	0.203752316	0.218371153	0.245476392	0.243236257	0.067281302	0.20205395	4.016784174	0.00521656	0.773451347	-2.43728468	9	94060853	9	F			AUH	NM 001698	Body				TRUE
cg25582541	0.423247414	0.465305471	0.489483748	0.558392377	0.497569107	0.523754121	0.067226324	0.492958706	3.271865933	0.013888178	0.781602075	-3.48123406	3	188625895	3	F									TRUE
cg06821828	0.256907457	0.278738404	0.257783217	0.334504769	0.349864335	0.310418407	0.067119478	0.298036098	5.851383153	0.000660127	0.773451347	-0.20593121	14	93698216	14	R									TRUE
cg27212541	0.246491319	0.254026485	0.241839763	0.299333806	0.31042555	0.333950454	0.067117414	0.28101123	6.94432153	0.000235722	0.773451347	0.90419772	3	49507385	3	R			DAG1;DAG1	NM 004393;N	TSS200;TSS20(	chr3:4950738	Island		
cg10033502	0.538643119	0.587826344	0.570582227	0.593152334	0.624930178	0.680314694	0.067115172	0.599241483	2.939293324	0.022053923	0.793816873	-3.96743091	2	152496744	2	F			NEB;NEB;NEB	NM 004543;N	Body;Body;Body				
cg01918222	0.506118478	0.507703332	0.529926814	0.592134778	0.566715192	0.586222925	0.06710809	0.54813692	6.915800684	0.000241751	0.773451347	0.877059081	16	87277142	16	R		rs62056197							TRUE
cg14395423	0.228107533	0.229602158	0.225819799	0.351921553	0.276830953	0.255949302	0.067057439	0.261371883	2.9462215	0.021839375	0.793784429	-3.95721377	X	74516489	X	F			UPRT;UPRT	NM 145052;N	Body;Body				TRUE
cg21161367	0.572206096	0.494442776	0.575415586	0.6395218	0.600328138	0.603239503	0.067008328	0.580858983	2.928835407	0.022382018	0.795185396	-3.98285918	1	108474727	1	F			VAV3	NM 006113	Body				TRUE
cg23645302	0.530751708	0.529480346	0.563474072	0.661410159	0.605618667	0.557626474	0.066983058	0.574726904	2.694509902	0.031259673	0.810402361	-4.32997587	4	69084723	4	F			FLJ41562	NM 0011299(	TSS1500				
cg02825211	0.644584066	0.655868336	0.661007026	0.700566716	0.749776477	0.711961531	0.066948432	0.687294025	5.173296715	0.001342617	0.773451347	-0.97356099	19	8808663	19	R			ACTL9	NM 178525	1stExon	chr19:880781:	Island		
cg09379146	0.535111411	0.522187405	0.531457707	0.606447974	0.580585494	0.602493917	0.066923621	0.563047318	7.895755082	0.000106044	0.773451347	1.75907754	3	156395056	3	F	rs35240871		TIPARP	NM 015508	5'UTR	chr3:1563918:	S Shore	RDMR	
cg11696466	0.627249521	0.595032829	0.608876093	0.676364062	0.685655042	0.669883802	0.066914821	0.643843558	7.119043695	0.000202285	0.773451347	1.068449931	X	119510970	X	R			ATP1B4;ATP1B	NM 0011424	Body;Body				TRUE
cg18241469	0.535585224	0.542272183	0.535425268	0.61122735	0.604863355	0.597865009	0.066891013	0.571206398	10.93820986	1.30E-05	0.773451347	3.958712607	3	168136028	3	F			C3orf50	NR 021485	Body				TRUE
cg22331840	0.654985094	0.653647921	0.661666838	0.754870705	0.716004246	0.699861878	0.066812325	0.69017278	4.930184197	0.001757646	0.773451347	-1.26476659	13	25504027	13	R			LOC646405	NR 026730	Body	chr13:255061:	N Shelf		
cg03706951	0.629820568	0.645186243	0.609188796	0.700214004	0.695390836	0.688873013	0.066760749	0.661445577	6.848430002	0.000256696	0.773451347	0.8125838	17	39465518	17	F									
cg08491641	0.129854234	0.152229532	0.173220089	0.1910184	0.273182121	0.191079233	0.066658633	0.185097268	2.841286881	0.025339846	0.802456617	-4.11226502	3	97806386	3	R			OR5AC2	NM 054106	1stExon				
cg17502267	0.314503263	0.359576295	0.367197657	0.431075595	0.380737651	0.429270544	0.066602192	0.380393501	3.613938836	0.008768888	0.776101911	-2.99297497	15	59981239	15	R			BNIP2	NM 004330	Body	chr15:599812:	Island		
cg13483953	0.577252562	0.556512726	0.580764563	0.619625066	0.641363178	0.653167105	0.066541833	0.604780867	6.209771498	0.000464111	0.773451347	0.174551343	6	23408789	6	R									TRUE
cg23131974	0.560276011	0.598682119	0.582438467	0.636954394	0.640637911	0.66329654	0.066497416	0.61371424	5.685413018	0.000781174	0.773451347	-0.38791458	10	1767723	10	F			ADARB2	NM 018702	Body				
cg24646009	0.186531008	0.222566372	0.262862863	0.238786843	0.330184435	0.302424394	0.066478476	0.257225986	2.459180821	0.043950477	0.829725495	-4.67965463	7	107221327	7	R			BCAP29;BCAP2	NM 018844;N	Body;Body;Bo(	chr7:1072203	S Shore		
cg12844277	0.383736816	0.386247629	0.376262321	0.421825376	0.46345422	0.460294396	0.066442409	0.41530346	5.725472017	0.000749832	0.773451347	-0.34364812	14	47544244	14	R		rs72190896	MDGA2;MDGA	NM 0011134!	Body;Body				
cg25026904	0.304732883	0.353111839	0.327052261	0.387943389	0.435766626	0.36036343	0.066392154	0.361495071	3.240476556	0.014498755	0.783559556	-3.52669529	4	168829894	4	F									TRUE
cg26807107	0.399109242	0.398063079	0.389000943	0.483601566	0.408312488	0.493349564	0.066363451	0.428572814	3.129628688	0.01689582	0.785810238	-3.68800654	16	25228603	16	R			AQP8	NM 001169	Body				
cg12950441	0.557128858	0.588598652	0.624053503	0.662054456	0.623008465	0.683343197	0.066208368	0.623031189	3.220026925	0.014911984	0.785810238	-3.55636592	X	113818537	X	R			HTR2C	NM 000868	TSS200	chrX:1138185:	Island		TRUE
cg00538247	0.419116493	0.419751863	0.461580257	0.518222771	0.495032665	0.485720477	0.066175767	0.466570754	4.749461043	0.002158809	0.773451347	-1.4868895	1	7113389	1	R			CAMTA1	NM 015215	Body				
cg03273860	0.420843071	0.428437553	0.446064007	0.527459412	0.460583333	0.50572762	0.066141911	0.464852499	3.934067422	0.005792067	0.773451347	-2.54954353	X	150815678	X	F			PASD1	NM 173493	Body				
cg06484993	0.569072531	0.614716459	0.579293299	0.645005957	0.651491966	0.664976228	0.066130621	0.620759407	5.285281038	0.001189172	0.773451347	-0.84231704	5	38259398	5	R			EGFLAM	NM 152403	Body	chr5:3825782!	S Shore		
cg13119853	0.156824513	0.205686104	0.178562845	0.219251337	0.245670678	0.274249826	0.066032793	0.213374217	3.894901207	0.006088499	0.773451347	-2.60303749	17	48939676	17	R			TOB1;TOB1	NM 005749;N	1stExon;3'UTR	chr17:489429	N Shelf		
cg04316925	0.467821552	0.511087731	0.49889803	0.582784536	0.540806225	0.551976078	0.065919842	0.525562359	4.516169276	0.002834519	0.773451347	-1.78082474	16	87471211	16	F			ZCCHC14	NM 015144	Body				TRUE
cg26916916	0.551501365	0.597572362	0.603057839	0.634279124	0.655825942	0.659686308	0.065886603	0.616987157	4.47589075	0.00297336	0.773451347	-1.8323979	17	9070303	17	R			NTN1	NM 004822	Body	chr17:906615:	S Shelf		
cg25488697	0.309074369	0.281122031	0.302205731	0.356886496	0.415333472	0.317654352	0.06582407	0.330379412	2.851405056	0.024977839	0.801369037	-4.09728849	1	38510383	1	R			POU3F1;POU3	NM 002699;N	3'UTR;1stExon	chr1:3851010:	Island		
cg09884341	0.568310763	0.625301953	0.621170338	0.70409989	0.649396711	0.658355501	0.065689683	0.637772526	3.340228078	0.012651898	0.780421619	-3.38258195	5	87974464	5	F			LOC645323;LC	NR 015436;NI	Body;TSS1500	chr5:8797609	N Shore		TRUE
cg21977075	0.370185859	0.401693451	0.412542352	0.450893544	0.46888434	0.461445821	0.065600681	0.427607561	5.646093564	0.000813369	0.773451347	-0.43157763	17	65040527	17	F			CACNG1	NM 000727	TSS200	chr17:650407:	N Shore		
cg04365696	0.845332415	0.852058618	0.826165891	0.933261757	0.927013796	0.859856115	0.065524915	0.873948099	3.360446538	0.01230935	0.780421619	-3.35350202	13	43834391	13	R			ENOX1;ENOX1	NM 017993;N	Body;Body				TRUE
cg05614028	0.512160742	0.548840219	0.536989408	0.617862375	0.597280476	0.579084866	0.065412449	0.565369681	5.076186941	0.001493672	0.773451347	-1.08884353	18	44785758	18	F						chr18:447874(	N Shore	RDMR	
cg26955881	0.275958755	0.355721287	0.346182733	0.400925887	0.34976602	0.423286302	0.065371811	0.358640164	2.53319675	0.039465338	0.822883069	-4.56972411	X	21393407	X	F			CNKSR2;CNKSI	NM 0011686	Body;Body;Bo(	chrX:2139183!	Island		
cg11022804	0.130523493	0.152621723	0.207583725	0.227635783	0.206526807	0.25253563	0.065323093	0.19623786	3.143035458	0.016584589	0.785810238	-3.66843549	X	152760227	X	F			BGN	NM 001711	TSS200				TRUE
cg08751025	0.555339806	0.619728025	0.616727426	0.659264539	0.648357871	0.679864747	0.065230633	0.629880402	3.590822368	0.009040813	0.776859249	-3.02552451	2	62591489	2	F									TRUE
cg09749813	0.436042403	0.455037594	0.463429081	0.498118713	0.483406083	0.56866326	0.065226326	0.484116189	3.026322769	0.01951354	0.789625816	-3.83932336	6	85474209	6	F			TBX18	NM 0010805(	TSS1500	chr6:8547270:	S Shore	DMR	
cg17594351	0.48336	0.521864581	0.523845692	0.548579228	0.584003189	0.592140202	0.065217449	0.542298815	4.301853156	0.003665916	0.773451347	-2.05802473	12	81101397	12	F	rs7313114	rs1185873	MYF6	NM 002469	TSS200	chr12:811020:	N Shore		
cg04362706	0.481775716	0.491204867	0.50445464	0.578512609	0.568007759	0.5264683	0.065184482	0.525070649	4.644134265	0.002438843	0.773451347	-1.61858786	1	57570305	1	F	rs12037367		DAB1	NM 021080	Body				TRUE
cg15936861	0.592221754	0.57657737	0.562431113	0.628893501	0.660297667	0.637323596	0.065094842	0.609624167	5.951138589	0.000597556	0.773451347	-0.09833298	12	130276151	12	R			TMEM132D	NM 133448	Body				TRUE
cg18348830	0.555881946	0.556616766	0.604215745	0.62392213	0.637975022	0.65004151	0.065074735	0.60477552	4.525268318	0.002804156	0.773451347	-1.76920783	3	54961956	3	R		rs4245920	LRTM1;CACNA	NM 020678;N	5'UTR;Body;1stExon				
cg27637606	0.594261603	0.656285206	0.667344816	0.728872165	0.715281408	0.668949298	0.065070415	0.671832416	2.865559321	0.024480558	0.801075951	-4.07634643	15	78420039	15	F			CIB2	NM 006383	Body	chr15:784235!	N Shelf	RDMR	
cg14431577	0.219563173	0.261875386	0.276259817	0.302770748	0.317075306	0.332926153	0.06502461	0.285078431	4.220968833	0.004046804	0.773451347	-2.16441971	12	70002985	12	F			LRRC10;LRRC1(	NM 201550;N	1stExon;3'UTR				
cg04326562	0.215826508	0.207453559	0.229684825	0.287306642	0.278715773	0.281938518	0.06499868	0.250154304	8.862564791	5.09E-05	0.773451347	2.537376741	19	18320186	19	F			PDE4C;PDE4C;	NM 0010988:	3'UTR;3'UTR;3	chr19:183191	S Shore	CDMR	
cg19826873	0.493090452	0.491873549	0.491361664	0.57787168	0.565406188	0.527610056	0.064854086	0.524535598	5.157076497	0.001366619	0.773451347	-0.99272116	2	178787741	2	R		rs76197733	PDE11A;PDE11	NM 0010771!	Body;Body;TSS200				
cg12695797	0.518138425	0.53719881	0.573506398	0.615150242	0.617200004	0.590914875	0.064807163	0.575351459	4.372100724	0.003366997	0.773451347	-1.96641002	6	127840704	6	R			C6orf174	NM 0010122:	TSS1500	chr6:1278367:	S Shelf		
cg05130482	0.544005971	0.574235059	0.553214295	0.627416826	0.617548083	0.62079844	0.064769341	0.589536446	7.379640739	0.000161892	0.773451347	1.307191703	8	98271949	8	R									TRUE
cg14393693	0.560320506	0.570677821	0.599361165	0.665580448	0.60044128	0.658565361	0.064742532	0.609157764	3.45371179	0.010853601	0.776859249	-3.21995964	6	166045279	6	R			PDE10A;PDE1(	NM 0011306!	Body;5'UTR				TRUE
cg16689609	0.582125916	0.639138785	0.654407956	0.682809707	0.659140441	0.727945427	0.064740973	0.657594705	2.781879875	0.027579851	0.804381388	-4.20028977	6	144682208	6	F			UTRN	NM 007124	Body				TRUE
cg26880412	0.378905207	0.359146488	0.356692057	0.405723906	0.387891226	0.495202952	0.064691444	0.397260306	2.458450974	0.043997234	0.829725495	-4.68073787	7	57188283	7	R			ZNF479	NM 033273	Body				
cg07376916	0.577807398	0.599628529	0.634639215	0.645349359	0.708085061	0.652476946	0.064612075	0.636331085	3.183055663	0.015691444	0.785810238	-3.61011184	20	15986081	20	F			MACROD2;MA	NM 080676;N	Body;Body				TRUE
cg00424467	0.547916114	0.508367767	0.542063529	0.651408167	0.544846274	0.595892673	0.064599901	0.565082421	2.511186738	0.040747364	0.82436524	-4.60242719	20	1377284	20	F						chr20:137325!	S Shelf		
cg05583965	0.580403987	0.62129115	0.658564549	0.703976204	0.695966908	0.653789279	0.064490902	0.652332013	3.003771202	0.020140488	0.790083167	-3.87246795	2	73867196	2	R									
cg23811512	0.231940299	0.276238721	0.182390928	0.325123871	0.264401566	0.294503094	0.064486194	0.26243308	2.571364088	0.037340338	0.819433132	-4.51299813	13	75928922	13	R			TBC1D4	NM 014832	Body				TRUE
cg08681437	0.175175062	0.186456147	0.201633706	0.267507621	0.243722173	0.245481282	0.064482054	0.219995999	6.660210805	0.000304272	0.773451347	0.629659593	6	28964249	6	R			ZNF311	NM 0010108:	Body				
cg14972889	0.476575664	0.494647059	0.516317486	0.529797377	0.546309822	0.604717462	0.064428151	0.528060812	3.216685926	0.014980687	0.785810238	-3.56121735	X	125687856	X	F			DCAF12L1	NM 178470	TSS1500	chrX:1256857:	S Shore	CDMR	
cg05257397	0.391823295	0.3659601	0.378445855	0.468995011	0.43273963	0.427601195	0.064368862	0.410927514	5.14832794	0.001379762	0.773451347	-1.00307127	15	28341500	15	R			OCA2	NM 000275	5'UTR	chr15:283397:	Island		
cg17362900	0.530039209	0.548277864	0.553497555	0.645402638	0.585368162	0.593946143	0.064300772	0.576088595	3.999320601	0.005332641	0.773451347	-2.46090371	6	33047944	6	R			HLA-DPB1	NM 002121	Body	chr6:3304841(	N Shore		
cg25783997	0.18258427	0.236479938	0.212689443	0.257386476	0.296548371	0.270596591	0.064259262	0.242714182	4.120856741	0.004579709	0.773451347	-2.29744445	2	185462928	2	R			ZNF804A	NM 194250	TSS200	chr2:1854632(	N Shore	CDMR	

cg09785391	0.462583597	0.519319138	0.492271221	0.443657241	0.429622332	0.445905388	-0.051663	0.46555982	-3.68808881	0.007954877	0.773451347	-2.88903423	18	5297098	18	F			ZFP161;ZFP16	NM 00114382	TSS1500;TSS1	chr18:529532	Island		
cg10274108	0.864824968	0.890796863	0.863036444	0.862752369	0.81308711	0.787697281	-0.05170717	0.847032506	-2.74979255	0.028875485	0.805418534	-4.24789151	4	38082931	4	R			TBC1D1	NM 015173	Body				
cg06201264	0.637465051	0.654689234	0.615990547	0.553669858	0.577213452	0.622133236	-0.05170943	0.610193563	-2.8388477	0.02542794	0.802491094	-4.11587614	X	106446861	X	R			NUP62CL	NM 017681	5'UTR	chrX:1064490	N Shelf		
cg10440578	0.827906977	0.786599842	0.85154911	0.770861223	0.771012828	0.768942127	-0.05174658	0.796145351	-3.3786357	0.012009709	0.780421619	-3.32737969	1	115397857	1	R			SYCP1	NM 003176	5'UTR	chr1:1153974	Island		
cg13891978	0.171850824	0.200027979	0.176384964	0.1688859	0.108566653	0.115556118	-0.0517517	0.15687874	-3.09266384	0.017786686	0.785810238	-3.74204896	14	63512037	14	F		rs78908869	KCNH5;KCNH5	NM 172375;N	TSS200;5'UTR;	chr14:635120	Island		TRUE
cg10162971	0.709454716	0.715672823	0.728159158	0.683716891	0.689094802	0.625116878	-0.05178604	0.691869211	-3.06052533	0.018601984	0.7871227	-3.78912893	2	10093493	2	R			GRHL1	NM 198182	Body	chr2:1009090	S Shore	CDMR	
cg17904575	0.756360078	0.735462345	0.73516393	0.677039851	0.703172979	0.691125691	-0.05188261	0.716387479	-5.55180358	0.000896794	0.773451347	-0.53715303	14	102290370	14	R			PPP2R5C;PPP2	NM 0011617	Body;Body;Body;Body;Body				TRUE
cg23489390	0.332395764	0.311360276	0.385693942	0.3085241	0.297826906	0.267404179	-0.05189827	0.317200861	-2.60505629	0.035563239	0.815698288	-4.46291548	2	36712570	2	R			CRIM1	NM 016441	Body				TRUE
cg09177545	0.832796747	0.819628266	0.842772894	0.827905121	0.745601486	0.765888187	-0.05193437	0.80576545	-2.5756885	0.037107177	0.818830892	-4.50657021	16	85458291	16	F	rs2054704	rs79586467							
cg04741094	0.321773253	0.353077916	0.315915436	0.286719153	0.282276254	0.265947467	-0.05194124	0.304284913	-4.62842236	0.002483963	0.773451347	-1.6383758	3	197209034	3	R									TRUE
cg10328768	0.284613957	0.346294867	0.292486215	0.264940577	0.246316209	0.256309591	-0.05194289	0.281826903	-3.22120807	0.014887776	0.785810238	-3.55465106	1	3210325	1	R			PRDM16;PRDM	NM 022114;N	Body;Body				
cg03133378	0.543734744	0.559466356	0.528890083	0.480529023	0.518456371	0.477165128	-0.05198022	0.518040284	-3.95905855	0.005611187	0.773451347	-2.51552381	7	99195931	7	R						chr7:9919568	Island		
cg18414754	0.652232487	0.692481446	0.69410408	0.628929793	0.637244823	0.616342412	-0.05210033	0.65355584	-4.17468759	0.004284182	0.773451347	-2.22573309	3	138668832	3	F			C3orf72	NM 0010400	Body	chr3:1386686	Island	DMR	TRUE
cg12767937	0.730443519	0.758166037	0.751475797	0.721462237	0.656826568	0.705408444	-0.05212937	0.720630434	-3.08935269	0.017868896	0.785810238	-3.74689555	17	42886235	17	F			GJC1;GJC1	NM 0010803	5'UTR;5'UTR				
cg16878059	0.709756642	0.757497415	0.728800727	0.682639434	0.66227027	0.694651609	-0.05216449	0.705936016	-3.79479993	0.006924172	0.773451347	-2.74073376	2	68692224	2	R			FBXO48	NM 0010246	Body	chr2:6869404	N Shore		
cg19278232	0.732724181	0.706313825	0.745545977	0.673580503	0.678615406	0.675890826	-0.05216575	0.702111786	-5.10874878	0.00144101	0.773451347	-1.05003509	6	49576124	6	F			RHAG	NM 000324	Body				TRUE
cg18097763	0.491413201	0.534973842	0.468948585	0.460742156	0.413689357	0.464229249	-0.05222496	0.472332732	-2.62119685	0.034743295	0.814167789	-4.43892304	6	32548402	6	F	rs28732277	rs67884866	HLA-DRB1	NM 002124	Body	chr6:3255185	N Shelf		
cg18182438	0.764553965	0.788436123	0.799127431	0.732086451	0.7498998	0.713431646	-0.05223321	0.757922569	-4.25854365	0.003864704	0.773451347	-2.11487332	13	38327937	13	F			TRPC4;TRPC4;T	NM 0011359	Body;Body;Body;Body;Body;Body				TRUE
cg15999104	0.752550467	0.765382714	0.74353339	0.738316334	0.683925972	0.682360073	-0.05228806	0.727678158	-3.34069809	0.01264382	0.780421619	-3.38190544	3	93780377	3	F			NSUN3;DHFRL	NM 022072;N	TSS1500;5'UT	chr3:9378164	N Shore		
cg02498120	0.65055788	0.66800638	0.635887673	0.592081218	0.584554091	0.620875151	-0.05231382	0.625327066	-4.32040807	0.003584217	0.773451347	-2.03375458	21	15095903	21	R						chr21:150956	Island		
cg20504925	0.815799397	0.783669725	0.868073823	0.766975927	0.791118132	0.752456473	-0.0523308	0.796348913	-2.46811131	0.043382492	0.82928137	-4.66639857	10	126304204	10	R		rs79648067				chr10:126303	Island		
cg26415571	0.555950969	0.552793711	0.561780796	0.519354279	0.520081227	0.473908413	-0.05239385	0.530644899	-4.08101882	0.004812818	0.773451347	-2.35078795	1	91172930	1	R						chr1:9117210	S Shore	DMR	
cg22113930	0.333196187	0.371109608	0.315425775	0.25483871	0.288146408	0.319206892	-0.05251319	0.31365393	-2.68738285	0.031581721	0.810676603	-4.34056351	15	26108410	15	F			ATP10A	NM 024490	TSS200	chr15:261075	Island		
cg19974223	0.807711886	0.829936175	0.84042711	0.790274904	0.774801962	0.755336922	-0.05255379	0.79974816	-4.46072724	0.003027561	0.773451347	-1.85187635	12	52281676	12	F			ANKRD33;ANK	NM 0011300	TSS200;TSS200				
cg08141518	0.666782167	0.657827103	0.687424817	0.618848358	0.615542895	0.619734491	-0.05263611	0.644359972	-6.23692409	0.000452162	0.773451347	0.202700223	X	133680974	X	R			MIR424;MGC1	NR 029946;N	TSS1500;TSS1	chrX:1336785	S Shore	CDMR	
cg16434502	0.83483871	0.80292695	0.818804552	0.792837079	0.735725355	0.769995093	-0.0526709	0.79252129	-3.44043816	0.011048932	0.776859249	-3.23890401	17	61434321	17	F			TANC2	NM 025185	Body				TRUE
cg01820463	0.79483592	0.779981213	0.785311347	0.766997545	0.733636428	0.701467269	-0.05267575	0.76037162	-3.37287037	0.012103825	0.780421619	-3.33565554	2	27616144	2	R			FTHL3;PPM1G	NR 002201;N	Body;Body;Bo	chr2:2761620	N Shore		
cg09464875	0.261120389	0.333527561	0.290510676	0.241113219	0.249152542	0.236666667	-0.05274207	0.268681842	-3.10021013	0.017600826	0.785810238	-3.73100678	2	168725510	2	F			B3GALT1	NM 020981	5'UTR				
cg24222165	0.773118578	0.816460587	0.823339044	0.768935978	0.747277792	0.738374165	-0.05277676	0.777917691	-3.58664751	0.009090891	0.776859249	-3.03141027	15	35663907	15	F			ATPBD4	NM 080650	3'UTR				
cg21173221	0.759297861	0.724731407	0.743726094	0.708372664	0.666718628	0.694069738	-0.05286478	0.716152732	-4.05362548	0.004980648	0.773451347	-2.38760204	2	60981462	2	R						chr2:6098319	N Shore		
cg01856069	0.84052324	0.858977436	0.842961165	0.810212552	0.821846554	0.751707317	-0.05289847	0.821038044	-2.96719826	0.02120316	0.792290172	-3.92629791	7	93474069	7	R									
cg05177746	0.298677546	0.354821924	0.366134865	0.312825767	0.289432254	0.258663735	-0.05290419	0.313426015	-2.58146148	0.036798266	0.81851826	-4.49798893	10	4720912	10	F	rs12098244	rs57548018	LOC10021600	NR 024475	TSS1500				
cg20327105	0.341361514	0.316307759	0.336787565	0.278450081	0.300399645	0.256705585	-0.05296718	0.305002025	-4.29250537	0.00370785	0.773451347	-2.07027118	1	170043996	1	R			KIFAP3	NM 014970	TSS200	chr1:1700436	Island		TRUE
cg05626073	0.644107136	0.658615621	0.685801364	0.606975479	0.590518622	0.632028322	-0.05300057	0.636341091	-3.78033568	0.007054937	0.773451347	-2.76074488	11	971527	11	R			AP2A2	NM 012305	Body	chr11:975211	N Shelf		
cg16149164	0.815340848	0.781917004	0.762881065	0.753383407	0.738064418	0.70956631	-0.05304159	0.760192175	-3.30672891	0.013242234	0.780421619	-3.43086167	14	105617308	14	F			JAG2;JAG2	NM 002226;N	Body;Body	chr14:105616	Island		
cg14063347	0.770006172	0.772764969	0.792592593	0.776610119	0.690723246	0.708715596	-0.05310492	0.751902116	-2.50078368	0.041371051	0.825508259	-4.61795055	9	88207974	9	F			AGTPBP1	NM 015239	Body				TRUE
cg03232933	0.835027299	0.849865515	0.820835204	0.780677803	0.788770053	0.776934879	-0.05311509	0.808685126	-6.19341735	0.00047148	0.773451347	0.157551832	21	18985641	21	F			BTG3;BTG3	NM 0011309	TSS1500;TSS1	chr21:189845	Island		
cg10769531	0.341232227	0.317268208	0.367408399	0.307213689	0.306760848	0.252541972	-0.05313078	0.315404224	-2.89071129	0.023622511	0.798033269	-4.03915855	7	110753971	7	R			LRRN3;IMMP2	NM 0010996	5'UTR;Body;5'UTR;5'UTR				TRUE
cg18320647	0.190422535	0.209820508	0.252717391	0.175431862	0.156256276	0.161618301	-0.053218	0.191044479	-3.42970159	0.011209705	0.776918821	-3.25424261	14	61201977	14	R			MNAT1	NM 002431	Body			DMR	
cg13355032	0.819986465	0.770220187	0.778045258	0.766370934	0.750411711	0.691294387	-0.05339163	0.76272149	-2.47380471	0.043024344	0.829032531	-4.65794621	12	71524030	12	R			TSPAN8	NM 004616	Body				
cg17968943	0.303180396	0.345719096	0.375397667	0.292803413	0.319130805	0.252050065	-0.05343763	0.314713574	-2.38877303	0.048705245	0.832214978	-4.78405536	19	1715374	19	R						chr19:171883	N Shelf		
cg19318364	0.667336683	0.620738636	0.619745575	0.597084162	0.539480019	0.610853559	-0.05346772	0.609206439	-2.53427765	0.039403465	0.822883069	-4.56811787	6	55774999	6	R									
cg16253870	0.357212318	0.390161931	0.436659368	0.34858519	0.360808709	0.31416078	-0.05349298	0.367931383	-2.53266695	0.039495702	0.822883069	-4.5705114	12	68959172	12	R									TRUE
cg24322139	0.559021624	0.603059772	0.615365144	0.550559152	0.513491635	0.552787503	-0.05353608	0.565714138	-3.14842856	0.016461124	0.785810238	-3.66056726	13	21723183	13	R			SAP18	NM 005870	3'UTR				TRUE
cg01963464	0.48572628	0.505754579	0.447973099	0.420544337	0.406233492	0.451908775	-0.05358912	0.453023427	-3.10839559	0.017401565	0.785810238	-3.71903482	2	228339337	2	F			AGFG1;AGFG1	NM 0011351	Body;Body;Bo	chr2:2283367	S Shore		
cg01896579	0.761150542	0.78510061	0.773972603	0.764550484	0.722670719	0.672059678	-0.05364762	0.746584106	-2.48149293	0.042545543	0.82822212	-4.64653081	4	76599597	4	F			G3BP2;G3BP2	NM 203505;N	TSS1500;TSS1	chr4:7659763	S Shore		
cg26277720	0.792090612	0.796065078	0.769689071	0.763231657	0.732197466	0.70140572	-0.05366997	0.759113267	-3.39971105	0.011672317	0.779165306	-3.29715909	14	101438491	14	F		rs73350964	SNORD114-14	NR 003207;N	Body;TSS1500;TSS1500				
cg01483139	0.704042995	0.660738714	0.671474515	0.649494557	0.577694236	0.648021828	-0.05368187	0.651911141	-2.53389197	0.039425531	0.822883069	-4.56869099	4	187549458	4	F			FAT1	NM 005245	Body				
cg00417719	0.514813016	0.487059303	0.490510411	0.460288066	0.473648534	0.39721123	-0.05374497	0.470588427	-2.71617385	0.030301683	0.808256584	-4.29779962	10	115670022	10	R									
cg05685643	0.844162649	0.873729367	0.847371024	0.806241985	0.801389693	0.796178344	-0.05381767	0.828178844	-5.96132502	0.00059155	0.773451347	-0.08742004	4	48083394	4	R			TXK	NM 003328	Body				
cg01594538	0.376422552	0.404928009	0.368437283	0.340312836	0.338239026	0.309782609	-0.05381779	0.356353719	-4.35122886	0.003452907	0.773451347	-1.9935537	16	54689221	16	F									TRUE
cg17976625	0.608130081	0.646934053	0.587943262	0.575451951	0.556355337	0.54973284	-0.05382242	0.587424587	-3.52104411	0.009918582	0.776859249	-3.12418696	17	28705858	17	R			CPD	NM 001304	TSS200	chr17:287053	Island		
cg19383211	0.422698321	0.481047938	0.5002457	0.445113478	0.409155937	0.387987013	-0.05391184	0.441041398	-2.4075098	0.047390507	0.831823398	-4.75629412	6	32527588	6	F			HLA-DRB6	NR 001298	Body				
cg07909692	0.615908592	0.625685836	0.680181067	0.618270799	0.558374495	0.583379501	-0.0539169	0.613633382	-2.59454645	0.036107947	0.817247752	-4.47853833	12	41728680	12	R			PDZRN4	NM 0011645	Body				TRUE
cg03476105	0.752312436	0.771943808	0.755993063	0.745510892	0.679356102	0.693594266	-0.05392935	0.733118428	-3.21854282	0.014942461	0.785810238	-3.55852085	7	96770912	7	F			ACN9	NM 020186	Body				
cg10517230	0.164558066	0.200099552	0.227199954	0.119107619	0.131767826	0.178994511	-0.05399587	0.170287921	-2.67174753	0.032300441	0.811377362	-4.36379395	17	48661425	17	R			CACNA1G;CAC	NM 198384;N	Body;Body;Body;Body;Body;Body;Body;Body;Body;Body;Body				TRUE
cg00979272	0.736283186	0.688888889	0.766365088	0.698221223	0.683392623	0.647743401	-0.05405997	0.703482402	-2.54828948	0.038610429	0.820850289	-4.54729453	14	61100882	14	R						chr14:611039	N Shelf		
cg16654595	0.778541329	0.771632047	0.777965088	0.758309487	0.716795616	0.690823228	-0.05407004	0.749011133	-3.40457425	0.011595923	0.778856741	-3.2901928	15	28339873	15	F		rs74007950	OCA2	NM 000275	5'UTR	chr15:283397	Island		
cg00091063	0.582748245	0.577232925	0.630091185	0.543272481	0.558208955	0.526376147	-0.05407159	0.56965499	-3.50742526	0.010100431	0.776859249	-3.14351385	3	38177531	3	F			ACAA1;ACAA1;	NR 024024;N	Body;Body;Bo	chr3:3817800	N Shore		
cg23563014	0.697398448	0.618480172	0.631166348	0.617430673	0.590943254	0.576074553	-0.05419883	0.621915575	-2.53532354	0.039343691	0.822883069	-4.56656364	10	44789077	10	R						chr10:447888	Island		TRUE
cg00576086	0.574208924	0.585709339	0.587525633	0.54887218	0.534549601	0.501019516	-0.0543342	0.555314199	-4.40312183	0.003243634	0.773451347	-1.92618741	5	1269066	5	R		rs35883631	TERT;TERT	NM 198255;N	Body;Body	chr5:1270778	N Shore		
cg14213105	0.507539411	0.515426997	0.540995608	0.495773361	0.468793343	0.436358894	-0.05434547	0.494147936	-3.39929677	0.01167885	0.779433001	-3.29775265	9	126980322	9	F	rs4142893								TRUE
cg21558706	0.826509236	0.795638733	0.78884961	0.780562835	0.750946367	0.716397635	-0.05436358	0.776484069	-3.12548519	0.016993266	0.785810238	-3.6940584	3	48103391	3	F			MAP4;MAP4;N	NM 030885;N	5'UTR;5'UTR;5'UTR				
cg09795093	0.820538528	0.845187264	0.848481375	0.800168229	0.779266751	0.77135026	-0.05447398	0.810832068	-5.11109608	0.001437295	0.773451347	-1.04724346	21	39493199	21	R			DSCR8;DSCR8;	NR 026839;N	TSS1500;TSS1500;TSS1500;TSS1500;TSS1500;Body				
cg04750100	0.756435644	0.709088141	0.725050916	0.708820404	0.674989176	0.643291707	-0.05449114	0.702945998	-2.93382107	0.022224963	0.793919605	-3.97550312	2	136595281	2	R			LCT	NM 002299	TSS1500				
cg25226247	0.706191514	0.691533948	0.715218643	0.643703379	0.662370252	0.643336015	-0.05451149	0.677058959	-6.24228373	0.000449844	0.773451347	0.208245444	6	50785152	6	F	rs10456638		TFAP2B	NM 003221	TSS1500	chr6:5078728	N Shelf		
cg09745638	0.876033862	0.900269058	0.865779057	0.866400073	0.783127736	0.828912144	-0.05454734	0.853420322	-2.65557117	0.033062041	0.812804767	-4.38783232	6	162294525	6	R		rs73603174	PARK2;PARK2;	NM 004562;N	Body;Body;Body				
cg07413957	0.657341552	0.634083045	0.709814324	0.641918528	0.606546957	0.588712586	-0.05468695	0.639736165	-2.55627381	0.038165953	0.820850289	-4.53542775	16	69478081	16	R			CYB5B	NM 030579	Body				TRUE
cg14020146	0.375838926	0.412005193	0.41864139	0.362270952	0.362506216	0.317644129	-0.05468807	0.374817801	-3.41150549	0.011487973	0.778856741	-3.28026883	X	23017980	X	F	rs41309601		DDX53	NM 182699	TSS200				
cg15797527	0.746146732	0.818732987	0.796528337	0.766418911	0.717209191	0.713693988	-0.05469532	0.759788358	-2.54912494	0.03856367	0.820850289	-4.54605285	6	135814781	6	R			AHI1;AHI1;AHI	NM 0011348	5'UTR;5'UTR;5	chr6:1358185	N Shelf		
cg12733040	0.660816482	0.599445325	0.592237295	0.554304897	0.578429681	0.555636896	-0.05470921	0.590145096	-2.98764769	0.020601836	0.791969901	-3.89618782	22	17303493	22	F	rs34868211	rs34126385	XKR3	NM 175878	TSS1500				
cg03665818	0.764234721	0.816648274	0.764029032	0.71738076	0.743041058	0.720284964	-0.05473508	0.754269802	-3.52361744	0.009884621	0.776859249	-3.12053764	16	54724064	16	F									TRUE
cg23720929	0.661230856	0.644136496	0.675629872	0.624875069	0.624374599	0.56753468	-0.05473763	0.632963595	-3.25146603	0.014281776	0.781979245	-3.51076782	3	195310887	3	R			APOD;APOD	NM 001647;N	1stExon;5'UTR				
cg03522971	0.777428811	0.80418251	0.77622628	0.762920221	0.736586929	0.693864469	-0.05482199	0.75853487	-3.12197758	0.017076227	0.785810238	-3.69918269	4	6537163	4	F									
cg06941009	0.592126958	0.536391437	0.568022747	0.532653372	0.47634584	0.522927281	-0.05487155	0.538077939	-2.92740161	0.022427402	0.795185396	-3.98497496	16	6249672	16	F			A2BP1;A2BP1	NM 0011423	5'UTR;5'UTR				TRUE
cg12990410	0.504957188	0.504113854	0.514097652	0.457935342	0.45934289	0.441161552	-0.05490964	0.48026808	-7.65238786	0.000129083	0.773451347	1.549364568	5	140501117	5	F			PCDHB4	NM 018938	TSS1500	chr5:1405028	N Shore	RDMR	
cg11492288	0.235365052	0.26861167	0.258279406	0.207548878	0.189304813	0.200539987	-0.05495415	0.226608301	-5.55025958	0.000898238	0.773451347	-0.53889209	6	30290596	6	R			HCG18;HCG18	NR 024052;N	Body;Body	chr6:3029416	N Shelf		
cg24505863	0.670479032	0.640034991	0.725423729	0.602939243	0.612659424	0.655365649	-0.05499115	0.651150345	-2.37253889	0.049874594	0.833631366	-4.80809361	X	112084143	X	R			AMOT	NM 133265	TSS200	chrX:1120835	Island		
cg24242384	0.711709357	0.711838791	0.703600248	0.659329409	0.658752328	0.644012058	-0.0550182	0.681540365	-8.23168511	8.15E-05	0.773451347	2.039125933	6	32551954	6	F	rs71827189	rs9281873	HLA-DRB1	NM 002124	Body	chr6:3255185	Island		
cg22376465	0.155026455	0.175590811	0.201101671	0.106815034	0.126014364	0.133797028	-0.05503084	0.149724227	-4.27337786	0.003795311	0.773451347	-2.09537041	2	136875349	2	F			CXCR4	NM 003467	Body	chr2:1368740	Island	DMR	
cg03917666	0.829491114	0.854226139	0.844820796	0.786253935	0.820842169	0.756316268	-0.05504189	0.81532507	-3.43289471	0.011161628	0.776918821	-3.2496794	10	3977608	10	F									TRUE
cg06908855	0.643666107	0.622850804	0.679092667	0.601901469	0.60125448	0.57696737	-0.05516209	0.620955483	-3.71223104	0.007707868	0.773451347	-2.85534879	7	93201042	7	F	rs34140967		CALCR;CALCR	NM 0011647	5'UTR;5'UTR	chr7:9320408	N Shelf		
cg16301890	0.382564841	0.415665382	0.39795651	0.368227823	0.326136056	0.336286861	-0.05517866	0.371139579	-4.20910561	0.004106241	0.773451347	-2.18010599	10	119301464	10	F	rs76393059		EMX2;EMX2OS	NM 0011659	TSS1500;Body	chr10:119301	Island	DMR	
cg23627149	0.272539444	0.296032181	0.280898876	0.247084101	0.235705324	0.200958773	-0.05524077	0.25553645	-4.30585905	0.003648105	0.773451347	-2.05278061	1	193155273	1	F		rs34137906	B3GALT2;B3GA	NM 003783;N	5'UTR;1stExon;Body				TRUE
cg01613122	0.285670498	0.296655518	0.347728203	0.288014514	0.212013309	0.264296541	-0.05524329	0.282396431	-2.40154823	0.047804827	0.831823398	-4.76512895	7	37951727	7	R		rs1132553	SFRP4	NM 003014	Body	chr7:3795562	N Shelf		
cg02979010	0.843505477	0.820734341	0.874465285	0.82740152	0.79592685	0.749604877	-0.05525729	0.818606392	-2.57183698	0.037314767	0.819266878	-4.51229522	12	72319077	12	F			TBC1D15;TBC1	NM 022771;N	3'UTR;3'UTR;Body;3'UTR				
cg04418423	0.744350908	0.753588517	0.790446092	0.71050759	0.704413793	0.707617858	-0.05528209	0.735152126	-4.63305716	0.002470558	0.773451347	-1.63253478	10	119082423	10	R			PDZD8	NM 173791	Body				TRUE
cg01963059	0.125176661	0.129389974	0.147634714	0.097654845	0.072075121	0.066309304	-0.05538736	0.106373437	-5.35378453	0.001104995	0.773451347	-0.76292008	1	116658288	1	F			C1orf161	NM 152367	Body				TRUE
cg07387429	0.432931157	0.492076229	0.479302832	0.451129211	0.410952146	0.37579357	-0.05547843	0.440364191	-2.51433062	0.040561634	0.824204985	-4.59775646	1	153234809	1	R								CDMR	
cg16362007	0.660719264	0.589052288	0.606286837	0.603766259	0.53699646	0.548832487	-0.05548773	0.590469226	-2.38624443	0.048885517	0.832586333	-4.78780046	2	191297422	2	F	rs4853704		MFSD6	NM 017694	5'UTR			DMR	
cg19780571	0.743856661	0.725950551	0.740946011	0.700011724	0.672039192	0.672075149	-0.05554239	0.709156548	-5.73174407	0.000745054	0.773451347	-0.33673713	10	101828642	10	F			CPN1	NM 001308	Body	chr10:101824	S Shelf		
cg02306639	0.770903254	0.768924798	0.750137771	0.729378394	0.705984288	0.68787024	-0.05557763	0.735533124	-4.78825432	0.002064807	0.773451347	-1.43880036	3	32026021	3	R			ZNF860	NM 0011376	5'UTR	chr3:3202196	S Shelf		
cg17707823	0.627995155	0.632763652	0.654757044	0.562171494	0.565603329	0.620597313	-0.05571457	0.610647998	-3.37483972	0.012071587	0.780421619	-3.33282821	6	169260618	6	F	rs76095730	rs73789472				chr6:1692611	N Shore		
cg01445827	0.229628584	0.307330708	0.255784359	0.2017932	0.233440986	0.190276446	-0.05574434	0.236375714	-2.70784054	0.030666497	0.808428213	-4.31017534	1	96952956	1	R									TRUE
cg25912938	0.340056676	0.30363111	0.335985225	0.315070365	0.222704808	0.274501394	-0.05579881	0.298658263	-2.45589635	0.044161295	0.829778235	-4.68452929	21	29910411	21	R			NCRNA00161;I	NR 026553;N	TSS1500;TSS1500				TRUE
cg10648815	0.745998241	0.769906053	0.737770858	0.706298758	0.702563276	0.677333838	-0.05582643	0.723311837	-4.94428809	0.001730007	0.773451347	-1.24763546	19	55013549	19	R			LAIR2;LAIR2	NM 002288;N	TSS1500;TSS1500				
cg05135828	0.685732963	0.668817527	0.711511963	0.646778419	0.66083707	0.590948803	-0.05583272	0.660771124	-2.86922959	0.024353324	0.800629909	-4.07091773	X	142721385	X	F			SLITRK4	NM 173078	5'UTR	chrX:1427214	N Shore	CDMR	
cg13863078	0.58867801	0.62103929	0.578448276	0.526496565	0.520809249	0.573241479	-0.05587276	0.568118812	-3.33365207	0.012765511	0.780421619	-3.39204983	4	177244109	4	R			SPCS3	NM 021928	Body	chr4:1772409	S Shelf		
cg01816482	0.847474414	0.834393916	0.837622469	0.783231913	0.774896596	0.793731041	-0.05587708	0.811891725	-7.75053442	0.000119172	0.773451347	1.634647513	3	193313692	3	R			OPA1;OPA1;OI	NM 130835;N	Body;Body;Bo	chr3:1933108	S Shelf		
cg08005660	0.687462864	0.662523144	0.71448541	0.630434783	0.660728193	0.605554893	-0.05591785	0.660198215	-3.21010006	0.015117112	0.785810238	-3.57078383	12	47226005	12	F						chr12:472249	S Shore		
cg10747483	0.429174484	0.48050728	0.464379947	0.437140509	0.370396601	0.398756661	-0.05592265	0.430059247	-2.88681541	0.02375331	0.798495973	-4.04491646	19	55038290	19	F	rs62131624	rs76168174				chr19:550382	Island		
cg24044028	0.752994012	0.771562767	0.79050177	0.752038766	0.697575399	0.697670947	-0.05592448	0.743723944	-3.3178064	0.013043809	0.780421619	-3.41488314	12	77623070	12	F	rs17043139								TRUE
cg06126713	0.298631607	0.256510562	0.311250773	0.21882112	0.265053763	0.214469453	-0.0560162	0.260789546	-3.056047	0.018718716	0.787317658	-3.79569595	7	16505617	7	R			SOSTDC1	NM 015464	TSS200				
cg14237746	0.425998732	0.473758531	0.403574401	0.394834711	0.377039454	0.363237603	-0.0560733	0.406407239	-3.12410479	0.017025864	0.785810238	-3.6960749	17	46692592	17	R			HOXB8	NM 024016	TSS1500	chr17:466903	S Shore		
cg06713076	0.530487099	0.587019545	0.548051948	0.516210882	0.494348475	0.48670268	-0.05609885	0.527136772	-3.67835661	0.008056874	0.773451347	-2.90263537	17	68942524	17	R									TRUE
cg15627871	0.68209725	0.702167766	0.679884902	0.670423099	0.630921664	0.594451783	-0.05611779	0.659991077	-3.07319709	0.018275865	0.786720137	-3.77055585	3	117321806	3	R									TRUE
cg22592108	0.6337241	0.619069395	0.61078535	0.574866801	0.572081073	0.548215473	-0.0561385	0.593123699	-5.81288863	0.000686208	0.773451347	-0.24780788	5	53304441	5	R			ARL15	NM 019087	Body				TRUE
cg04015501	0.832311892	0.848090068	0.861867769	0.805666052	0.784989858	0.783161967	-0.05615028	0.819347768	-5.66720289	0.000795904	0.773451347	-0.40810998	13	113201847	13	R			TUBGCP3	NM 006322	Body	chr13:113201	Island		
cg17015133	0.802854834	0.825483092	0.807798892	0.777452086	0.706129675	0.784003615	-0.05618381	0.783953699	-2.76431219	0.028281461	0.804381388	-4.22634716	1	155111332	1	R			RAG1AP1;RAG	NM 018845;N	3'UTR;3'UTR;3	chr1:1551129	N Shore		
cg17894592	0.384361425	0.391809382	0.372699333	0.344105409	0.295236547	0.34084726	-0.05622697	0.354843226	-4.1033818	0.004680401	0.773451347	-2.32081513	4	139052047	4	F									
cg08699680	0.781812069	0.771203156	0.80156658	0.729651785	0.776941308	0.679294082	-0.05623154	0.75674483	-2.43863424	0.045286531	0.830804608	-4.71014259	8	32452965	8	F	rs11988011		NRG1;NRG1;N	NM 013960;N	Body;TSS1500;TSS1500;Body;Body;Body;Body;TSS1500;Body;Body;Body;Body;Body				
cg04809990	0.574151039	0.571557156	0.54388643	0.528971699	0.501514036	0.490137546	-0.05632378	0.535036318	-4.49483734	0.002907137	0.773451347	-1.8081082	20	16728895	20	R			OTOR	NM 020157	TSS200				
cg03731616	0.608305425	0.633655218	0.640166316	0.570330054	0.603494053	0.539289819	-0.05633768	0.599206814	-3.37043396	0.012143837	0.780421619	-3.33915401	3	123603618	3	R			MYLK;MYLK;M	NM 053027;N	TSS1500;TSS1	chr3:1236025	S Shore		
cg22495968	0.354142526	0.29211702	0.346052919	0.258505003	0.291131267	0.273616631	-0.05635319	0.302594228	-3.27201912	0.013885267	0.781602075	-3.48101245	2	5622155	2	R									TRUE
cg01614536	0.860953819	0.872282609	0.875697136	0.854276874	0.808359708	0.77712742	-0.05638985	0.841499594	-3.11419144	0.017261932	0.785810238	-3.71056135	7	95065605	7	F			PON2;PON2	NM 000305;N	TSS1500;TSS1	chr7:9506407	S Shore		
cg07236367	0.549074473	0.538525441	0.589054563	0.550222832	0.484848485	0.47238406	-0.0563997	0.530684976	-2.52187774	0.040119342	0.823470242	-4.58654329	6	118244455	6	F	rs74583845		SLC35F1	NM 0010298	Body	chr6:1182413	S Shelf		
cg22621161	0.749906332	0.732526882	0.743504436	0.680410636	0.684506251	0.691689008	-0.05644392	0.713757258	-8.23086197	8.15E-05	0.773451347	2.038452668	10	116654257	10	F	rs942143	rs34295789	FAM160B1	NM 0011350	Body				
cg09505607	0.551054155	0.57096207	0.56974026	0.539183143	0.461218837	0.522021168	-0.05644445	0.535696606	-2.92002037	0.022662585	0.796113368	-3.99586901	10	57390872	10	F	rs77405171					chr10:573903	Island	DMR	
cg14027817	0.677586207	0.685535367	0.658820452	0.626805006	0.627277904	0.598509687	-0.05644981	0.645765771	-5.27542506	0.001201861	0.773451347	-0.85379561	X	15690643	X	F						chrX:1569310	N Shelf		
cg04585185	0.694117647	0.663484873	0.66815624	0.624122954	0.625983014	0.606136627	-0.05650539	0.647000226	-5.60697497	0.000846878	0.773451347	-0.47522886	21	17961737	21	R			C21orf34;MIR	NR 027790;N	Body;TSS1500;Body				
cg10499429	0.383818121	0.348464619	0.357894737	0.334251101	0.325295152	0.260610766	-0.05667349	0.335055749	-2.82665986	0.02587298	0.802600013	-4.13392396	16	18816941	16	R			SMG1	NM 015092	3'UTR	chr16:188123	S Shelf		
cg26528484	0.305786936	0.26825311	0.326106926	0.222600519	0.244878422	0.262567325	-0.05670024	0.271698873	-3.4543762	0.010843922	0.776859249	-3.21901192	2	103387474	2	R			TMEM182	NM 144632	Body				TRUE
cg06323052	0.622714771	0.682156134	0.676395616	0.639556473	0.58713355	0.584147205	-0.05680976	0.632017292	-2.77020921	0.028043881	0.804381388	-4.21759915	4	56720686	4	F			EXOC1;EXOC1;	NM 018261;N	5'UTR;5'UTR;5	chr4:5671970	S Shore		
cg06712846	0.69092352	0.685240796	0.677585569	0.641123074	0.640691716	0.601039073	-0.05696534	0.656100625	-4.87210272	0.001876751	0.773451347	-1.33562465	4	138864252	4	F	rs7664009								
cg08319412	0.777464177	0.800976342	0.804027754	0.756252265	0.711531262	0.743715512	-0.05698974	0.765661219	-4.38033546	0.003333753	0.773451347	-1.95571869	16	5149577	16	F						chr16:514725	S Shore		
cg05529816	0.808609739	0.792345277	0.850840082	0.788514899	0.759914712	0.732314891	-0.05701687	0.7887566	-3.03012251	0.019409963	0.789625816	-3.83374254	17	4802735	17	R			CHRNE;C17orf	NM 000080;N	Body;TSS1500	chr17:480226	Island	DMR	TRUE
cg14100973	0.534408179	0.557418884	0.592581378	0.496459132	0.505297474	0.511461032	-0.0570636	0.53293768	-4.01096875	0.005254905	0.773451347	-2.44514502	4	87280816	4	F			MAPK10;MAPI	NM 138980;N	5'UTR;1stExon;5'UTR;1stExon;5'UTR				TRUE
cg15701842	0.607834507	0.659611993	0.664148352	0.614749082	0.588572364	0.556705571	-0.05718928	0.615270312	-2.94268944	0.021948476	0.793784429	-3.96242219	2	169609566	2	F			LASS6	NM 203463	Body				TRUE
cg21074911	0.39185205	0.363680742	0.41538132	0.342329545	0.331613508	0.325396825	-0.05719141	0.361708998	-4.39597136	0.003271621	0.773451347	-1.93544611	14	60040732	14	F	rs76743811		C14orf38	NM 0011643	Body	chr14:600432	N Shelf		
cg12706330	0.646022622	0.681061193	0.692229336	0.650769465	0.625	0.571768781	-0.0572583	0.644475233	-2.6958037	0.03120158	0.810402361	-4.32805397	10	85898700	10	F			GHITM	NM 014394	TSS1500	chr10:858990	N Shore		
cg01082910	0.641966142	0.687281214	0.700617284	0.653945666	0.59223301	0.611764706	-0.05730709	0.647968004	-2.86486455	0.024504722	0.801238506	-4.07737414	10	36053547	10	F		rs74133236				chr10:360541	N Shore		TRUE
cg00992586	0.632154143	0.687079106	0.715551299	0.646755309	0.622268343	0.593812331	-0.05731619	0.649603422	-2.54299812	0.038907945	0.821045416	-4.55515845	3	8000912	3	F									
cg00905042	0.71712279	0.742487479	0.732520617	0.717131474	0.674447428	0.628582646	-0.05732311	0.702048739	-2.74624568	0.029022574	0.805651692	-4.25315542	4	174114298	4	F			GALNT7	NM 017423	Body				TRUE
cg17368726	0.77183666	0.761077324	0.778260195	0.715144972	0.74391657	0.680108086	-0.05733485	0.741723968	-3.72123965	0.007617845	0.773451347	-2.84279908	7	108169094	7	F						chr7:1081662	S Shelf		
cg00059399	0.738675295	0.731404612	0.726573141	0.722545509	0.637650878	0.664437279	-0.05733979	0.703547786	-2.8800235	0.023983172	0.799689074	-4.05495656	5	2008272	5	R						chr5:2008187	Island		
cg18984151	0.155001137	0.189428021	0.13475616	0.103419516	0.100694444	0.102776962	-0.05743147	0.131012707	-4.35853305	0.003422571	0.773451347	-1.98404728	3	47555476	3	F			C3orf75	NM 0010317	TSS1500	chr3:4755480	S Shore		
cg27122213	0.628564155	0.686254471	0.629349817	0.612641417	0.551443519	0.607206804	-0.05762557	0.619243364	-2.69160091	0.031390704	0.810402361	-4.33429722	14	57274763	14	F	rs12878110		OTX2	NM 021728	5'UTR	chr14:572746	Island	DMR	
cg18552939	0.610815047	0.648059198	0.598120385	0.570274818	0.580124679	0.533562053	-0.05767769	0.590159363	-3.49731351	0.010237783	0.776859249	-3.15787839	15	23932620	15	R			NDN	NM 002487	TSS200	chr15:239315	S Shore	CDMR	
cg16631698	0.629728765	0.616	0.659428411	0.612633649	0.580673872	0.538790994	-0.05768622	0.606209282	-2.93809559	0.02209124	0.79383557	-3.96919754	10	3500383	10	F	rs76845269					chr10:350033	Island		
cg22416672	0.733145751	0.718142449	0.749628951	0.646560091	0.667176611	0.714057776	-0.05770756	0.704785272	-3.30690108	0.013239126	0.780421619	-3.43061322	20	62148107	20	F	rs380158					chr20:621510	N Shelf		
cg15686216	0.79335733	0.818776078	0.853086916	0.78717359	0.762122449	0.742485911	-0.05781279	0.792833712	-3.36044379	0.012309396	0.780421619	-3.35350597	1	215794543	1	F			KCTD3	NM 016121	3'UTR				
cg13131061	0.703799099	0.730573641	0.733095738	0.684600108	0.646221597	0.663120567	-0.05784207	0.693568458	-4.75349283	0.002148822	0.773451347	-1.48188115	2	225268095	2	R			FAM124B;FAM	NM 0011227	TSS1500;TSS1500				
cg10116636	0.612890232	0.60773177	0.597389724	0.58298006	0.558327082	0.502977667	-0.05790897	0.577049423	-3.04482926	0.019014553	0.788442786	-3.81215259	10	24301907	10	R			KIAA1217	NM 0010985	5'UTR				TRUE
cg20253212	0.263410379	0.327148111	0.313416218	0.266625521	0.20769832	0.25540491	-0.05808199	0.27228391	-2.79503918	0.027066298	0.803102356	-4.18077864	4	41694822	4	F			LIMCH1;LIMCH	NM 014988;N	Body;Body;Body;Body;Body				
cg22553555	0.663965822	0.693781095	0.735119726	0.643671119	0.647546959	0.627036985	-0.05820386	0.668520284	-3.38833739	0.011853108	0.780421619	-3.31346186	12	121643760	12	F	rs74728193					chr12:121647	N Shelf		
cg03814733	0.275300546	0.24345191	0.304907196	0.26401137	0.204982091	0.180000419	-0.05822192	0.245442255	-2.44479112	0.044881845	0.83011027	-4.70100836	X	149106755	X	F			CXorf40B;LOC1	NM 0010138	TSS200;TSS20	chrX:1491061	S Shore		
cg02789485	0.17198989	0.195083579	0.181753506	0.142416616	0.107973032	0.123189183	-0.05841605	0.153734301	-5.58904966	0.000862747	0.773451347	-0.49530183	12	75783428	12	R			GLIPR1L2	NM 152436	TSS1500	chr12:757847	N Shore		
cg25405719	0.573919833	0.559766133	0.636955433	0.535923595	0.506833713	0.552541	-0.0584477	0.560989951	-2.74037078	0.02926794	0.806044853	-4.26187518	11	81697779	11	R		rs34131790							
cg11754185	0.326358297	0.320770722	0.294196438	0.246718576	0.288036267	0.230808995	-0.05858721	0.284481549	-3.69690791	0.007863661	0.773451347	-2.87672002	13	54707971	13	R									TRUE
cg27200236	0.259168203	0.256816183	0.314183958	0.177414425	0.264542423	0.211883603	-0.05877596	0.247334799	-2.39825097	0.048035576	0.831823398	-4.77001463	4	24296454	4	F									TRUE
cg12044123	0.192949907	0.210185184	0.180204911	0.138548845	0.156951004	0.111347112	-0.05883101	0.165031161	-4.49805008	0.00289607	0.773451347	-1.80399475	6	28554864	6	R			SCAND3;SCAN	NM 052923;N	1stExon;5'UTR	chr6:2855486	Island	RDMR	TRUE
cg21248987	0.672441672	0.678369196	0.726082268	0.65046621	0.640444634	0.609392164	-0.05886338	0.662866024	-3.51042293	0.010060097	0.776859249	-3.13925783	7	3385318	7	R			SDK1	NM 152744	Body				
cg08425482	0.432878679	0.459669254	0.446717412	0.406340058	0.346341463	0.409193515	-0.0591301	0.41685673	-3.39409863	0.011761155	0.780421619	-3.30520197	7	143747422	7	F			OR2A5	NM 012365	TSS200				
cg07184856	0.534008225	0.559548793	0.56049961	0.490265072	0.509666081	0.476729153	-0.05913211	0.521786156	-5.34738081	0.001112576	0.773451347	-0.77031373	6	25736615	6	F		rs75144769				chr6:2573269	S Shelf		
cg03170665	0.694834563	0.690038856	0.700771854	0.643021072	0.629623541	0.635536295	-0.05915479	0.665637697	-9.34066344	3.63E-05	0.773451347	2.89269011	2	114333496	2	R			FAM138B	NR 026821	TSS1500				
cg17342916	0.798351001	0.807404237	0.80800464	0.778007228	0.718660037	0.739612903	-0.0591599	0.775006674	-4.1193744	0.004588157	0.773451347	-2.29942517	3	104556025	3	R									TRUE
cg12443030	0.781080608	0.795934202	0.804900911	0.699309593	0.731933866	0.773116907	-0.05918512	0.764379348	-3.32057055	0.012994796	0.780421619	-3.4108981	1	75565024	1	R									TRUE
cg24437311	0.183234421	0.175798645	0.271187728	0.150695546	0.159860904	0.142005366	-0.05921966	0.180463768	-2.44984455	0.044552469	0.829846682	-4.69351012	3	44753069	3	F			ZNF502;ZNF50	NM 0011344	TSS1500;TSS1	chr3:4475409	N Shore		
cg00890110	0.481789137	0.520297952	0.510598387	0.466712899	0.422436671	0.445662313	-0.0592912	0.474582893	-4.21510794	0.004076949	0.773451347	-2.17216674	X	119247023	X	R			RHOXF1	NM 139282	Body	chrX:1192494	N Shelf		
cg05938207	0.712790946	0.727380248	0.761585271	0.722881498	0.655870445	0.644859813	-0.05938157	0.704228037	-2.68014799	0.03191219	0.81121464	-4.35131228	6	32489750	6	F	rs41562819	rs41544215	HLA-DRB5	NM 002125	Body	chr6:3248974	Island		
cg25134401	0.680488919	0.73213268	0.715982829	0.680329496	0.63311994	0.636987035	-0.05938932	0.67984015	-3.46929886	0.010628975	0.776859249	-3.19774017	17	80730489	17	R			TBCD	NM 005993	Body				TRUE
cg25816031	0.73656272	0.7325028	0.733993399	0.703064911	0.668334281	0.653244422	-0.05947177	0.704617089	-4.8148175	0.002003059	0.773451347	-1.4060012	2	158087662	2	F									TRUE
cg08778908	0.663568773	0.641017964	0.656225731	0.618402874	0.580628134	0.583333333	-0.05948271	0.623862802	-5.08154449	0.001484862	0.773451347	-1.08244756	13	48988353	13	R			LPAR6;LPAR6;L	NM 0011624	TSS1500;5'UTR;5'UTR;Body				
cg00010742	0.489434609	0.452097824	0.493643298	0.428638941	0.396801383	0.431168831	-0.05952219	0.448630814	-4.23531649	0.00397618	0.773451347	-2.14547615	1	91182989	1	F			BARHL2	NM 020063	TSS200	chr1:9118324	N Shore		
cg21026199	0.796099633	0.777903044	0.824353784	0.77002665	0.72139699	0.728330946	-0.05953396	0.769685175	-3.65698521	0.008285876	0.773451347	-2.93254658	4	174912278	4	F									
cg16903122	0.755793017	0.754864815	0.753859181	0.731550587	0.682479323	0.671677549	-0.05960318	0.725037412	-3.9961155	0.005354251	0.773451347	-2.46524329	1	44584429	1	R			KLF17	NM 173484	TSS200				
cg16501628	0.811774636	0.812782694	0.839595888	0.795754328	0.736234174	0.753290261	-0.05962482	0.791571997	-3.73293377	0.007502688	0.773451347	-2.82652447	14	45600560	14	R			FKBP3	NM 002013	Body	chr14:456033	N Shelf		
cg07284231	0.639146568	0.7056488	0.708963482	0.638307219	0.590605071	0.64583647	-0.05967003	0.654751268	-2.67329505	0.032228549	0.811303767	-4.3614945	8	700689	8	F									
cg01488159	0.679476207	0.742163292	0.718815186	0.659366912	0.624441524	0.677601547	-0.05968157	0.683644111	-3.14431459	0.016555216	0.785810238	-3.66656908	4	153856503	4	R						chr4:1538571	N Shore	RDMR	
cg16875420	0.654900139	0.665698097	0.652346736	0.624924288	0.597224602	0.571365736	-0.05981012	0.627743266	-4.53502622	0.002771993	0.773451347	-1.75676351	7	53305866	7	R									TRUE
cg22158476	0.550144928	0.581558817	0.592910652	0.529322034	0.518108652	0.497744977	-0.05981291	0.54496501	-4.58800741	0.002604326	0.773451347	-1.68944501	13	23433383	13	F									
cg03488097	0.780481137	0.764355955	0.79277671	0.767603997	0.709535709	0.680896235	-0.05985929	0.749274957	-2.84856446	0.025078916	0.801369037	-4.10149252	2	3184399	2	F	rs77368607					chr2:3184187	Island		
cg16503797	0.747015915	0.711353033	0.74226445	0.712470566	0.642749472	0.66519174	-0.06007387	0.703507529	-3.24575994	0.014394001	0.783139541	-3.51903636	18	19476805	18	R						chr18:194768	N Shore		
cg19735739	0.705365182	0.700074399	0.723158758	0.681142483	0.662319868	0.604823835	-0.06010405	0.679480754	-3.17203067	0.015932241	0.785810238	-3.62616437	1	191120792	1	F									
cg20981919	0.624173181	0.597839345	0.593410508	0.559744194	0.537610619	0.537749737	-0.06010616	0.575087931	-5.71788155	0.000755661	0.773451347	-0.352019	3	25616035	3	R			RARB;RARB	NM 016152;N	Body;Body				
cg11258102	0.511159499	0.548945148	0.613382183	0.50241838	0.494240838	0.496309963	-0.06017255	0.527742669	-2.57809375	0.036978146	0.818830892	-4.50299492	1	117078712	1	F	rs35768283		CD58;CD58;CD	NM 001779;N	Body;Body;Bo	chr1:1170770	S Shore		
cg04671659	0.683196462	0.683495822	0.695954907	0.64912847	0.626188734	0.606784888	-0.0601817	0.657458214	-5.43206704	0.001016841	0.773451347	-0.67300714	5	42979395	5	F		rs34922908							
cg18588281	0.627345845	0.587247944	0.624637214	0.538056897	0.567888999	0.552569007	-0.0602387	0.582957651	-4.68025993	0.002338502	0.773451347	-1.57323037	2	48842061	2	R		rs7592776	STON1-GTF2A	NM 172311	Body	chr2:4884475	N Shelf		
cg03513163	0.412387252	0.379810504	0.413162706	0.367871318	0.331510992	0.324870397	-0.06036925	0.371602195	-4.27802566	0.003773852	0.773451347	-2.08926654	5	140431149	5	R			PCDHB1	NM 013340	1stExon				TRUE
cg22927009	0.65792235	0.669015767	0.669197861	0.591991458	0.649428476	0.573426573	-0.06042982	0.635163748	-3.29288487	0.013494789	0.780421619	-3.45084917	9	115833890	9	F						chr9:1158329	Island		
cg00424354	0.47027972	0.49566507	0.4697109	0.4281026	0.456389345	0.369806279	-0.06045249	0.448325652	-2.86800801	0.024395594	0.800961418	-4.07272449	11	100555339	11	F	rs56302425					chr11:100557	N Shelf		
cg15711973	0.29257217	0.331858407	0.272395395	0.248967926	0.254509513	0.211905532	-0.060481	0.268701491	-3.45875865	0.010780314	0.776859249	-3.21276214	2	241638367	2	F						chr2:2416404	N Shelf		
cg22301128	0.427329193	0.367675159	0.45566398	0.376412542	0.325491937	0.367297344	-0.06048884	0.386645026	-2.56236735	0.037830307	0.820264016	-4.52637076	4	77011716	4	F			ART3;ART3;AR	NM 0011300	Body;Body;Body				TRUE
cg02405213	0.798970901	0.833225806	0.825583602	0.808025285	0.727020945	0.741218005	-0.06050536	0.789007424	-2.85476178	0.024858951	0.801369037	-4.0923211	9	5042618	9	R		rs74285178	JAK2	NM 004972	Body	chr9:5042797	N Shore		
cg18017082	0.588585805	0.642937884	0.583360593	0.588200616	0.533828117	0.511294941	-0.0605202	0.574701326	-2.61064145	0.035277256	0.815557552	-4.45461323	21	15455198	21	F						chr21:154562	N Shore		
cg16537483	0.631257631	0.681510363	0.672891685	0.634757601	0.588306064	0.580822711	-0.0605911	0.631591009	-3.33600393	0.012724753	0.780421619	-3.38866317	3	152019539	3	R			MBNL1;MBNL	NM 207295;N	Body;Body;Body;Body;Body;Body;Body				TRUE
cg13739333	0.392059553	0.468695562	0.443765903	0.371826779	0.394618834	0.356283101	-0.06059743	0.404541622	-3.05919838	0.018636491	0.7871227	-3.79107461	6	32495746	6	R			HLA-DRB5	NM 002125	Body				
cg17315639	0.339572707	0.320987654	0.310280231	0.255896688	0.278772897	0.254152058	-0.06067298	0.293277039	-5.93140236	0.000609388	0.773451347	-0.11951589	8	80877113	8	R			MRPS28	NM 014018	Body				TRUE
cg21721825	0.270082501	0.306761055	0.258040597	0.226693928	0.232133015	0.193897398	-0.06071994	0.247934749	-3.98105664	0.005457075	0.773451347	-2.48565211	12	97300410	12	R			NEDD1;NEDD1	NM 152905;N	TSS1500;TSS1	chr12:973008	N Shore		

cg09992309	0.592350103	0.544825598	0.648101266	0.548979312	0.347354138	0.49108454	-0.13261966	0.528782493	-2.59062346	0.036313486	0.817750792	-4.48436982	7	16223374	7	R	ISPD;ISPD	NM	00110142	Body;Body
cg16180082	0.681047628	0.54238957	0.709508812	0.438001119	0.064856914	0.059947336	-0.45671355	0.415958563	-4.4272361	0.003151179	0.773451347	-1.89501961	6	159466542	6	F	TAGAP;TAGAP;	NM	152133;N	TSS1500;TSS1500;TSS1500

#	Chr	Start	End	Length	n	ID	Class	990479624	990479624	990479624	990479624	990479624	990479624	Gene.Symbol	dM	p	p.adj	Chromatin state in HMEC cells	Direction	Diff.methylation
1	1	155294935	155295267	333	4	806	gene;tss;islan	0.3337	0.3165	0.3147	0.3198	0.3005	0.3069	FDPS; RUSC1; RU	0.735	0.92	0.999	active promoter	Hypo	-0.012566667
3	19	13365923	13366101	179	4	19914	gene;island	0.8415	0.823	0.8264	0.8304	0.8448	0.8753	CACNA1A (margi	0.58	0.928	0.999	heterochromatin	Hyper	0.019866667
4	18	67872746	67872919	174	4	19159	gene	0.0975	0.0799	0.064	0.0678	0.0656	0.0609	RTTN (margin: RT	0.559	0.287	0.999	active promoter	Hypo	-0.0157
6	X	152938750	152938907	158	4	41718	tss	0.3389	0.4273	0.4062	0.3732	0.3248	0.3704	RN7SL687P; PNC	0.514	0.598	0.999	weak enhancer and weak transcription	Hypo	-0.034666667
9	5	1416793	1417003	211	4	31588	gene;island	0.865	0.883	0.879	0.902	0.8463	0.8868	SLC6A3 (margin:	0.497	0.681	0.999	heterochromatin	Hyper	0.0027
10	3	3885955	3886273	319	4	27685	gene	0.5769	0.5622	0.5504	0.5927	0.5981	0.6194	LRRN1; SUMF1 (r	0.496	0.726	0.999	heterochromatin	Hyper	0.040233333
12	13	113299697	113300120	424	5	11947	island	0.8874	0.9093	0.9101	0.9008	0.8769	0.8865	C13orf35 (margir	0.493	0.955	0.999	heterochromatin	Hypo	-0.0142
14	22	36236649	36236760	112	4	26896	gene;tss	0.1561	0.1684	0.1443	0.1485	0.1555	0.2017	RBFOX2 (margin:	0.49	0.758	0.999	strong enhancer	Hyper	0.0123
15	12	25348252	25348358	107	5	9098	gene	0.0617	0.0757	0.071	0.0902	0.0597	0.075	LYRM5; CASC1; K	0.489	0.961	0.999	active promoter	Hyper	0.0055
16	2	183902764	183903098	335	4	22992	gene;island	0.0846	0.0995	0.1031	0.121	0.0995	0.1091	NCKAP1 (margin:	0.488	0.941	0.999	active promoter	Hyper	0.014133333
17	17	79846205	79846485	281	4	16956	gene;island	0.9395	0.9398	0.9329	0.9267	0.9267	0.9187	RP11-498C9.16; /	0.486	0.825	0.999	transcription elongation	Hypo	-0.013366667
18	X	152938698	152938907	210	5	41275	gene;island	0.3471	0.495	0.4909	0.4025	0.3251	0.3986	RN7SL687P; PNC	0.481	0.814	0.999	weak enhancer	Hypo	-0.068933333
19	20	3184938	3185276	339	4	25385	gene	0.0706	0.0956	0.0977	0.1055	0.1039	0.097	ITPA; DDRGK1 (m	0.481	0.987	0.999	active promoter	Hyper	0.014166667
20	4	187517794	187518154	361	5	30266	gene	0.9086	0.9186	0.9056	0.9171	0.9107	0.9077	FAT1 (margin: FA	0.479	0.965	0.999	transcription elongation	Hyper	0.0009
21	9	131154899	131155026	128	4	41017	island	0.8899	0.8948	0.8869	0.9001	0.8936	0.919	URM1; RP11-339	0.478	0.304	0.999	weak transcription	Hyper	0.0137
24	1	50513749	50513927	179	4	523	gene	0.9457	0.9455	0.9445	0.9407	0.9412	0.9336	ELAVL4 (margin:	0.473	0.906	0.999	poised promoter	Hypo	-0.006733333
25	7	23571311	23571645	335	5	36976	gene	0.0753	0.0705	0.0721	0.0685	0.0496	0.0642	TRA2A (margin: T	0.473	0.936	0.999	active promoter	Hypo	-0.011866667
27	6	32138723	32138839	117	5	34121	gene;island	0.8775	0.8982	0.8885	0.8913	0.8791	0.8763	PPT2; PPT2-EGFL	0.467	0.929	0.999	transcription elongation	Hypo	-0.005833333
29	2	112812621	112812775	155	6	23614	tss	0.1282	0.1447	0.1307	0.1251	0.1033	0.1289	TMEM87B (marg	0.464	0.357	0.999	weak promoter	Hypo	-0.015433333
31	1	27986306	27986807	502	5	2929	island	0.0883	0.0983	0.1054	0.0893	0.0895	0.0952	RP11-288L9.4; RF	0.46	0.835	0.999	weak promoter	Hypo	-0.006
32	1	1248233	1248492	260	4	30	gene;island	0.8317	0.8654	0.8251	0.8496	0.8346	0.8081	PUSL1; ACAP3; C	0.457	0.814	0.999	transcription elongation	Hypo	-0.009966667
33	17	21194718	21194806	89	4	16515	gene	0.8882	0.9079	0.8948	0.9159	0.896	0.9155	MAP2K3 (margin	0.457	0.534	0.999	transcription elongation	Hyper	0.012166667
34	4	118006747	118006832	86	6	30608	tss	0.5244	0.5074	0.5646	0.5254	0.4965	0.5118	TRAM1L1 (margi	0.457	0.334	0.999	weak promoter	Hypo	-0.0209
35	8	80942046	80942378	333	4	39413	gene;island	0.1042	0.086	0.0877	0.0873	0.0846	0.0731	MRPS28; TPD52;	0.456	0.831	0.999	active promoter	Hypo	-0.010966667
36	1	9324688	9325015	328	5	201	gene;island	0.8733	0.8619	0.864	0.8938	0.8602	0.8568	H6PD (margin: H	0.455	0.932	0.999	weak transcription	Hyper	0.003866667
38	15	101084442	101084565	124	4	13527	gene;island	0.9135	0.9169	0.92	0.9212	0.9069	0.9255	CERS3; RP11-526	0.45	0.948	0.999	heterochromatin	Hyper	0.001066667
42	12	66123127	66123496	370	4	10615	island	0.7677	0.7897	0.8121	0.7954	0.8055	0.8236	(margin: RPSAP5	0.443	0.912	0.999	weak promoter	Hyper	0.018333333
44	17	29886672	29886890	219	4	17279	tss	0.967	0.9667	0.9656	0.9601	0.958	0.9557	MIR193A; RNU6/	0.441	0.786	0.999	weak promoter	Hypo	-0.0085
48	11	77300486	77300560	75	5	7596	tss	0.0927	0.107	0.0923	0.0859	0.0795	0.0904	AQP11; CLNS1A;	0.438	0.994	0.999	weak promoter	Hypo	-0.012066667
49	13	113474153	113474413	261	5	11273	gene;island	0.8901	0.8635	0.8823	0.8762	0.8568	0.8803	ATP11A (margin:	0.437	0.989	0.999	weak transcription	Hypo	-0.007533333
50	5	65222276	65222365	90	4	32148	tss	0.073	0.0691	0.0723	0.0692	0.0512	0.071	ERBB2IP; CTD-20	0.437	0.495	0.999	active promoter	Hypo	-0.007666667
51	5	1218507	1218653	147	4	31577	gene;island	0.8887	0.8877	0.915	0.8958	0.8847	0.8696	SLC6A19; SLC6A1	0.435	0.967	0.999	heterochromatin	Hypo	-0.013766667
52	6	80657412	80657555	144	7	35139	tss;island	0.1027	0.114	0.1042	0.1062	0.1143	0.08	ELOVL4; GAPDHP	0.434	0.954	0.999	weak promoter	Hypo	-0.0068
54	6	32073324	32073700	377	5	34101	gene	0.8385	0.8416	0.8625	0.8815	0.8666	0.878	TNXB; ATF6B (ma	0.433	0.963	0.999	repressed	Hyper	0.027833333
56	2	109403293	109403692	400	5	22859	gene	0.0679	0.0672	0.0814	0.0782	0.0624	0.0761	RANBP2; CCDC13	0.43	0.991	0.999	active promoter	Hyper	6.66667E-05
58	16	19896246	19896644	399	4	15145	tss	0.1745	0.1737	0.1666	0.1494	0.1715	0.136	AC134300.1; GPR	0.43	0.977	0.999	weak promoter	Hypo	-0.0193
60	10	27541298	27541418	121	4	5005	tss	0.8902	0.8916	0.9007	0.8841	0.8651	0.8907	RP11-85G18.6; A	0.428	0.901	0.999	weak promoter	Hypo	-0.0142
61	14	101438430	101438663	234	4	12638	tss	0.8365	0.8496	0.8565	0.8689	0.8498	0.8268	AL132709.8; SNC	0.428	0.793	0.999	weak enhancer	Hyper	0.000966667
62	13	113832355	113832595	241	4	11296	gene	0.5763	0.5981	0.5896	0.5613	0.5615	0.5532	PROZ; PCID2 (ma	0.427	0.926	0.999	transcription elongation	Hypo	-0.029333333
63	15	81294134	81294324	191	4	13471	gene;island	0.113	0.0991	0.1037	0.1056	0.0959	0.1088	MESDC1; C15orf/	0.427	0.619	0.999	active promoter	Hypo	-0.001833333
64	12	85430123	85430336	214	7	9246	gene	0.1151	0.1075	0.1049	0.1087	0.1072	0.1431	LRRIQ1; TSPAN1	0.426	0.816	0.999	active promoter	Hyper	0.0105
68	16	85670135	85670348	214	4	14901	gene;island	0.8666	0.8708	0.8788	0.8575	0.85	0.852	GSE1 (margin: GS	0.423	0.97	0.999	weak enhancer	Hypo	-0.0189
69	4	81186795	81187198	404	5	30510	tss;island	0.0633	0.0755	0.0702	0.0752	0.0806	0.0801	FGF5 (margin: FG	0.422	0.66	0.999	active promoter	Hyper	0.008966667
70	16	85242446	85242716	271	4	16177	island	0.8999	0.8883	0.906	0.9133	0.9001	0.9137	(margin: CTC-786	0.422	0.723	0.999	weak transcription	Hyper	0.010966667
72	10	134973605	134973796	192	5	5458	tss;island	0.1697	0.1633	0.1722	0.1471	0.1836	0.169	KNDC1 (margin: (	0.421	0.841	0.999	poised promoter	Hypo	-0.001833333
73	10	133000130	133000471	342	6	4846	gene	0.5937	0.6187	0.6266	0.6487	0.6672	0.6396	TCERG1L (margin	0.42	0.977	0.999	heterochromatin	Hyper	0.038833333
74	19	45281006	45281287	282	5	22152	island	0.0487	0.0588	0.0577	0.0606	0.0755	0.077	CBLC (margin: BC	0.419	0.999	0.999	weak enhancer	Hyper	0.015966667
76	14	21152202	21152358	157	4	12298	tss	0.1015	0.0807	0.1029	0.1015	0.1098	0.1033	Y_RNA; RNASE4;	0.418	0.99	0.999	active promoter	Hyper	0.009833333
77	11	77300486	77300763	278	7	8696	island	0.0897	0.0886	0.0881	0.0809	0.0659	0.0671	AQP11; CLNS1A;	0.417	0.979	0.999	weak promoter	Hypo	-0.0175
78	17	7893344	7893701	358	4	18011	island	0.0653	0.0572	0.0534	0.0612	0.0679	0.0686	(margin: GUCY2D	0.417	0.985	0.999	weak promoter	Hyper	0.007266667
79	16	89163343	89163800	458	5	14952	gene;island	0.911	0.9163	0.9249	0.9233	0.9267	0.9185	ACSF3 (margin: A	0.417	0.997	0.999	weak transcription	Hyper	0.005433333
81	2	220306470	220306674	205	4	23073	gene;island	0.0449	0.0563	0.0506	0.0503	0.0522	0.0669	SPEG (margin: DE	0.415	0.899	0.999	strong enhancer	Hyper	0.005866667
82	5	86563744	86564119	376	6	32212	tss;island	0.0948	0.1137	0.1182	0.1337	0.1268	0.1389	RASA1 (margin: F	0.415	0.68	0.999	active promoter	Hyper	0.024233333
85	16	2509755	2510115	361	5	15630	island	0.1107	0.1159	0.1232	0.1311	0.1109	0.1162	CCNF; C16orf59;	0.414	0.983	0.999	weak promoter	Hyper	0.0028
86	17	29886672	29887049	378	5	18219	island	0.9664	0.9646	0.9606	0.9576	0.9534	0.9557	MIR193A; RNU6/	0.414	0.949	0.999	weak promoter	Hypo	-0.0083
88	4	41694736	41694847	112	4	30041	gene	0.2287	0.2549	0.2473	0.2156	0.1895	0.234	LIMCH1; RP11-22	0.414	0.95	0.999	heterochromatin	Hypo	-0.0306
90	6	36562212	36562537	326	4	34370	gene	0.0825	0.0698	0.0825	0.0736	0.0685	0.0619	SRSF3 (margin: S	0.414	0.888	0.999	active promoter	Hypo	-0.010266667
91	11	43601969	43602179	211	4	7264	tss;island	0.8309	0.8084	0.8024	0.8192	0.8274	0.8232	HSD17B12; MIR1	0.412	0.991	0.999	poised promoter	Hyper	0.009366667
92	15	37391424	37391721	298	4	13305	gene;tss;islan	0.1045	0.1007	0.111	0.1037	0.1177	0.1102	RP11-128A17.1; I	0.412	0.951	0.999	active promoter	Hyper	0.005133333
97	15	62989935	62990138	204	5	13391	gene;island	0.8224	0.8356	0.8674	0.8832	0.8536	0.8513	TLN2; RP11-625H	0.41	0.634	0.999	heterochromatin	Hyper	0.0209
98	19	571107	571416	310	5	20310	tss;island	0.1235	0.1258	0.1467	0.1184	0.1025	0.1251	BSG; AC009005.2	0.409	0.973	0.999	strong enhancer	Hypo	-0.016666667
99	3	9943828	9943937	110	4	28181	tss	0.8537	0.8588	0.8631	0.8801	0.8539	0.8562	JAGN1; IL17RE (m	0.409	0.821	0.999	weak enhancer	Hyper	0.004866667
100	6	33037413	33037690	278	6	34235	gene	0.3714	0.4023	0.4068	0.408	0.4227	0.3862	HLA-DPB1; RPL32	0.409	0.992	0.999	heterochromatin	Hyper	0.012133333
101	19	13262683	13263065	383	4	19913	gene;island	0.0595	0.054	0.0492	0.062	0.0614	0.0659	IER2; STX10; CTC	0.408	0.981	0.999	active promoter	Hyper	0.008866667
102	22	36697013	36697055	43	5	26900	gene	0.8627	0.8709	0.9018	0.8887	0.8701	0.8601	MYH9 (margin: M	0.408	0.932	0.999	transcription elongation	Hypo	-0.0055
104	12	40499811	40500139	329	4	9653	tss	0.0702	0.0763	0.0664	0.0712	0.0803	0.0745	SLC2A13 (margin	0.408	0.984	0.999	weak promoter	Hyper	0.004366667
105	5	65222276	65222522	247	5	32890	island	0.0694	0.0739	0.0727	0.071	0.0527	0.077	ERBB2IP; CTD-20	0.408	0.747	0.999	active promoter	Hypo	-0.0051
107	6	50818685	50819236	552	4	36258	island	0.7695	0.7918	0.7905	0.809	0.8024	0.8081	TFAP2B; RPS17P5	0.406	0.963	0.999	poised promoter	Hyper	0.022566667
108	4	2341196	2341463	268	5	29937	gene;island	0.8629	0.8751	0.8803	0.8599	0.8642	0.8574	ZFYVE28 (margin	0.406	0.947	0.999	heterochromatin	Hypo	-0.012666667
109	14	89259551	89259748	198	4	12568	tss;island	0.1341	0.1405	0.1398	0.1547	0.1803	0.1688	EML5 (margin: RI	0.406	0.794	0.999	active promoter	Hyper	0.0298
110	1	76262648	76262984	337	4	590	gene	0.7721	0.7945	0.768	0.7651	0.7452	0.7655	ACADM; RABGGT	0.405	0.966	0.999	weak transcription	Hypo	-0.0196
112	10	112432175	112432418	244	4	4759	gene;island	0.0954	0.0962	0.0986	0.1165	0.1135	0.1166	RBM20 (margin:	0.404	0.992	0.999	weak promoter	Hyper	0.0188
114	12	85430025	85430336	312	10	9913	tss	0.1413	0.1222	0.1071	0.1331	0.1337	0.1569	LRRIQ1; TSPAN1	0.404	0.844	0.999	active promoter	Hyper	0.0177
115	20	41818574	41818905	332	5	25789	tss;island	0.3158	0.3033	0.2966	0.2885	0.3153	0.327	RP1-269M15.3; P	0.404	0.994	0.999	repressed	Hyper	0.005033333
117	15	38364951	38365373	423	5	14040	island	0.0638	0.0633	0.0691	0.0593	0.0605	0.0725	RP11-1008C21.2	0.403	0.71	0.999	strong enhancer	Hypo	-0.0013
118	10	43278214	43278349	136	4	4569	gene;island	0.0368	0.0302	0.0277	0.0276	0.0276	0.026	BMS1 (margin: B	0.402	0.58	0.999	active promoter	Hypo	-0.0045
120	9	114557067	114557553	487	4	40996	island	0.9084	0.9047	0.9099	0.909	0.9161	0.9011	RP11-430K21.2; (	0.402	0.919	0.999	heterochromatin	Hyper	0.001066667
121	2	214016113	214016366	254	4	23897	tss;island	0.0826	0.0812	0.086	0.0874	0.0891	0.0906	RP11-105N14.1; I	0.401	0.963	0.999	active promoter	Hyper	0.005766667
123	16	70285806	70285978	173	5	16091	island	0.0549	0.0413	0.0409	0.0414	0.0399	0.0401	RP11-296I10.6; E	0.401	0.933	0.999	weak promoter	Hypo	-0.005233333
124	13	101186107	101186274	168	5	11535	tss	0.911	0.904	0.9059	0.9093	0.9004	0.9056	PCCA; GGACT; RF	0.401	0.87	0.999	heterochromatin	Hypo	-0.001866667